INFORMATION TO USERS

This manuscript has been reproduced from the microfilm master. UMI films the text directly from the original or copy submitted. Thus, some thesis and dissertation copies are in typewriter face, while others may be from any type of computer printer.

The quality of this reproduction is dependent upon the quality of the copy submitted. Broken or indistinct print, colored or poor quality illustrations and photographs, print bleedthrough, substandard margins, and improper alignment can adversely affect reproduction.

In the unlikely event that the author did not send UMI a complete manuscript and there are missing pages, these will be noted. Also, if unauthorized copyright material had to be removed, a note will indicate the deletion.

Oversize materials (e.g., maps, drawings, charts) are reproduced by sectioning the original, beginning at the upper left-hand corner and continuing from left to right in equal sections with small overlaps.

ProQuest Information and Learning
300 North Zeeb Road, Ann Arbor, MI 48106-1346 USA
800-521-0600

UMI®

THE PHOTOCHEMISTRY OF ALKYLCYCLOBUTENES AT 228-NM. AN INVESTIGATION OF THE RYDBERG EXCITED STATE REACTIVITY

By

BRUCE H.O. COOK, B.Sc.

A Thesis

Submitted to the School of Graduate Studies

in Partial Fulfillment of the Requirements for the Degree

Doctor of Philosophy

McMaster University

©Copyright by Bruce H.O. Cook, July 2000

THE PHOTOCHEMISTRY OF ALKYLCYCLOBUTENES AT 228-NM

DOCTOR OF PHILOSOPHY (2000) McMaster University
(Chemistry) Hamilton, Ontario

TITLE : The Photochemistry of Alkylcyclobutenes at 228-nm. An Investigation of the Rydberg Excited State Reactivity.

AUTHOR : Bruce H.O. Cook, B.Sc. (Laurentian University)

SUPERVISOR : Professor William J. Leigh

NUMBER OF PAGES : xviii, 184

Abstract

In apparent contradiction with the Woodward-Hoffmann rules of pericyclic reactions, the photochemical ring-opening of alkylcyclobutenes to 1,3-dienes has been shown to proceed nonstereospecifically. There is now substantial evidence to support a mechanism in which the reaction occurs adiabatically to produce the symmetry-allowed diene in the excited singlet state. Relaxation to the ground state provides the observed mixture of diene isomers. Although the ring-opening is presumed to occur from the π,π^* excited state alone, the potential involvement of the low-lying Rydberg π,R(3s) has never been completely ruled out.

In order to assess the contribution of the Rydberg state to the photochemistry of cyclobutenes, a series of 1,2-dialkyl substituted derivatives were irradiated at 228-nm where the π,R(3s) state can be excited selectively. Under these conditions, it was found that these cyclobutenes continue to give rise to ring-opening products in substantial yields. Furthermore, with *cis*- and *trans*-1,2,3,4-tetramethylcyclobutene, the reaction proceeds with conrotatory (thermal) stereospecificity.

The possibility of reaction from upper vibrational levels of the ground state was investigated. The quantum yields for ring-opening at 228-nm for a series of cyclobutenes were determined, and compared to values calculated with the assumption that reaction proceeds entirely via a hot ground state mechanism.

The calculated quantum yields were based on rate constants from RRKM theory and the rate of relaxation from upper vibrational levels of the ground state. Hot ground state reactivity was shown to be insignificant by the lack of any correlation between the experimental and calculated quantum yields.

The ring-opening reaction from the Rydberg state was shown to be dependent on the incipient torsional mobility about the central C1-C2 bond of the cyclobutene. Derivatives with small ancillary rings attached to the central bond displayed reactivity similar to the π,π^* state, where those with large ancillary rings gave products enriched in the conrotatory diene isomers. Both the π,π^* (adiabatic) and Rydberg state ring-opening reactions can be rationalized in terms of these results. The pathway to ring-opening on the Rydberg state potential energy surface likely encounters a barrier associated with twisting about the central bond. If the barrier is sufficiently large, the state can cross with the π,π^* surface and products of adiabatic ring-opening are formed. When there is free rotation about the central bond, conrotatory ring-opening from the Rydberg state occurs.

Acknowledgments

It is at this time that I have the opportunity to extend my thanks to the many people who have either influenced my research, or my life, over the past five years. At the top of this list is Professor Willie Leigh. Willie, I thank you for educating me in countless ways during my stay in your group. You have been a teacher, a supervisor, and an advisor to me, and I am grateful. I also wish to thank my supervisory committee members, Dr. Ron Childs and Dr. Nick Werstiuk for their input to my research, and advice along the way. Of course, none of this would have been possible without the assistance of the amazing research support staff in our department including Dr. Don Hughes, Brian Sayer, George Timmins, Mike Palme, and Mike Malott. They are always willing to help in what is often a thankless job.

The WJL research group has been a great place to be. To Dr. J.A. Postigo, Dr. Nick Toltl, Ed Lathioor, Cerrie Rogers, Dr. Christine Bradaric, Dr. Corinna Kerst, Dr. Rabah Boukherroub, Tracy Morkin, Tom Owens, Cam Harrington, and Dr. Xiaojin Li : thanks for all of the good times and lively discussions.

Finally, I would like to thank my family; Mom, Dad, and David for your support over this long haul. I finally did it. And to Kerry : I'm glad that you were here for the last couple of years. Your endless encouragement and love was a welcome addition to the completion of my studies, and my life. I thank you all.

Table of Contents

List of Figures

List of Tables

Chapter 1

Introduction

1.1. The General Photochemistry of Cyclobutenes

The irradiation of cyclobutene (**1**) at 185 nm in *n*-heptane solution results in the formation of 1,3-butadiene (**2**), acetylene (**3**), ethylene (**4**), and methylenecyclopropane (**5**) (eqn.1.1).[1] Although this was not the first example to illustrate the array of photoproducts that result from cyclobutene photolysis, it nicely demonstrates the available reactions in the photochemistry of these compounds. For instance, **2** is derived from electrocyclic ring-opening, the acetylene/ethylene pair are from [2+2] cycloreversion, and **5** is the product of skeletal rearrangement.

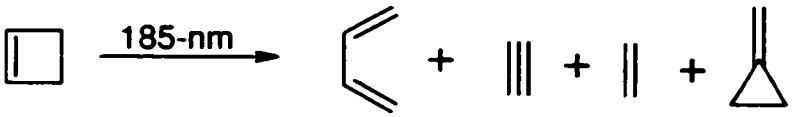

1 **2** **3** **4** **5**

[1.1]

Alkenes and cycloalkenes generally show a rich photochemistry,[2,3] but none of the various derivatives studied is considered to be of as fundamental importance as cyclobutenes. The thermal and photochemical electrocyclic interconversions of cyclobutene and butadiene lie at the foundation of the Woodward-Hoffmann rules,[4] and although the thermal reaction is well understood, its photochemical counterpart is still in the midst of scrutiny. In order to completely comprehend the origin of the photoproducts derived from cyclobutenes, it is important to be aware of the excited states available and their characteristics.

1.2. The UV Absorption Spectra of Alkylcyclobutenes

Although the carbon-carbon double bond is perhaps the simplest of chromophores, the electronic absorption spectra of simple alkenes can be complicated. There are at least four excited singlet states which are accessible with far-uv excitation of alkyl-substituted alkenes; these are the valence π,π^* and π,σ^* states and the π,R(3s) and π,R(3p) Rydberg states.[5-11] The relative energies of these states depend on the substitution on the C=C double bond. Typically, with increased alkyl substitution on the carbon-carbon double bond, the energy of the π,π^* state changes only slightly due to a parallel increase in the energy of both the π and π^* molecular orbitals. In contrast, the Rydberg states decrease in energy due to the increased energy of the π MO and the fact that the

energy of the carbon 3s and 3p atomic orbitals remains roughly constant.[11-13] The energies (E_n) of the π,R(3s) Rydberg states of alkenes correlate with the vertical π-ionization potentials.[11,13] Due to this shift in excited state energies, the Rydberg absorptions actually appear at longer wavelengths than the valence π,π^* absorption in highly substituted alkenes. Figure 1.1 illustrates how this inversion of excited state energies occurs.

Figure 1.1. Relative energies of the molecular and atomic orbitals of increasingly alkyl-substituted alkenes.

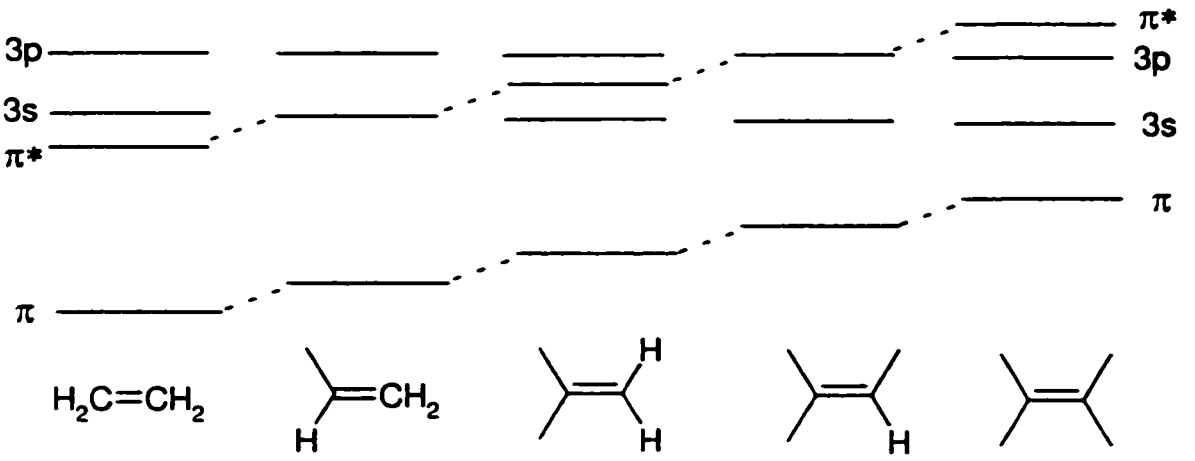

The ultraviolet absorption spectra of alkylcyclobutenes[14-17] and other tetraalkylalkenes,[9,11,12,18] reflect these effects and show at least two overlapping yet distinct absorptions in the far UV. They have been assigned as the π,π^* (*ca.* 180-nm to 200-nm), the π,R(3p) (*ca.* 190-nm to 210-nm), and the π,R(3s) (*ca.*

210-nm to 230-nm) excitations.[8,9,11] The broad structure of the π,π^* absorption is believed to completely shield the observation of the π,σ^* state.[11] The UV spectra of 2,3-dimethyl-2-butene (**6**) in the gas phase, and as a thin film at 23 K, are shown in Figure 1.2.

Figure 1.2. The UV absoprtion spectra of 2,3-dimethyl-2-butene a) in the gas phase and b) as a thin film at 23 K.[19]

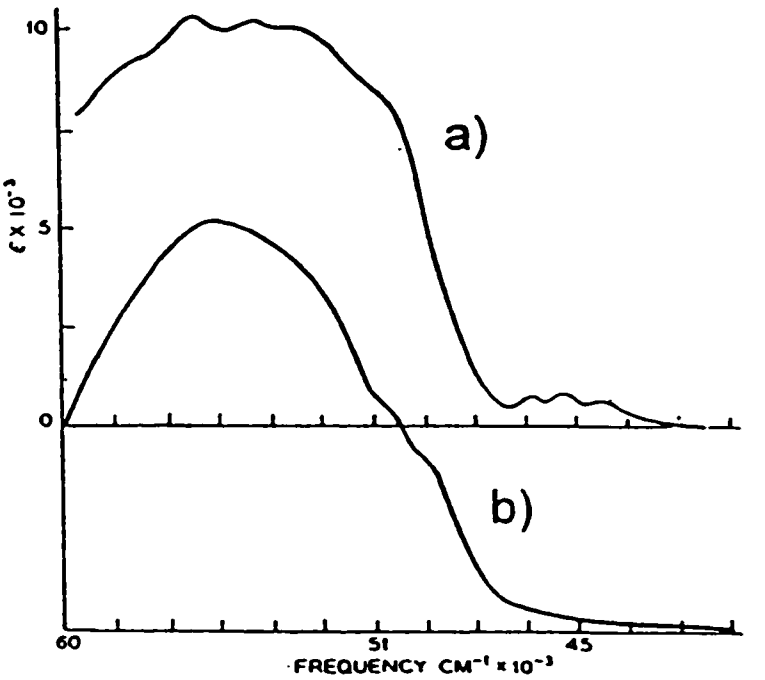

The Rydberg state absorptions of alkenes are much more evident in the gas phase than in condensed phases.[9,11] The state is susceptible to high pressures primarily because the excited electron exists in a spatially diffuse orbital and resembles a lone or ionized electron.[11] In solution, for instance, the

electron repulsion from solvent molecules is believed to increase the energy of the Rydberg states and render the transition broad and very weak.[13] With highly alkyl-substituted alkenes the Rydberg π,R(3s) absorption is not completely suppressed in solution, but only broadened to the point where the fine structure is lost and the absorbance maximum is significantly reduced in comparison to the valence π,π^* transition. Accordingly, the π,R(3s) state is accessible in both the gas and solution phase photochemistry of tetraalkyl-substituted alkenes. However, the energies of the valence π,π^* and Rydberg π,R(3s) transitions are such that it is generally very difficult to determine where the Rydberg band ends and the valence band begins.[10,11,13]

1.3. Ring-Opening of Cyclobutenes. The Ground State and π,π^* Excited State Reactions.

It is believed that the cyclobutene ring-opening products are primarily formed in the π,π^* state while the cycloreversion products result from the Rydberg state (although possibly not exclusively).[14-16,20] The reasons for these assignments will follow.

1.3.1. The Woodward-Hoffmann Rules

In the 1960's R.B. Woodward and R. Hoffmann developed a set of theoretical rules to predict the general reactivity and stereochemistry of pericyclic reactions.[4] Dr. Hoffmann won the 1981 Nobel Prize in Chemistry for his contribution to this theory. Pericyclic reactions can be defined as reactions which proceed through a cyclic transition state with all bond forming and bond breaking taking place concertedly.[4] These reactions are divided into four categories : cycloadditions, electrocyclic reactions, sigmatropic reactions and group transfer reactions. The Woodward-Hoffmann rules successfully predicted the stereochemistry of many pericyclic reactions including those shown in equation 1.2; a) the photochemical and thermal ring-opening of cyclohexadienes[21,22] (**7** to **8**) (6π electrocyclic), b) the Diels-Alder reaction[23] (**9** + **10**) (thermal 4π+2π cycloaddition), c) thermal and photochemical 1,n-sigmatropic shifts[24] (**12** to **13**), and d) the ring-closure of 1,3-dienes[25] (**15** to **14**)(4π electrocyclic). The ring-opening of cyclobutenes, the reverse reaction of the latter example, received much attention as a thermal electrocyclic reaction[26-31] and was shown to obey the Woodward-Hoffmann rules. However, despite its importance in the development of the theoretical understanding of pericyclic reactions (and the orbital symmetry rules), the photochemical counterpart was virtually ignored until very recently.

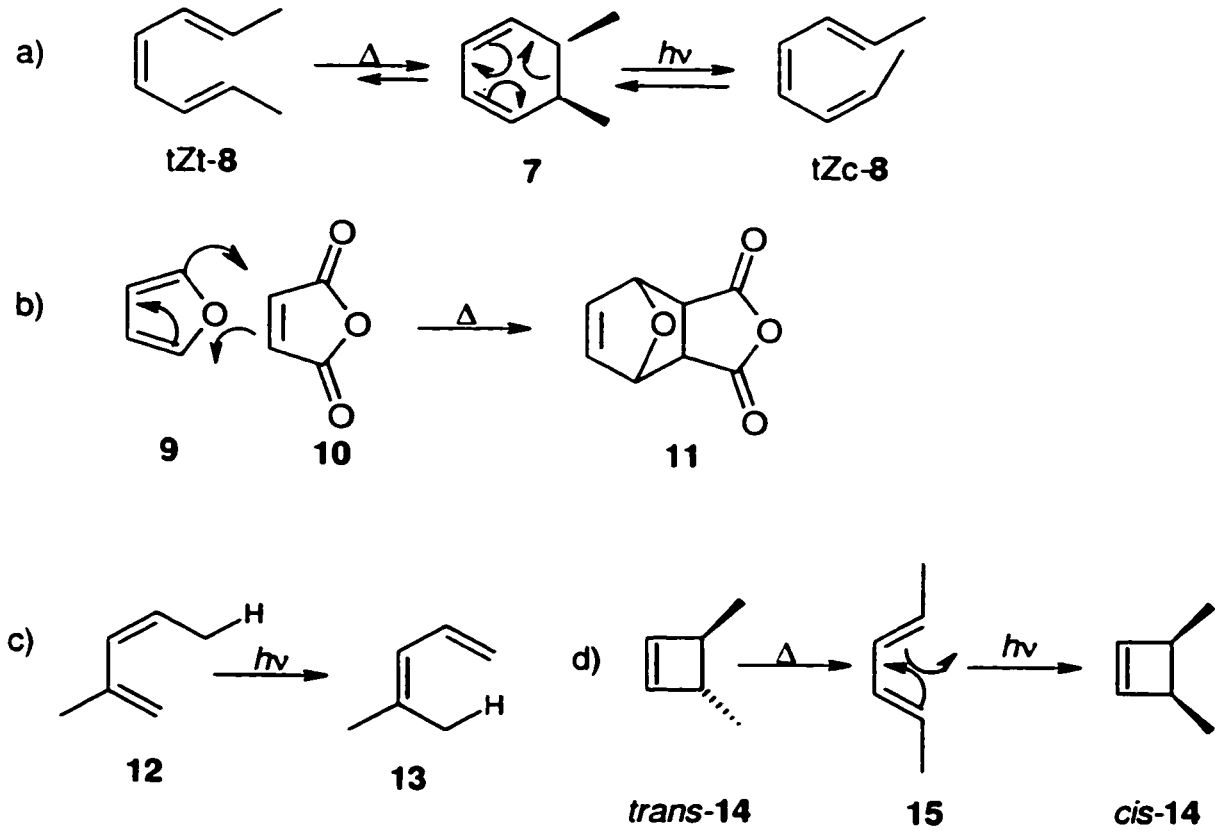

[1.2]

1.3.2. Orbital Symmetry and the Electrocyclic Ring-Opening of Cyclobutenes

The Woodward-Hoffmann rules state that the sterochemistry of pericyclic reactions is determined by orbital symmetry. The interconversions of cyclobutene and butadiene represent the prototypical example of a 4π electrocyclic reaction. An orbital correlation diagram can be constructed based on the frontier molecular orbitals (FMO) of both cyclobutene and butadiene. The correlations demonstrate the preferred stereochemistry for the reaction. For

instance, the FMOs of cyclobutene which are involved in the electrocyclic ring-opening are the σ, π, $\sigma^*$and π^* MOs which transform into the four π FMOs of butadiene; ψ_1, ψ_2, ψ_3 and ψ_4. The transformation can occur with either conrotatory (together) or disrotatory (opposite) twisting of the methylene groups. Different molecular symmetry elements are preserved throughout these two reaction coordinates : C_2 symmetry for the conrotatory process and σ_v symmetry for the disrotatory one. This is demonstrated in Figure 1.3.

Figure 1.3. The C_2 and σ_v symmetry elements which are preserved in the conrotatory and disrotatory rotation of the methylene groups of cyclobutene.

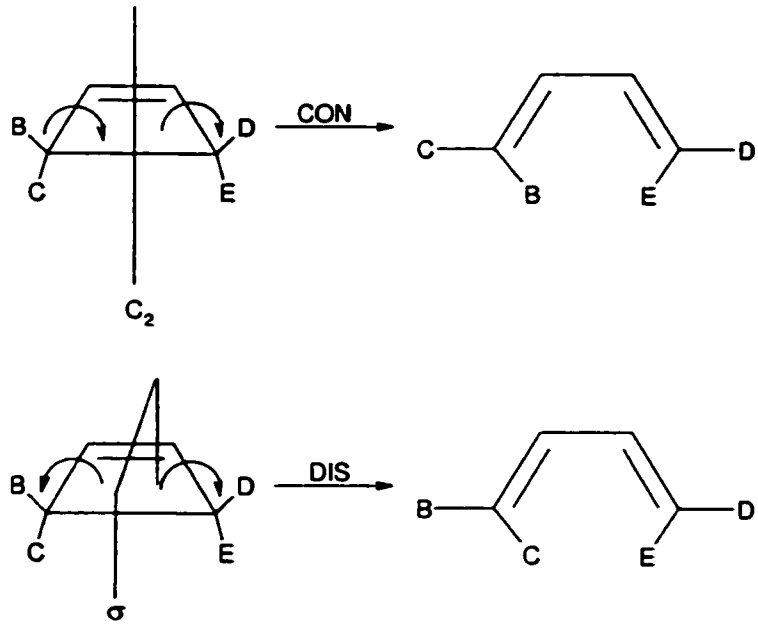

The cyclobutene and butadiene molecular orbitals are assigned as either symmetric (S) or antisymmetric (A) with respect to these two symmetry elements. Figure 1.4 shows the relevant FMOs of both transformations. If the matching symmetric (S) and antisymmetric (A) orbitals in the reactant and product are paired, the symmetry-allowed reaction paths can be found.

Figure 1.4. The orbital correlation diagram for the interconversion of cyclobutene and 1,3-butadiene depicting the ground state ring-opening reaction.

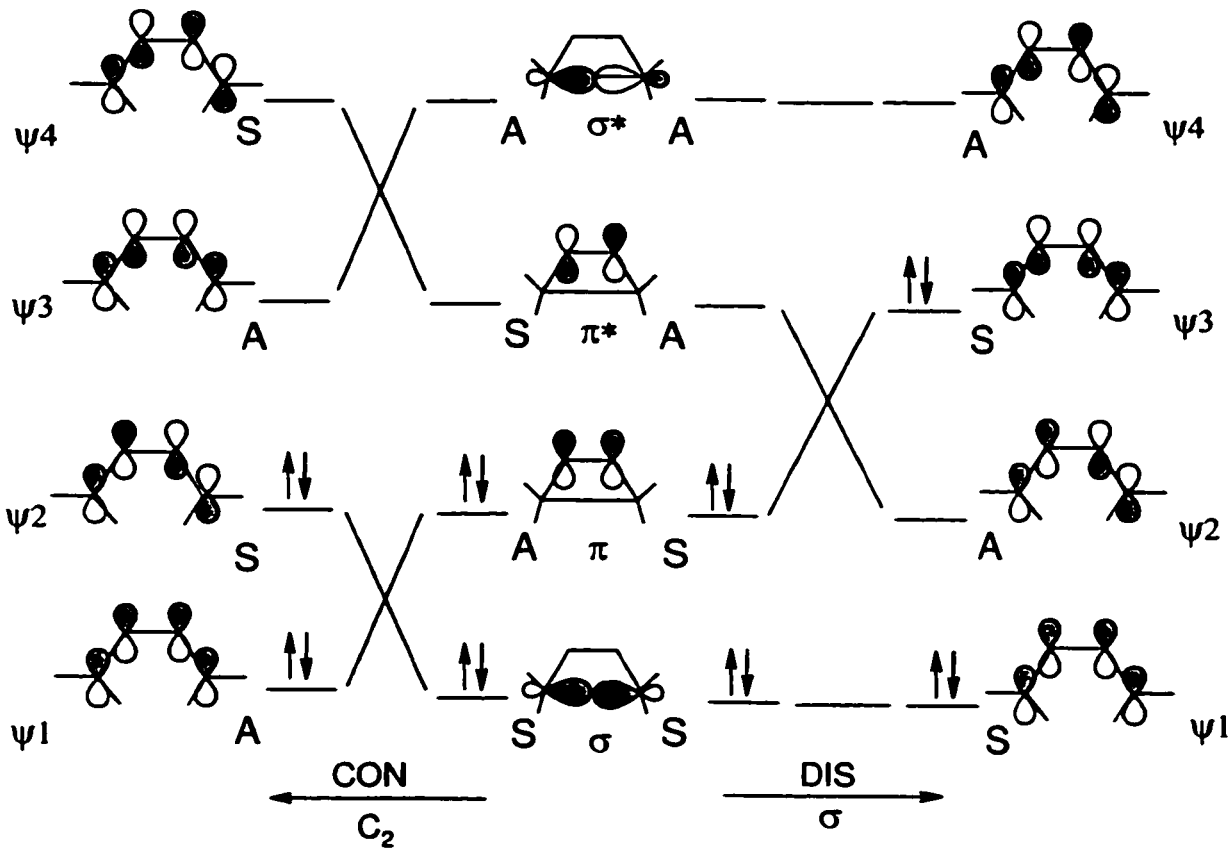

Figure 1.4 indicates that in the ground state the conrotatory pathway is preferred since it results in the ground state diene, as opposed to the doubly excited electronic state of the diene which correlates via disrotatory ring-opening.

The assessment of the excited state reaction in Figure 1.5, is similar with the exception that one of the π electrons is promoted to the π^* MO. In this case, the disrotatory pathway results in interconversion of the reactant and product without a change in electronic state, while the conrotatory pathway does not. The same stereochemistry is predicted for the reverse reaction (butadiene ring-closure).

Figure 1.5. The orbital correlation diagram for the interconversion of cyclobutene and 1,3-butadiene depicting the excited state ring-opening reaction.

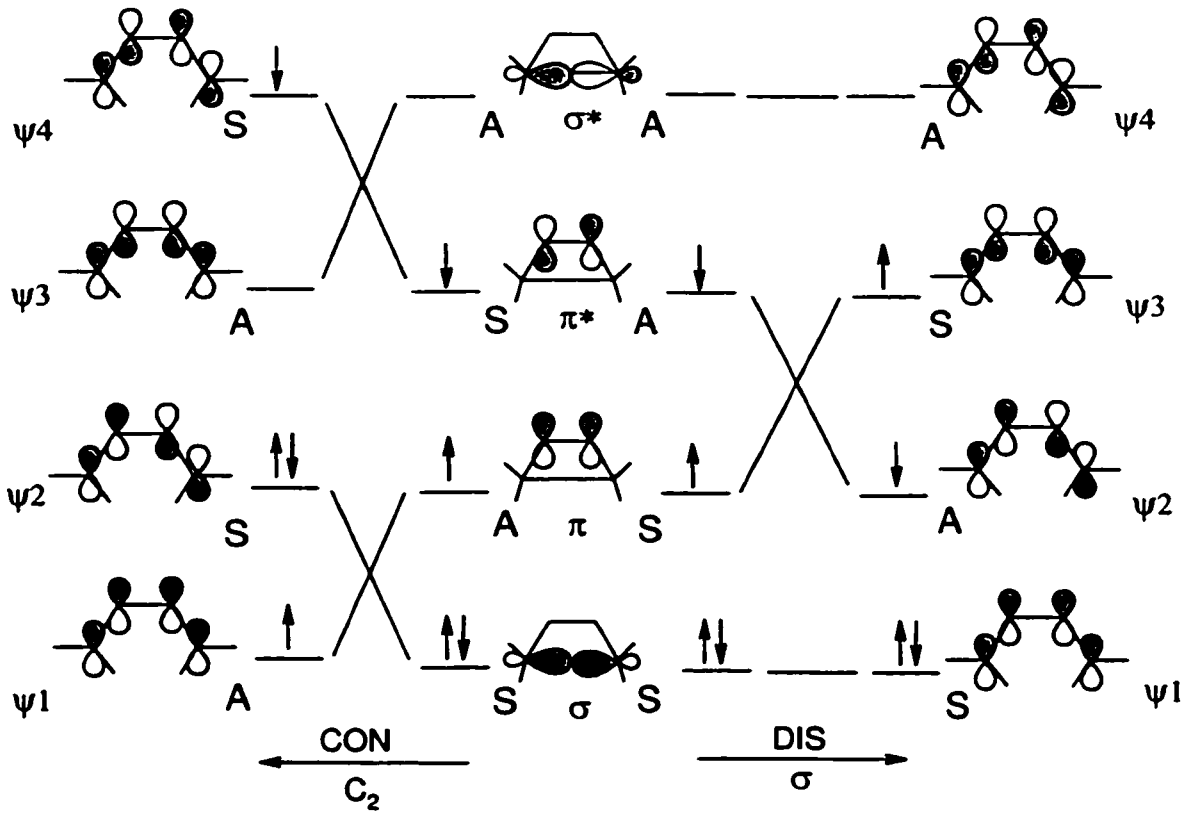

An interesting aspect of the orbital symmetry correlations is that the stereochemistry of the ground and excited state electrocyclic reactions alternates as the number of electrons involved in the process increases.[4] For instance, the butadiene system (4π electrons) which has been discussed here, reacts with ground state conrotatory, and excited state disrotatory motion. In contrast, the hexatriene system in equation 1.2.a (6π electrons) is predicted to react with

ground state disrotatory, and excited state conrotatory, stereochemistry. Table 1.1 demonstrates this phenomenon with the two possibilities being designated as having either 4k or 4k+2 electrons.

Table 1.1. The predicted stereochemistry for the electrocyclic reactions of conjugated systems.

π electrons	System	Ground State	π,π^* Excited State
4	4k	CON	DIS
6	4k+2	DIS	CON
8	4k	CON	DIS
10	4k+2	DIS	CON

1.3.3. The Ground State Ring-Opening of Cyclobutenes

The thermally induced electrocyclic ring-opening of cyclobutenes was studied very thoroughly in the 1950s and 1960s. The reaction was shown to be stereospecific in every case where the stereochemistry could be determined (eqns. 1.3 and 1.4).[26-31] Bicyclo[4.2.0]oct-7-ene (**16**) [29] was shown to be the smallest bicyclic derivative in which the conrotatory product could be identified (eqn. 1.4).

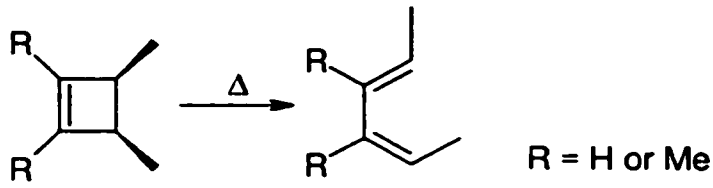

[1.3]

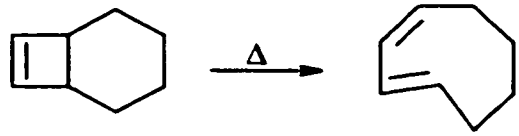

16 *E,Z*-**17**

[1.4]

The Arrhenius activation parameters for the ring-opening of several of the cyclobutenes were also determined and offer an insightful comparison. For instance, systems in which conrotatory rotation always results in internal motion of an alkyl group (i.e. *cis*-**18**, **20**, **22**) have higher activation energies than others (eqn. 1.5).[29] As well, bicyclic cyclobutenes which give highly strained products from conrotation (*cis*-**24**, **26**) also have exceedingly high activation energies for ring-opening (eqns. 1.6 and 1.7).[27,28] The experimental Arrhenius activation parameters of a series of cyclobutenes depicting these trends are given in Table 1.2.

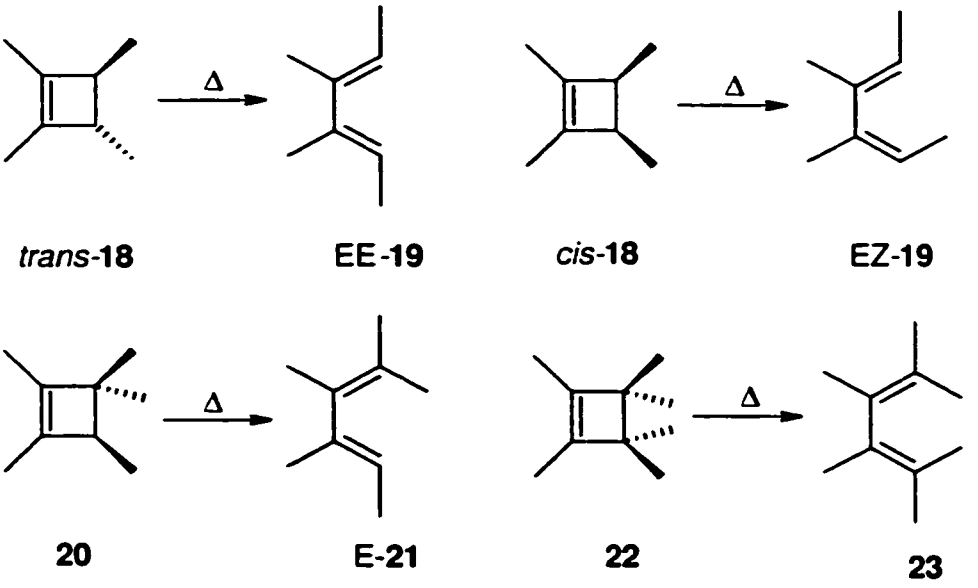

trans-**18** EE-**19** *cis*-**18** EZ-**19**

20 E-**21** **22** **23**

[1.5]

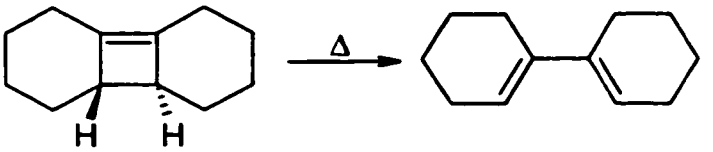

trans-**24** **25**

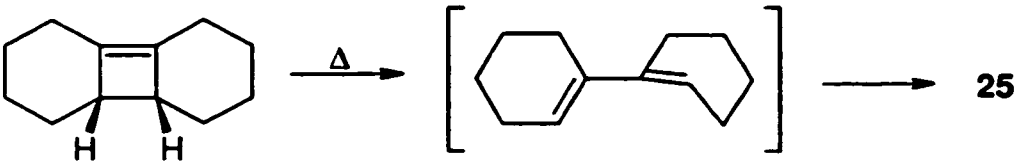

cis-**24** *E,Z*-**25** **25**

[1.6]

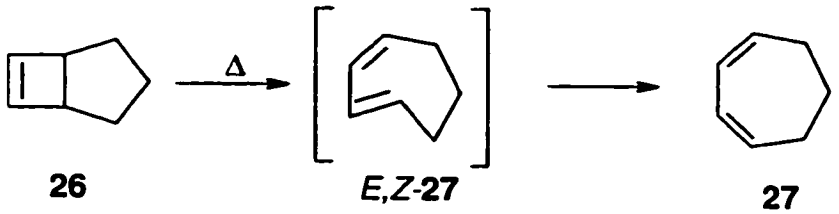

26 *E,Z*-**27** **27**

[1.7]

Table 1.2. Arrhenius activation energies and pre-exponential factors for the thermal ring-opening of selected alkylcyclobutenes.

Compound	*trans*-**18**[29]	*cis*-**18**[29]	**20**[29]	**22**[29]
E_a (kcal/mol)	32.0	35.8	34.0	40.0
log(A)	13.25	13.32	12.8	14.95

Compound	*cis*-**24**[28]	*trans*-**24**[28]	**26**[27]
E_a / kcal/mol	41.6	29.2	45.9
log(A)	12.96	14.23	14.31

1.3.4. The Photochemical Ring-Opening of Cyclobutenes

Most textbooks suggest that the photochemical ring-opening of cyclobutenes obeys the Woodward-Hoffmann rules. This opinion is evidently based on the report by Saltiel and coworkers on the photochemistry of the tricyclic cyclobutenes *cis*- and *trans*-**24** (eqn.1.8).[32] They reported that while the cis derivative gave both ring-opening (**25**) and cycloreversion (**28**) products upon excitation, only *E*-**28** was obtained from trans-**24**. It was argued that disrotatory ring-opening of the trans isomer would give the highly strained *E,Z*-**25** and therefore did not occur.

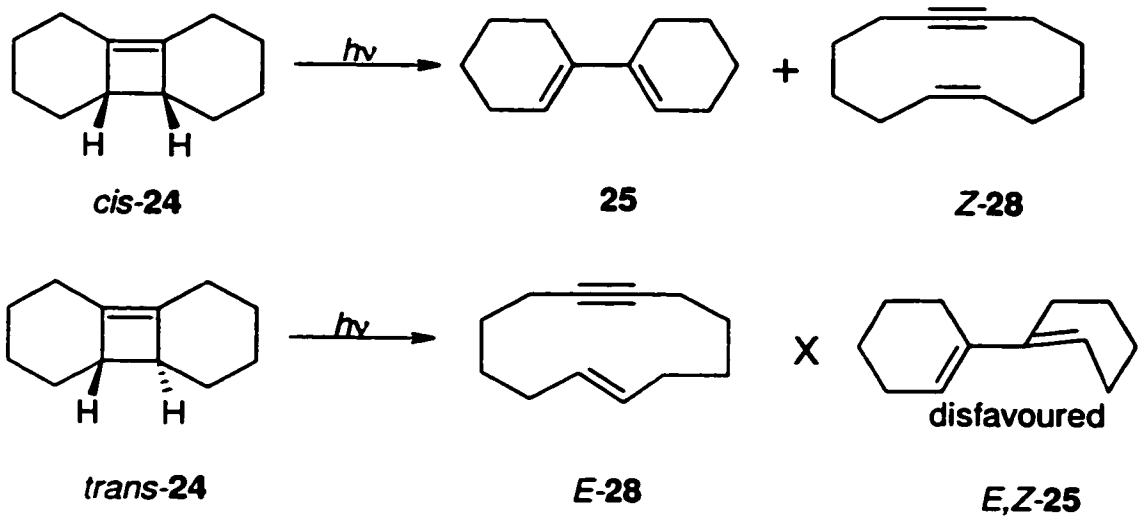

cis-**24** **25** *Z*-**28**

trans-**24** *E*-**28** *E,Z*-**25**

[1.8]

However, in 1987, Clark and Leigh described the 185-nm excitation of *cis*- and *trans*-3,4-dimethylcyclobutene (**14**) and the two bicyclic derivatives, **26** and **16**.[33] Not only did all the irradiations give products of ring-opening (**15**, **27**, **17**) and cycloreversion (**3**/**29**, **3**/**30**, **3**/**31**), it was shown that in cases where the stereochemistry of the reaction could be determined, the ring-opening proceeded nonstereospecifically, in apparent violation of the Woodward-Hoffmann rules (eqn. 1.9 and 1.10). The photochemistry of the isomers **24** was also reinvestigated at this wavelength and the ring-opening was observed in both cases.[34]

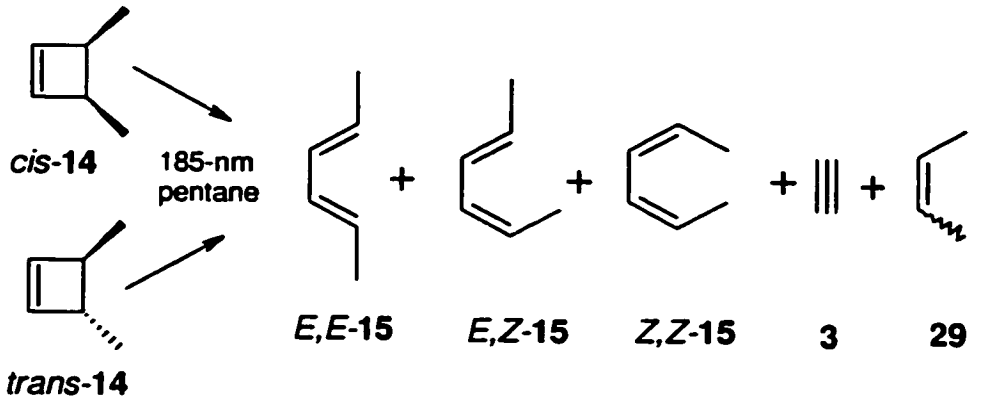

[1.9]

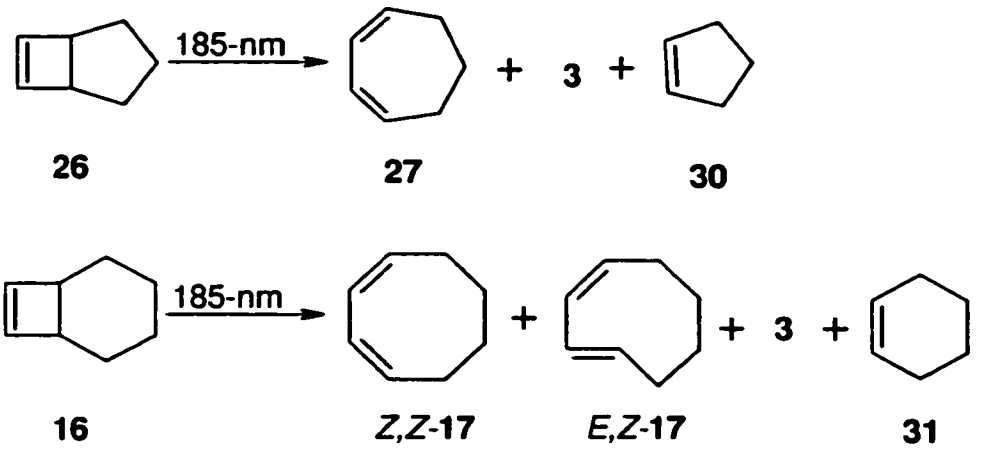

[1.10]

The nonstereospecificity of the photochemical ring-opening of cyclobutenes is quite general, as a variety of monocyclic cyclobutenes (**18**, **32**),[14,35] (eqn. 1.11) and bicyclic cyclobutenes (**16**, **36**)[15,36-38] (eqn. 1.12) have all been shown to open nonstereospecifically upon photolysis in solution.

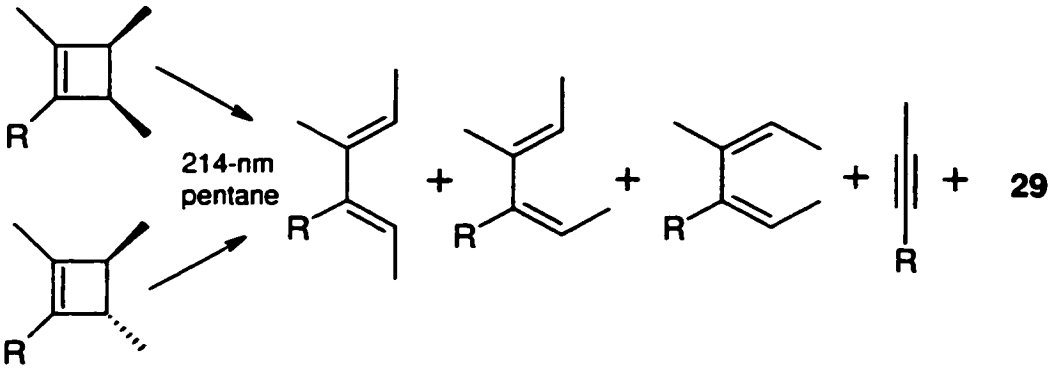

32 : R = H
18 : R = Me

33 : R = H
19 : R = Me

34 : R = H
35 : R = Me

[1.11]

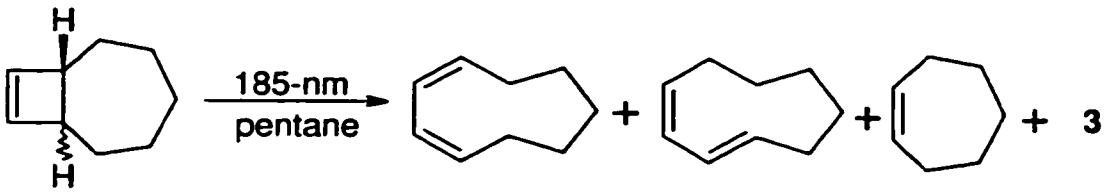

36 *Z,Z*-**37** *E,Z*-**37** **38**

[1.12]

With these discoveries it was clear that a new mechanism to depict the excited state ring-opening was required. Three possibilities have been proposed : i) adiabatic ring-opening, which initially obeys the Woodward-Hoffmann rules by forming the allowed diene in the excited state; ii) competitive ring-opening involving both the π,π^* and π,R(3s) excited states; and iii) competitive ring-opening from the π,π^* state and upper vibrational levels of the ground state after initial internal conversion.

1.3.5 Adiabatic Ring-Opening of Cyclobutenes

The proposed adiabatic reaction mechanism is shown in equation 1.13; notice that all of the common diene excited state reaction pathways[39] are accounted for including *E,Z*-isomerization, conformer interconversion, and cyclobutene formation.

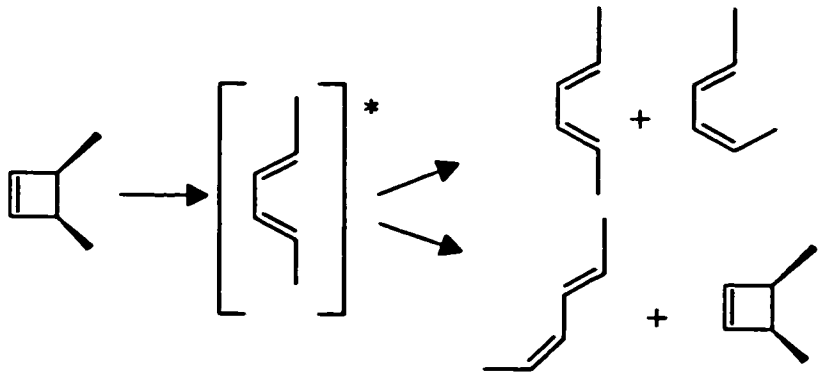

[1.13]

One way to provide evidence in support of this mechanism is to compare the distribution of photoproducts upon irradiating a given cyclobutene to those from irradiating its *formally-allowed ring-opening product.* However, this approach also brings its implicit problems. It has been shown that 1,3-dienes exist in two rapidly equilibrating ground state conformations about the central single bond; the s-*trans* and the s-*cis*, with the former being some 2 kcal/mol more stable in the parent 1,3-butadiene.[40,41] Rotation about the central bond of the diene occurs with an energy barrier of approximately 2-5 kcal/mol.[42] Furthermore, the photochemistry of 1,3-dienes, and polyenes in general, has been shown to be conformation-dependent.[39,43,44] This has been demonstrated by the wavelength and structural effects in the photochemistry of cyclic and acyclic dienes.[39,45] For instance, 254-nm excitation of 1,3-pentadiene (**39**) results in both *E,Z*-isomerization and cyclobutene formation (**40**) whereas 229-

nm irradiation leads only to *E,Z*-isomerization. In the latter example, the s-*trans* conformer is exclusively excited (eqn. 1.14).[46]

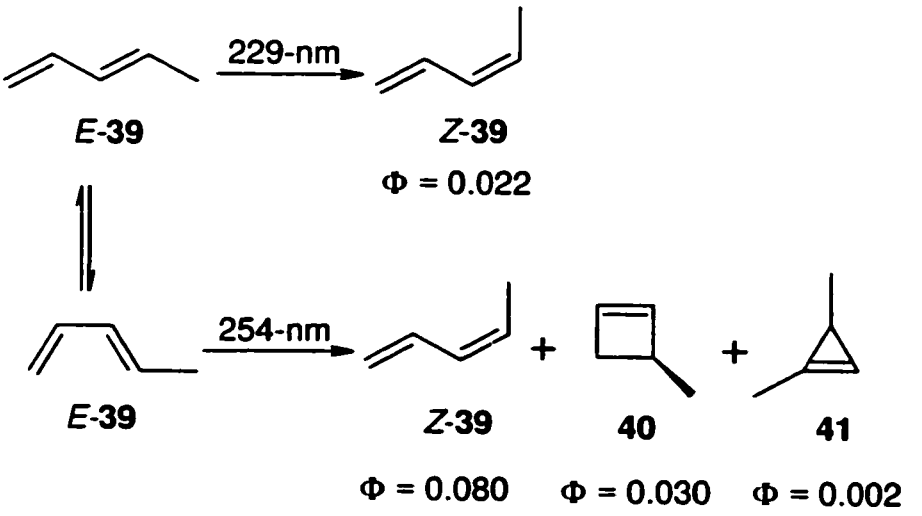

[1.14]

In addition, cyclic dienes show an increased tendency towards cyclobutene formation because they are constrained to the s-*cis* conformation,[36,39,47,48] although it has been shown that some of the product arises from secondary thermal isomerization (i.e. *E,Z*-**27** to **26**).[47,49] As the ring size of the diene is increased and the torsional flexibility of the central bond increases, the quantum yield for ring-closure is drastically reduced. This trend is illustrated in equations 1.15-1.18.

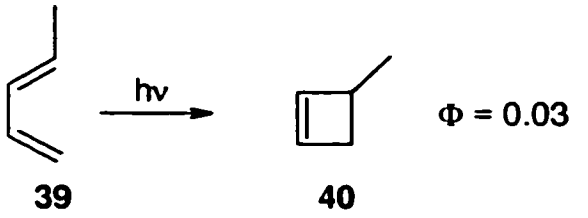

[1.15]

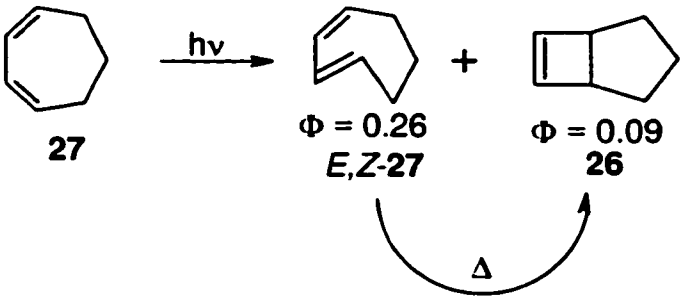

[1.16]

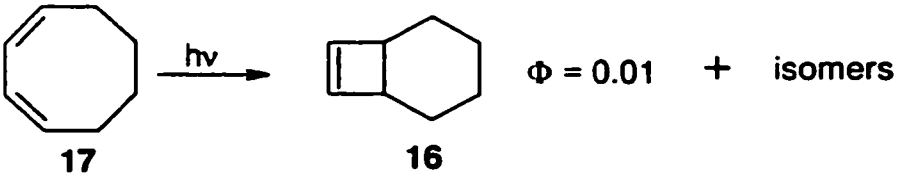

[1.17]

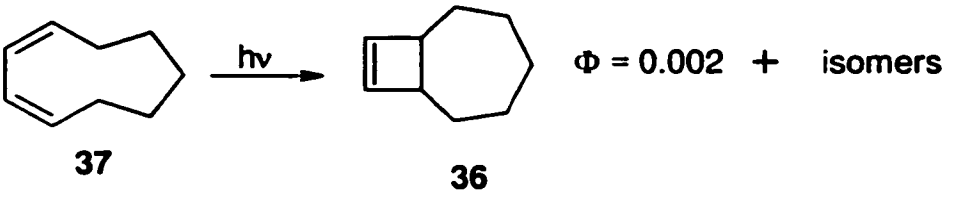

[1.18]

In order to investigate the possibility of an adiabatic cyclobutene ring-opening mechanism, it was necessary to identify a means by which only the

photochemistry of the s-*cis* diene could be observed, since the *primary* photochemical ring-opening product in this mechanism is the s-*cis* conformer of the diene. This was accomplished by using cyclobutenes which would produce 1,3-dienes where the central single bond is restricted in an ancillary ring.

The adiabatic mechanism was thoroughly investigated by Leigh and coworkers. A system which provided excellent evidence was that of *cis*-4,4,6,7-tetramethylbicyclo[3.2.0]hept-1[5]-ene (**42**) and its ring-opening products (**43**).[50] In this particular asymmetric system, the conrotatory products can be distinguished and the relative yields of the E,Z and Z,E dienes were compared. It was shown that the E,Z/Z,E ratio upon irradiation of **42**, closely matches that obtained from irradiation of *E,E*-**43** (eqn. 1.19).

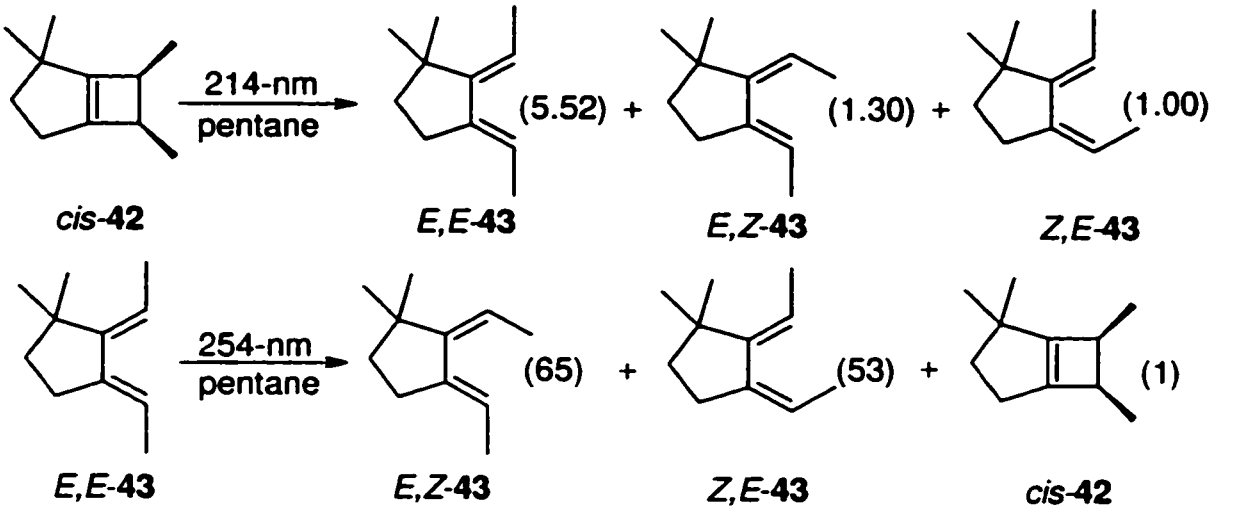

[1.19]

The generality of this phenomenon was later shown by the study of bicyclic cyclobutenes, **44-46**, and their corresponding dienes (eqn. 1.20).[16] With this series of derivatives the product ratios from photolysis of the cyclobutenes were compared to those calculated from the quantum yields for isomerization of the dienes (eqn. 1.21). The calculation provides a ratio of the allowed / forbidden isomers expected from the cyclobutene, and is based on the assumption that the ring-opening produces only the disrotatory isomer in the excited state. Accordingly, the quantum yields of cyclobutene ring-opening to each isomer and each diene isomerization reaction were determined experimentally and the theoretical ratios of diene isomers were calculated using equation 1.21. For example, the mechanistically predicted E,E/E,Z ratio is found by subtracting the quantum yields of all the reactions which deplete the E,E isomer from unity, and dividing by the quantum yield of formation of the E,Z isomer from the E,E. Furthermore, the E,E/Z,Z ratio from irradiation of the trans cyclobutenes (the ratio of conrotatory products) can be compared to that from isomerization of the E,Z dienes (the formally-allowed ring-opening products). The results are summarized in Table 1.3 along with the calculated ratios using equation 1.21.

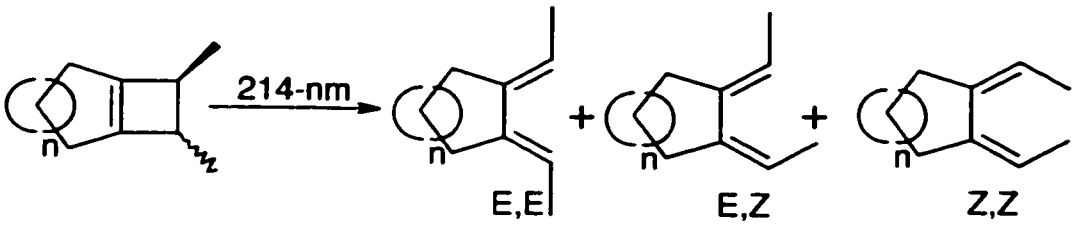

n=1 : **44** n=1 : **47**
2 : **45** 2 : **48**
3 : **46** 3 : **49**

[1.20]

$$(E,E/E,Z)_{\text{from CB}} = (1-\Phi_{E,E\rightarrow E,Z} - \Phi_{E,E\rightarrow CB} - \Phi_{E,E\rightarrow other})/\Phi_{E,E\rightarrow E,Z}$$

[1.21]

In almost every case, the quantum yield ratio from reaction of the cyclobutene matched the predicted ratio within experimental error. The investigation of this series of cyclobutenes and resultant dienes provides considerable support for a ring-opening mechanism which occurs adiabatically in the excited singlet state.

Table 1.3. Quantum yield ratios for ring-opening of **44-46** at 214-nm and isomerization of dienes **47-49** at 254-nm in pentane. (obs : observed from the cyclobutene, calc : calculated from eqn. 1.21)

	EE/EZ_{obs}	EE/EZ_{calc}	EZ/EE_{obs}	EZ/EE_{calc}	EE/ZZ_{obs}	EE/ZZ[a]
cis-**44**	2.0±0.4	2.2±0.4	-	-		-
trans-**44**	-	-	2.2±0.3	1.4±0.2	3.7±0.7	4.3±0.4
cis-**45**	4.1±0.3	3.7±0.4	-	-	-	-
trans-**45**	-	-	3.5±0.4	2.6±0.4	9.2±1.8	8.6±0.8
cis-**46**	5.6±0.9	3.7±0.8	-	-	-	-
trans-**46**	-	-	4.8±0.8	5.6±1.1	-	-

a. EE/ZZ ratio formed from irradiation of the EZ isomer.

In further support of this mechanism, two independent studies showed that initial disrotatory motion, and thus Woodward-Hoffmann based reactivity, is important in the photochemical ring-opening. Mathies and coworkers demonstrated with UV-resonance Raman spectroscopy that at the onset of the reaction (within 15 fs), carbons 3 and 4 of cyclobutene (**1**) undergo disrotatory twisting prior to bond cleavage.[51]

In addition, Leigh and Postigo determined the quantum yields for ring-opening (Φ_{RO}) of a series of monocyclic cyclobutenes which were increasingly substituted at C3 and C4 (Fig. 1.6). A pattern in the Φ_{RO} values revealed that

steric effects and buttressing at the C3 and C4 positions were influential on the efficiency of the reaction (eqn. 1.22).[35] Essentially, the quantum yield for ring-opening decreases as the syn methyl substitution, and the steric interaction involved with initial rotation of the methylene groups, increases. The maximum quantum yield for ring-opening occurs when the methyl groups are trans to one another and the amount of interaction from either mode of disrotatory motion is the least. Notice that the Φ_{RO} of *cis*-**18** is considerably lower than that of the trans.

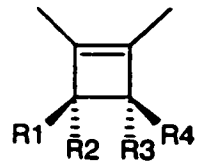

50 : R1=R2=R3=R4 = H
51 : R1 = CH_3
cis-**18** : R1=R4 = CH_3
trans-**18** : R1=R3 = CH_3
20 : R1=R2=R3 CH_3
22 : R1=R2=R3=R4 = CH_3

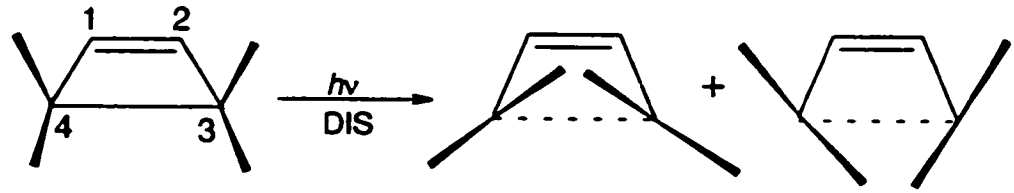

[1.22]

Figure 1.6. The total ring-opening quantum yields for 214-nm irradiation of **50**,**51**,**18**, **20**, and **22**, as a function of methyl substitution.[35]

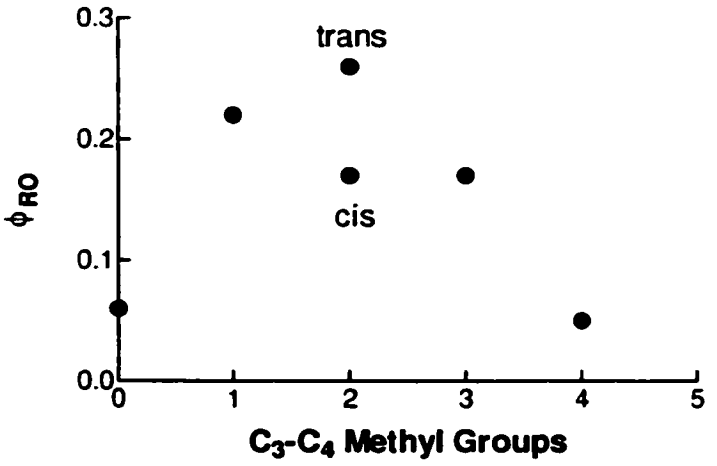

All of these studies support a ring-opening mechanism which initially obeys the Woodward-Hoffmann rules to form the formally-allowed diene in the excited state. From this excited state, the mixture of dienes is produced by *E,Z*-isomerization as the diene relaxes to the ground state.

1.3.6. Theoretical Investigations of the Photochemical Interconversions of Cyclobutenes and Butadienes

Early theoretical work on the photochemical cyclobutene-diene interconversions attempted to depict the true ground state, and excited state, reaction pathways in the context of a symmetry controlled reaction. Van der Lugt

and Oosterhoff established the potential energy surfaces of the 2^1A_g, ^1B_u, and ^1A_g states using simple valence bond calculations.[52] The results were later confirmed at a higher level of theory (SCF *ab initio* calculations) by Grimbert, Segal and Devaquet.[53] Figure 1.7. shows an example of the resulting reaction coordinate diagram.

Figure 1.7. A depiction of the calculated reaction coordinate diagrams for the interconversions of cyclobutene and butadiene.

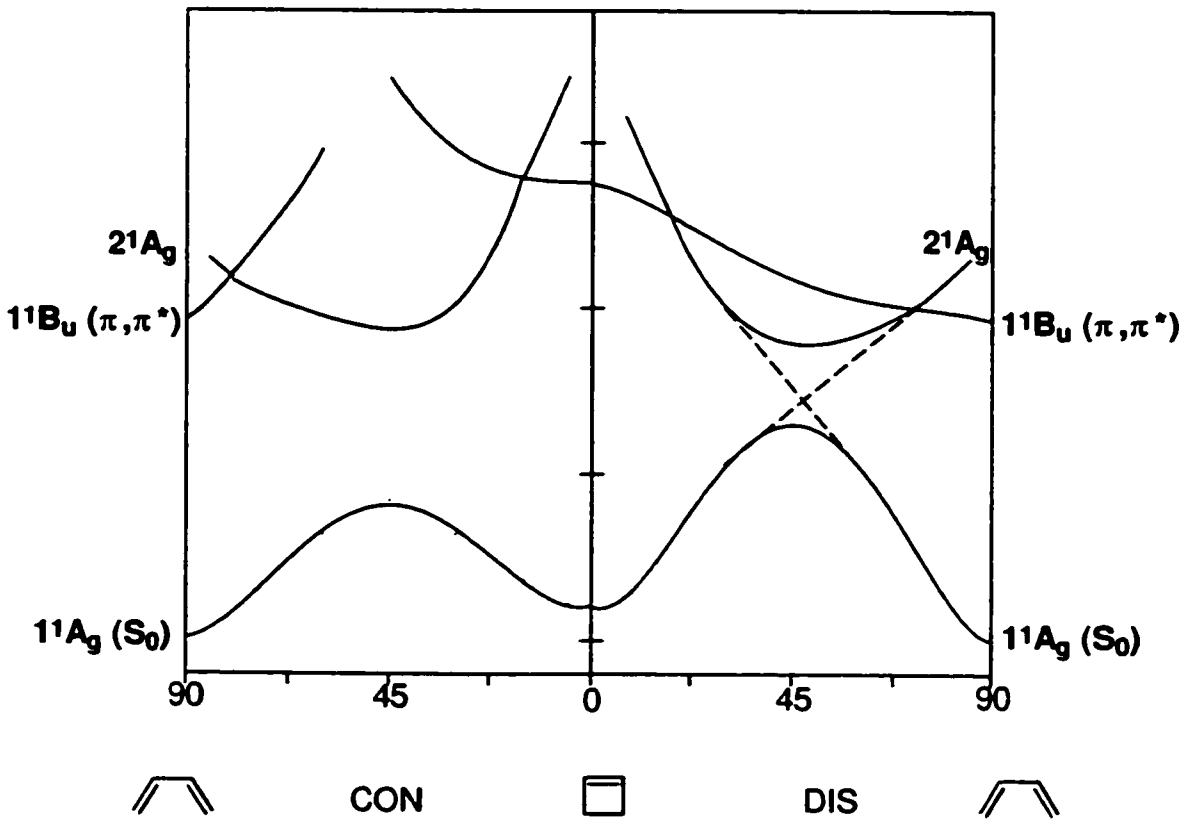

It was proposed that following excitation of butadiene to the S_1, the disrotatory path immediately crosses to the 2A excited state potential energy surface.[52,53] Approximately half-way between the cyclobutene and diene along the reaction coordinate, the excited species arrives at a symmetry-imposed avoided crossing to the ground state (indicated by the dashed lines in Figure 1.7). After internal conversion from the energy well, the reaction can then either proceed to the product cyclobutene or back to the starting diene. The large energy gap associated with the avoided crossing suggests that the excited molecule possesses a finite lifetime as it comes to rest in the energy well.

1.3.6.a. The Conical Intersection Model for the Photochemistry of Butadiene

As theoretical methods improved, Michael Robb, Massimo Olivucci, Fernando Bernardi and others, began modeling the excited state potential energy surfaces of photochemical reactions, and took interest in the cyclobutene-1,3-diene interconversions. This group has been instrumental in promoting the importance of conical intersections in organic photochemistry. There is now a considerable amount of literature which suggests that with polyatomic molecules, symmetry restrictions become less important and states of the same symmetry can cross.[54-58] In the vicinity of this crossing the two energy surfaces have the shape of a double cone, or funnel, leading to the use of the term conical intersection. The concept of a conical intersection between

electronic states is not new however, and was initially proposed independently by Michl[59] and Zimmerman[60] as early as 1966. In contrast to the avoided crossing model, a conical intersection is not associated with an energy well and the excited molecule can simply approach the funnel and pass directly through the intersection point between the two surfaces (radiationless decay) (Fig. 1.8). Accordingly, if the excited state pathway to the funnel is relatively free of barriers, the excited molecule will have a very short lifetime, likely on the order of a few bond vibrations.[61] In agreement with this, the lifetime of the excited state in the interconversion of cyclohexadiene to hexatriene has been established to be between 10-15 fs.[62,63] Indeed, a large number of photochemical reactions have been predicted via calculations to proceed via a conical intersection (CI).[54-56,64,65]

Figure 1.8. A three dimensional representation of a conical intersection between the S_1 and S_0 energy surfaces of a generic compound.

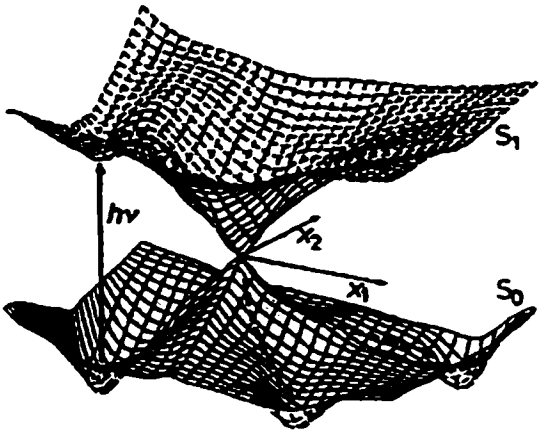

Olivucci and coworkers have thus provided theoretical evidence that all of the 1,3-diene photochemical reactions are initiated on the S_1 surface and are dependent on conical intersections.[54,57,58,66,67] Furthermore, all of the photoproducts from excitation of butadiene can be accounted for on the same excited state potential energy surface (PES) in which there exist multiple conical intersections differing only slightly in geometry.[66,67]

The reaction path begins in similar fashion to the avoided crossing model, with excitation of *s-cis*-butadiene populating the 1B state. The excited butadiene then crosses to the low lying 2A state through the first conical intersection (surface crossing) encountered in the reaction. On the 2A state surface, in a region where asynchronous, disrotatory rotation of the termini occurs along the s-cis/s-trans conformerization pathway, there lie three conical intersections with the ground state (termed s-cisoid, central and s-transoid). The butadiene at these points is tetraradicaloid in structure with all of the double bonds broken, and the terminal methylene groups rotated and twisted. (**52**) The stereochemistry of the ring-closure reaction (and ultimately cyclobutene formation) is induced due to the increased energy barrier to conrotatory rotation (+2 kcal/mol) of the termini on the excited state potential energy surface.[66]

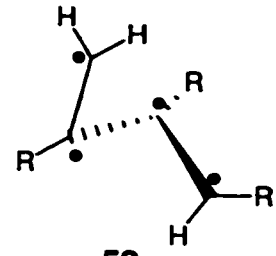

52

The product distribution obtained depends on a number of factors which include the geometry of the diene at the CI, the trajectory of the approach to the CI, and the topography of the ground state PES.[55,56,66] For instance, if the excited molecule has followed a pathway associated with twisting about the termini, isomerization will occur; if it is undergoing rotation about the central bond, conformer interconversion or ring-closure will occur. The s-transoid CI favours the former and the s-cisoid favours the latter.[66,67] Figure 1.9 shows a two-dimensional representation of this reaction through one of the conical intersections.

Figure 1.9. A two-dimensional reaction coordinate diagram for 1,3-butadiene depicting one conical intersection (CI) between the excited and ground states, and the resulting reactivity.

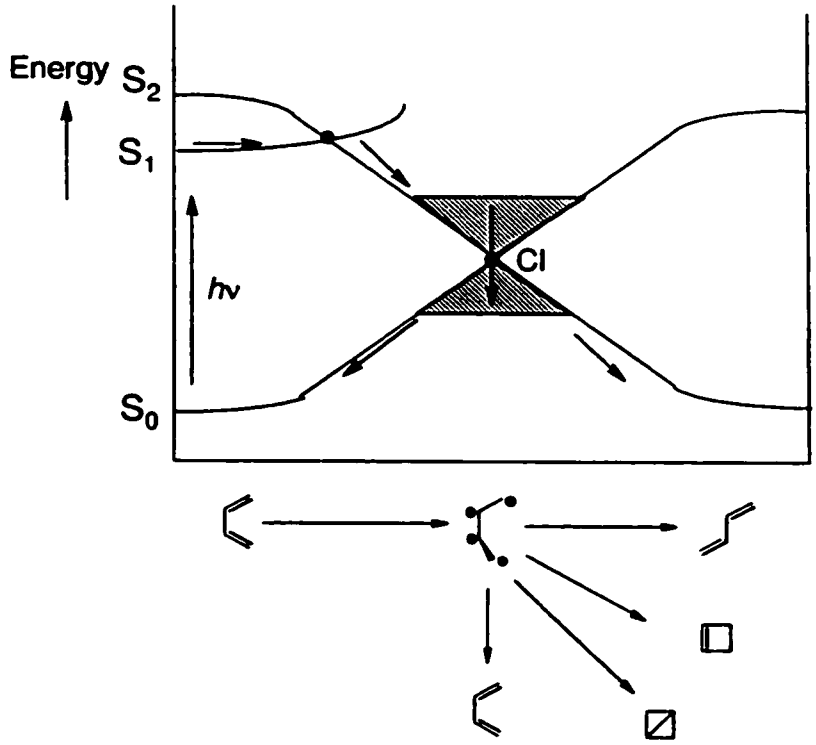

This mechanism is in agreement with a number of experimental observations. Squillacote and coworkers have shown that the s-*cis* conformer of **53** undergoes ring-closure and conformer interconversion in a ratio of 5:1 in addition to *E,Z*-isomerization. However, the s-*trans* conformer does not cyclize, and only undergoes conformer interconversion and *E,Z*-isomerization. Furthermore, the two conformers show much different propensities towards *E,Z*-

isomerization (eqn. 1.23).[68] In this case, the s-*cis* conformer likely approaches the cisoid CI and favours ring-closure where the products of the s-*trans* conformer are indicative of the transoid CI.[66,67]

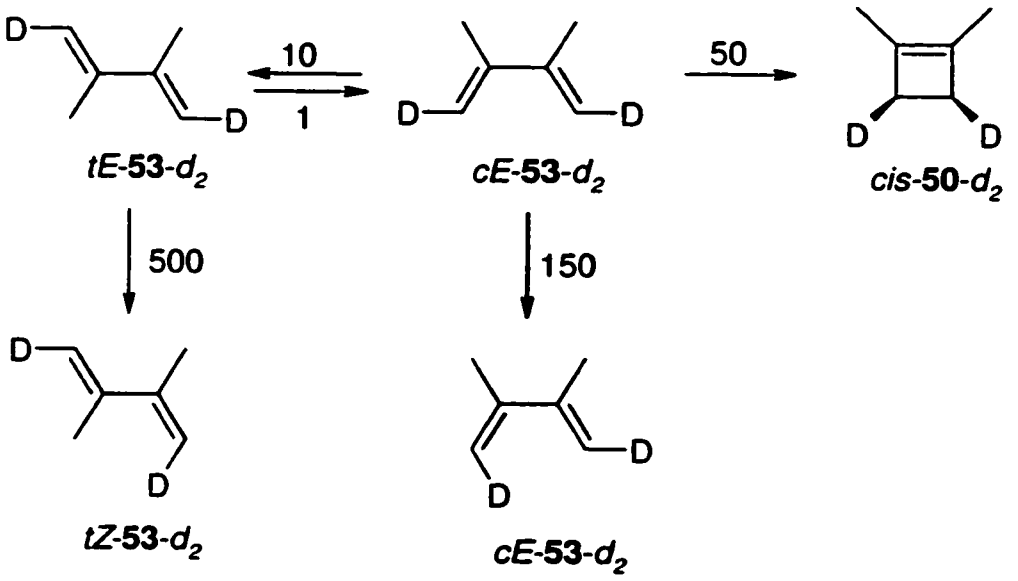

[1.23]

Leigh and Postigo demonstrated that even the most facile reaction of dienes, *E,Z*-isomerization, is affected by the degree of mobility of the central bond of the diene,[69] an important feature of the conical intersection model. Table 1.4 gives the isomerization quantum yields for **47**, **54**, and **55** at 254-nm. Note that the derivative which has the most strain in the central bond, **55**, has markedly decreased quantum yields in comparison to the other two.

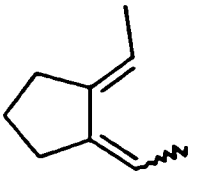

47

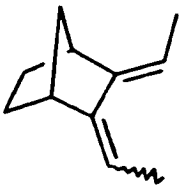

54

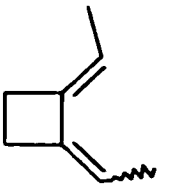

55

Table 1.4. Quantum yields for *E,Z*-isomerization of dienes **47**, **54**, and **55** at 254-nm in pentane.[70]

Diene	$\Phi_{EE\text{-}EZ}$	$\Phi_{EZ\text{-}EE}$	$\Phi_{EZ\text{-}ZZ}$
47	0.24±0.02	0.39±0.04	0.09±0.01
54	0.30±0.03	0.28±0.03	0.06±0.01
55	0.12±0.02	0.11±0.03	0.011±0.005

1.3.6.b. The Conical Intersection Model for the Photochemical Ring-Opening of Cyclobutenes

As a computational study of the photochemical ring-opening of cyclobutenes, Olivucci and coworkers modeled the reaction path of 1-methylbicyclo[4.2.0]octene (**56**).[71] They found three separate conical intersections leading to products (CI1, CI2, and CI3). Each CI structure is of almost equal energy and possesses tetraradicaloid character where both double bonds are broken and the central bond is twisted, much like that described in the

diene conical intersection model (**52**). The initial stage of the reaction involves rotation about the double bond, essentially inducing ring-opening, as the conical intersection region is approached. In the second phase of the reaction, each CI structure leads to three diene isomers by disrotatory (D) or conrotatory (C) rotation about the methylene termini. The pathways leading to products can be assigned within this terminology as C_+, C_-, D_+, or D_-, depending on the direction of the rotation from the CI geometry. An example of the reaction proceeding through CI1 is given in equation 1.24. This representation seems to suggest that the stereochemistry of the ring-opening reaction is determined randomly, and depends only on the conical intersection that is encountered in a particular system.

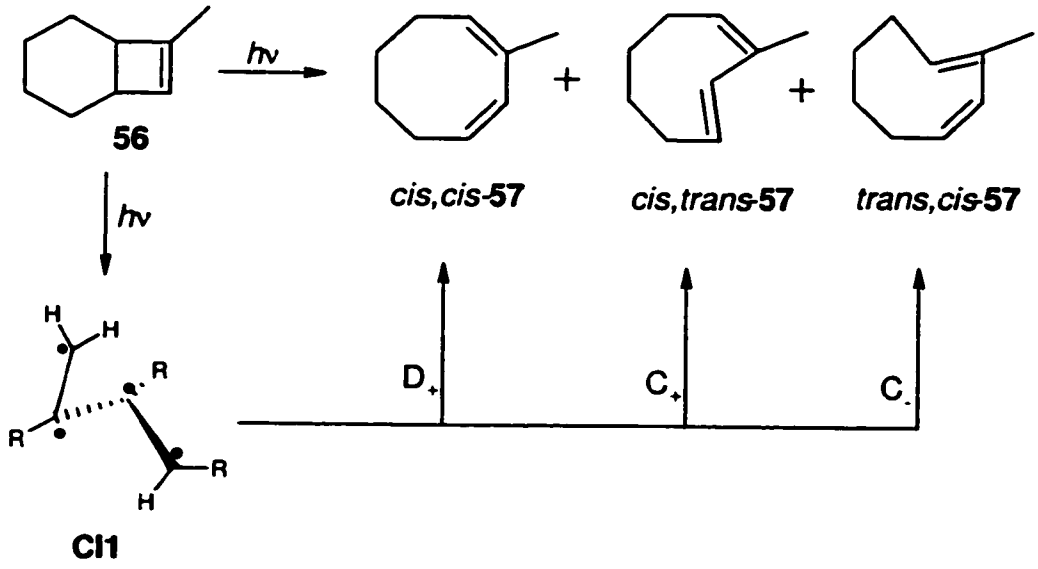

[1.24]

It is beneficial to draw connections between the ring-opening mechanism proposed by Leigh[16,20,50] and the theoretically-derived conical intersection models. Both mechanisms suggest that the ring-opening proceeds via a diene intermediate with excited state character. However, the similarities end there. The results of Leigh and coworkers suggest that the initial product of the ring-opening is the excited s-*cis* diene. In terms of a conical intersection model then, the reaction must proceed directly to the cisoid region of the excited PES and then pass through an intersection point. Whether or not this is the exact route is still uncertain. Unfortunately, much of the recent efforts of studying excited state potential energy surfaces by computational methods have been dedicated to the photochemistry of higher polyenes i.e. hexatriene,[72-76] octatetraene,[77] retinal analogs,[78-80] and carotene analogs[81], and interest in the simple moieties has diminished.

1.4. Cycloreversion of Alkylcyclobutenes & the π,R(3s) State

1.4.1. The Rydberg State Chemistry of Alkenes

Excitation to a Rydberg state results in promotion of an electron in a valence molecular orbital to an unoccupied atomic orbital. This leaves the core of the molecule electron deficient and the single electron in a spatially diffuse

region. Accordingly, the Rydberg states of alkenes have been commonly depicted as having radical cation character (eqn. 1.25).[3,12,13,82-84]

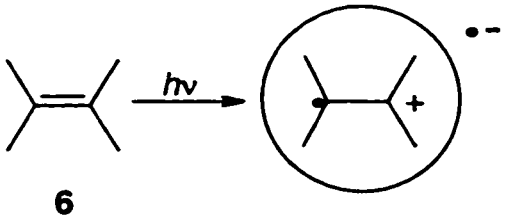

6

[1.25]

The electron-deficient character of alkene Rydberg states has been demonstrated by the excitation of various alkenes in nucleophilic solvents.[84-86] For example, irradiation of 2,3-dimethyl-2-butene (**6**) and 1,2-diemethylcyclopentene (**60**) in methanol results in addition of the alcohol and products of free radical disproportionation (eqns. 1.26 and 1.27).

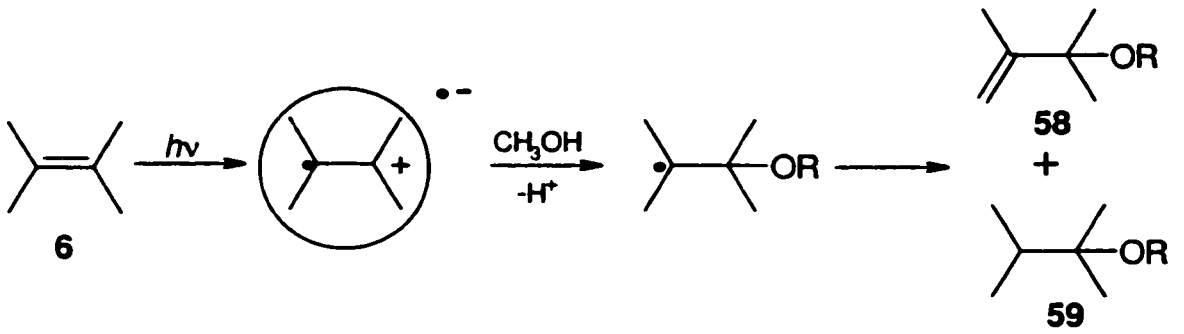

6 58 59

[1.26]

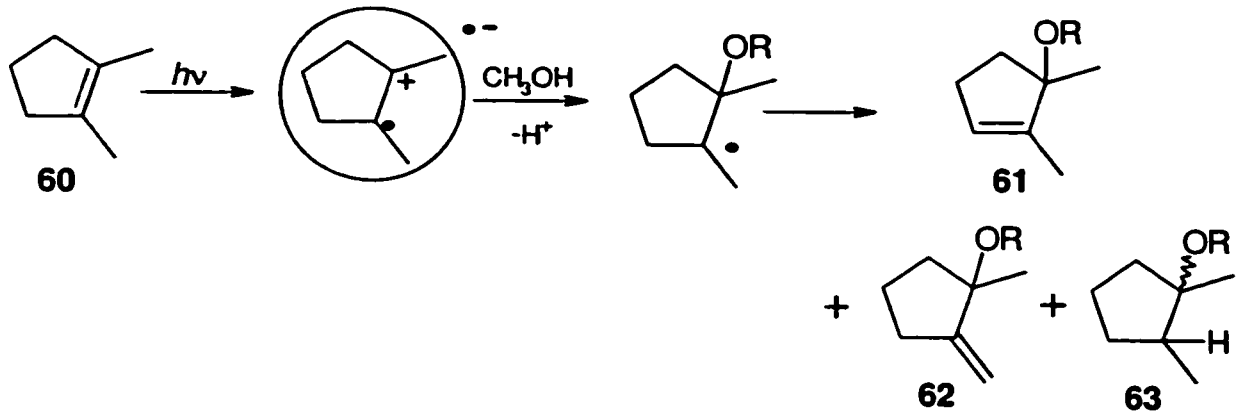

[1.27]

In non-nucleophilic solvents, alkenes with low-lying Rydberg states undergo 1,2-carbon or hydrogen migrations to give carbene intermediates.[2,3,82,83,87,88] This is viewed as being analogous to the Wagner-Meervein rearrangement of carbocations. For instance, excitation of **6** in the absence of nucleophiles gives two rearrangement products, **65** and **66**, which are derived from the carbene intermediate, **64**, formed by a 1,2-methyl shift (eqn. 128).[82] Similarly, irradiation of cyclopentene (**30**) produces methylenecyclobutane (**68**) and bicyclo[2.1.0]pentane (**69**) which are believed to be the products of hydrogen migration and C-H insertion in the cyclobutyl carbene **67** (eqn. 1.29).[87]

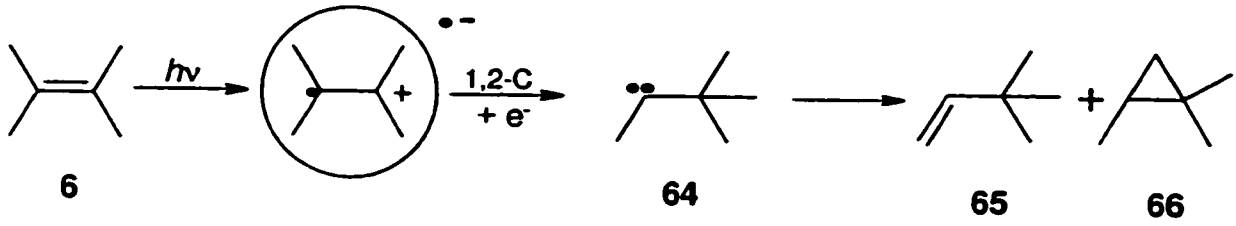

6 64 65 66

[1.28]

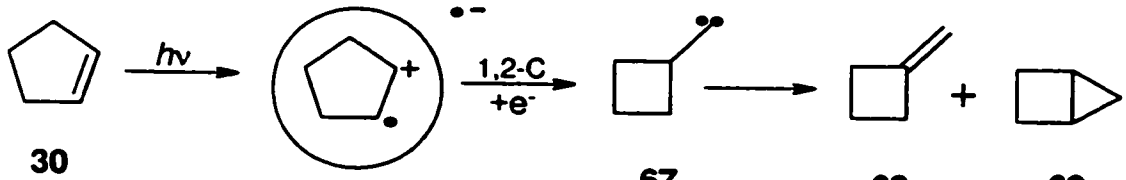

30 67 68 69

[1.29]

1.4.2. The Rydberg State Chemistry of Cyclobutenes

The contribution of the Rydberg excited state to the photochemistry of alkylcyclobutenes has been thought to be limited to the cycloreversion process. It was proposed that this rearrangement proceeds via a carbene intermediate[14,15,89,90] on the basis that the unsymmetrical 1-methylcyclobutenes **70** and **71** interconvert upon photolysis in solution (eqn. 1.30).[89]

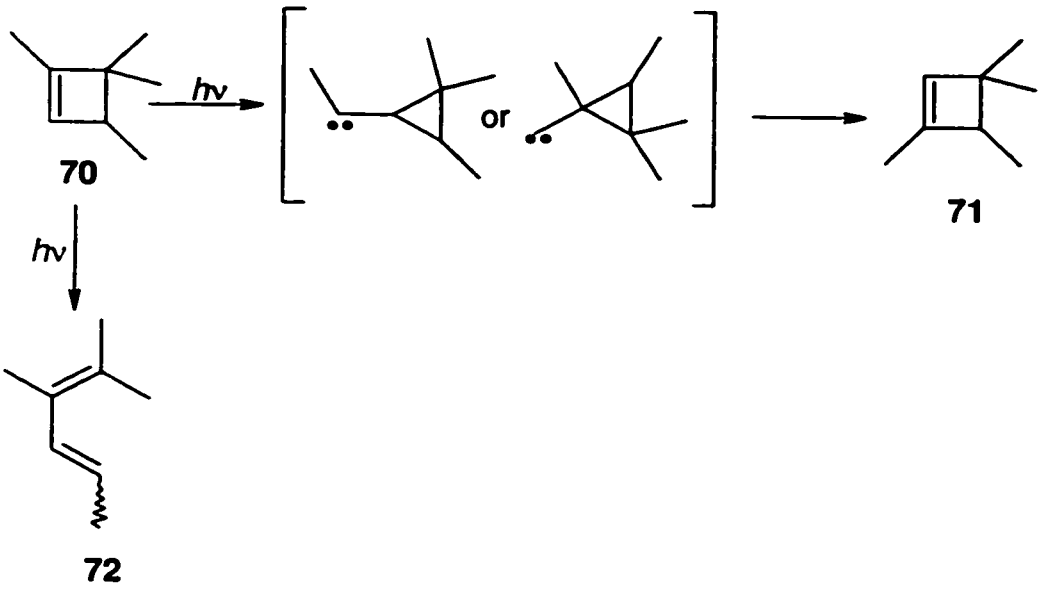

[1.30]

A combined spectroscopic and photochemical study of 1-substituted bicyclooctenes **16**, **56**, and **73** also supports the association of cycloreversion with the Rydberg state.[15] Two different substituents were chosen for their ability to systematically stabilize (-CH_3) or destabilize (-CF_3) the Rydberg state of bicyclo[4.2.0]oct-7-ene (**56**). The gas phase UV spectra of these three compounds verify the proposed substituent effect on the π,R(3s) state energies, and it was found that the quantum yield for cycloreversion of **73** at 193-nm is reduced by a factor of 4 relative to the other derivatives. The quantum yield for ring-opening of this derivative is over three times higher than that of the methyl substituted cyclobutene (Table 1.5).

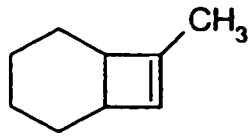

56

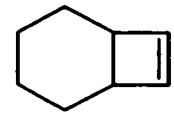

16

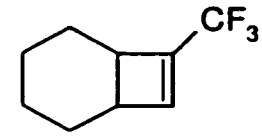

73

Table 1.5. Quantum yields for ring-opening (RO) and cycloreversion (CR) for the 193-nm irradiation of substituted bicyclooctenes, **56**, **16**, and **73**, in pentane.[15]

Cyclobutene	Φ_{RO}	Φ_{CR}
56	0.087	0.13
16	0.175	0.14
73	0.292	0.03

As the π,R(3s) state is destabilized, the yield of cycloreversion products is dramatically decreased and that of ring-opening increases. These observations are consistent with the idea that the Rydberg state is primarily responsible for the cycloreversion process, while the valence π,π^* state is primarily responsible for ring-opening.

1.5. Objectives

In summary, there is now considerable experimental evidence in place to support a ring-opening mechanism in which initial disrotation yields the symmetry-allowed product in the first excited singlet state.[16,35,50] The reaction products are then derived from relaxation of the excited diene, via *E,Z*-isomerization.

However, it is clear that there is substantial overlap between the π,π^* and Rydberg π,R(3s) in the far UV. Irradiations in this region undoubtedly result in population of both states.[14,17] It is therefore difficult to be absolutely confident in the conclusions regarding the reactivity, or lack thereof, of either state when assessing the photochemistry of cyclobutenes at 193- or 214-nm. Due to this uncertainty, a clear and unambiguous assessment of the contribution from the Rydberg state is imperative to a *full understanding* of cyclobutene photochemistry. In addition, it is also essential to any confident interpretations of either the ring-opening or cycloreversion mechanisms.

Therefore, the objective of this research was to investigate the photochemistry of a variety of alkylcyclobutenes using monochromatic 228-nm light, conditions under which population of *the Rydberg excited state alone* should be possible. By obtaining a better understanding of the photochemistry of the π,R(3s) state it was proposed that a better understanding of the π,π^* state would follow. This understanding can be achieved by not only demonstrating the

reactions which are characteristic of the Rydberg state but by also elucidating the mechanism by which they occur. The ultimate goal of this research was to firmly establish the mechanism for the photochemical ring-opening of cyclobutenes.

Chapter 2

The Photochemistry of Simple Cyclobutenes at 228-nm

2.1. Introduction

The known, pertinent differences between the valence π,π^* and Rydberg π,R(3s) excited states of cyclobutenes have been outlined in Chapter 1. With 1,2-dialkylcyclobutenes, the π,π^* absorption is observed at shorter wavelengths (*ca.* 190-nm to 210-nm)[14,15] and this valence excited state is thought to be primarily responsible for electrocyclic ring-opening.[4,14,15] The Rydberg state transitions are observed between 205-nm and 230-nm[14,15] and this state is believed to react via a carbene intermediate to form products of formal cycloreversion.[14,15,89] Since the Rydberg state of alkenes is susceptible to reaction with nucleophiles, methanol can be used as a solvent to effectively decrease its lifetime and thus limit the formation of its photoproducts. The initial goal of this research was to obtain a *direct* comparison of the reactivity of the two excited states. Three simple monocyclic cyclobutenes were irradiated at 193-, 214-, and 228-nm in both the gas phase and solution to allow this comparison.

2.2. Results

2.2.1. Preparation of the Cyclobutenes and their Photoproducts

1,2-Dimethylcyclobutene (**50**) was prepared by direct irradiation of 2,3-dimethyl-1,3-butadiene (**53**) (eqn. 2.1).[35] Purification was accomplished with semi-preparative gas chromatography.

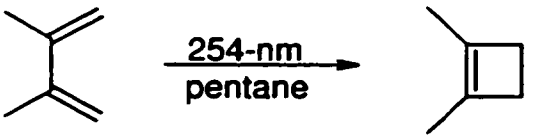

53 **50**

[2.1]

cis- and trans-1,2,3,4-Tetramethylcyclobutene (**18**) were prepared by the synthetic scheme[14,35] shown in equation 2.2. This route required the photosensitized 2+2 addition of 2-butene (as a mixture of isomers) (**29**) to 1,2-dimethylmaleic anhydride (**74**), followed by lead(IV)tetraacetate oxidation of **75**.[35,91] Separation and purification of the two isomers of **18** were accomplished using semi-preparative gas chromatography.

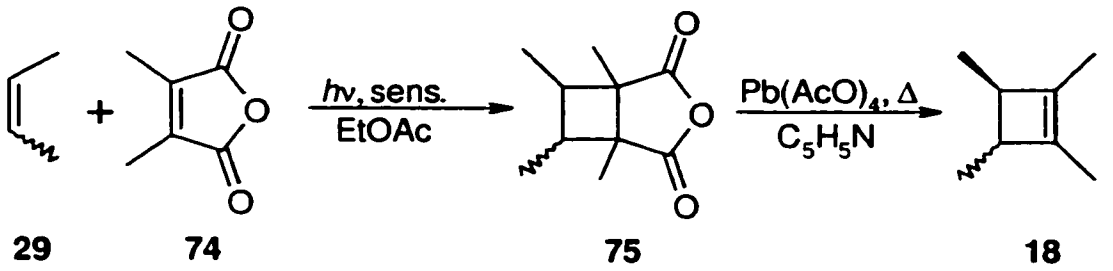

[2.2]

The E,E and E,Z diene isomers (**19**) of *cis*- and *trans*-**18** were also prepared by a known method, involving a reductive coupling reaction followed by dehydration (eqn. 2.3).[92] The Z,Z isomer was prepared by triplet sensitized irradiation of *E,Z*-**19**.[14] The three diene isomers were separated and purified using semi-preparative gas chromatography.

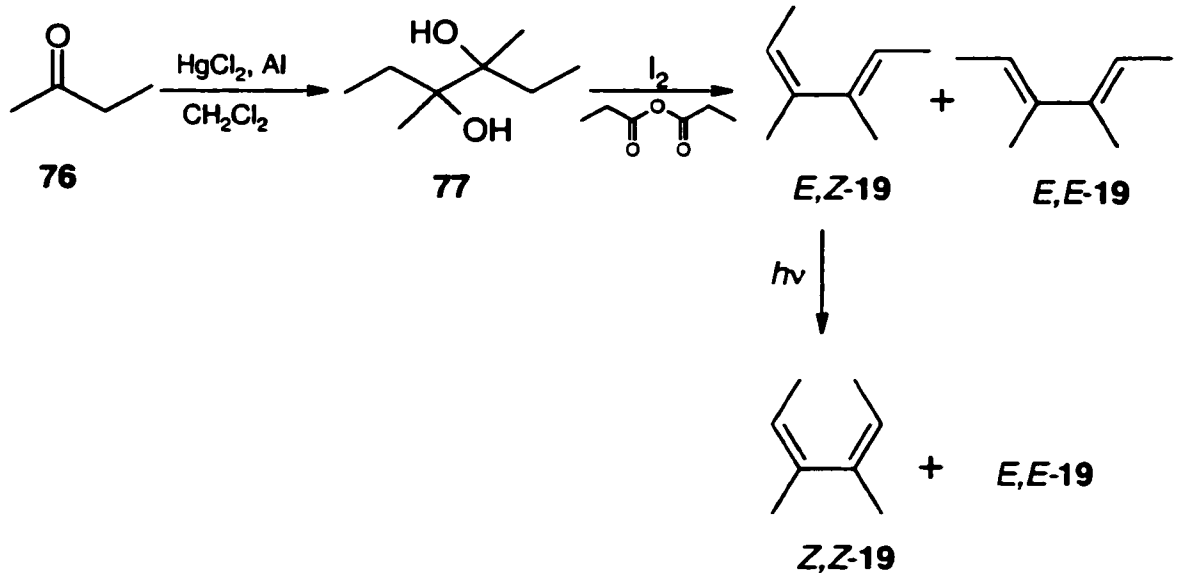

[2.3]

2.2.2. UV Absorption Spectra of 1,2-Dimethylcyclobutene (**50**) and *cis*- & *trans*-Tetramethylcyclobutene (**18**)

The UV absorption spectrum of **50** was obtained in both hexane solution (*ca.* 0.01 M) and in the gas phase (1 atm) with SF_6 as a buffer gas. The gas phase UV absorption spectra of *cis*- and *trans*-**18** were also obtained at atmospheric pressure with SF_6 as a buffer gas. The spectra of the three derivatives are shown in Figure 2.1. The most intense band (190- to 200-nm) is assignable to the π,π^* transition, where the weaker Rydberg absorption bands are observed at 210- to 230-nm for **50**, and between 200- to 230-nm for *cis*- and *trans*-**18**.[11] In all three cases, the Rydberg bands exhibit similar fine structure.

Figure 2.1. UV absorption spectra of a) 1,2-dimethylcyclobutene (**50**) in the gas phase (200 torr) (solid line) and in pentane solution (dashed line), b) *cis*-1,2,3,4-tetramethylcyclobutene (*cis*-**18**), and c) *trans* -1,2,3,4-tetramethylcyclobutene (*trans*-**18**) in the gas phase (*ca.* 200 torr) in 1 cm Suprasil cells with SF_6 as a buffer gas (total pressure of 1 atm).

a)

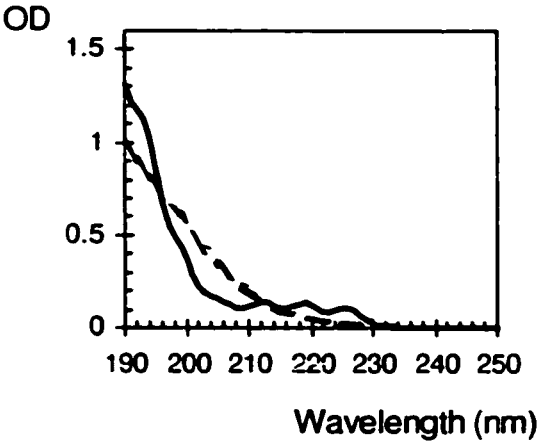

b)

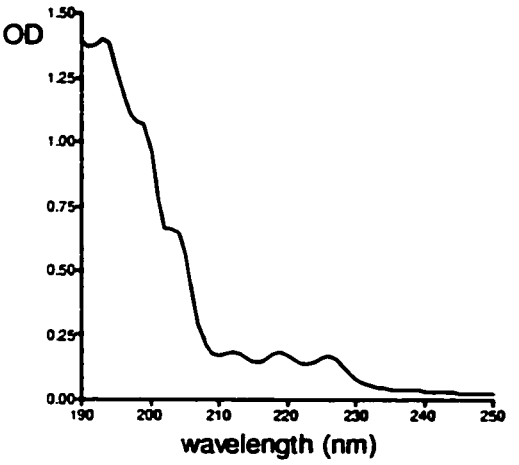

c)

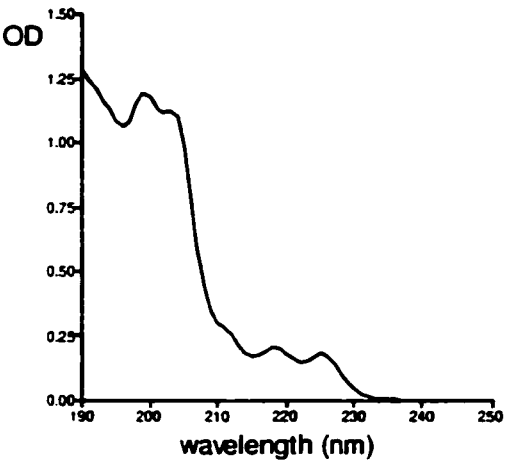

2.2.3. Irradiation of **50** and *cis*- and *trans*-**18** in the Gas Phase and in Hydrocarbon Solution

The direct irradiations of the cyclobutenes used either an unfocussed ArF excimer laser, a zinc resonance lamp, or a cadmium resonance lamp for 193-, 214-, or 228-nm excitation, respectively. Gas phase samples were composed of *ca.* 200 torr of the cyclobutene and 560 torr of SF_6. Solution samples were *ca.* 0.05 - 0.1 M in hexanes or isooctane (**50** only). Products of ring-opening (RO) (**53, 19**) and cycloreversion (CR) (**35, 29**) were observed in all experiments and identified by co-injection with authentic samples (eqn. 2.5). No other products were detected in yields greater than *ca.* 5% under the analytical conditions. Table 2.1 contains the yields of the major products as determined by triplicate GC analysis at the maximum conversion (*ca.* 8%). The FID response factors for the analytes were accounted for by the construction of calibration curves.

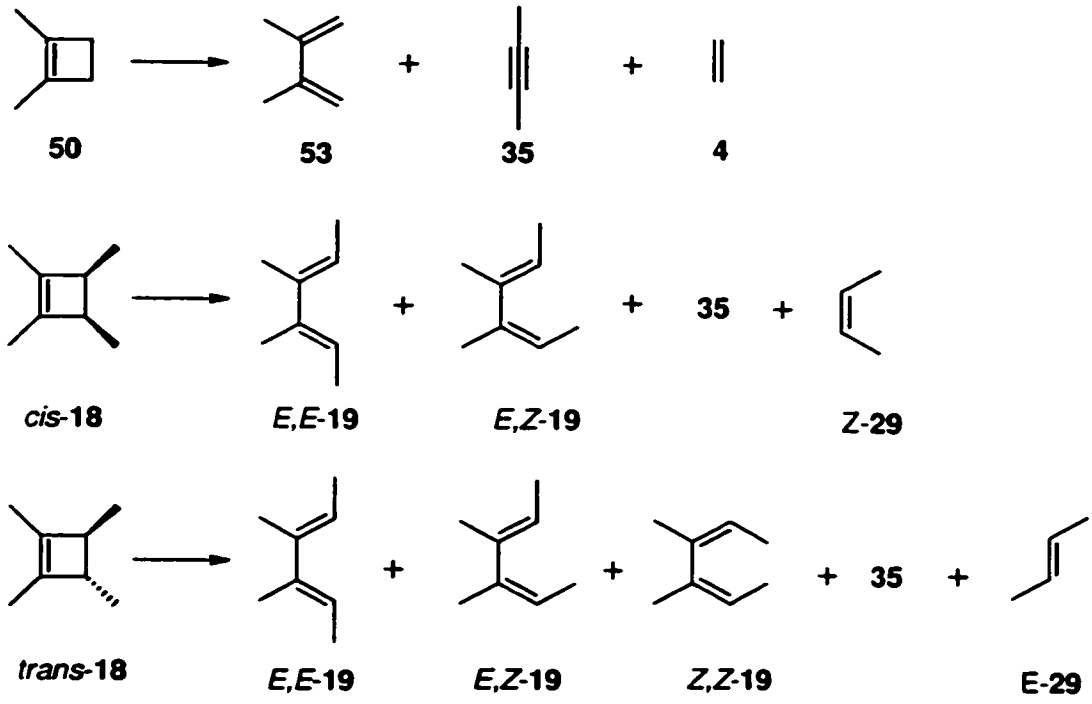

[2.5]

Table 2.1. Product yields from photolysis of **50** and *cis*- and *trans*-**18** in the gas phase (1 atm, SF_6) and as deoxygenated 0.05 M solutions in isooctane (**50**) or hexane (**18**) at 25 °C.[a]

Compound	λ_{ex} (nm)	Gas Phase				Hydrocarbon Solution			
		35 + 4	**53**			**35 + 4**	**53**		
50	193	28 ± 2	72 ± 5			40 ± 3	55 ± 4		
	214	31 ± 4	64 ± 4			50 ± 1	45 ± 3		
	228	32 ± 1	62 ± 3			56 ± 4	44 ± 4		
		35 + 29	***E,E*-19**	***E,Z*-19**	***Z,Z*-19**	**35 + 29**	***E,E*-19**	***E,Z*-19**	***Z,Z*-19**
cis-**18**	193	39 ± 2	20 ± 2	41 ± 2	<1	34 ± 2	40 ± 2	25 ± 2	<1
	214	50 ± 1	7.0 ± 0.5	42 ± 1	<1	48 ± 2	21 ± 2	31 ± 2	<1
	228	55 ± 3	<1	45 ± 2	<1	59 ± 7	<1	40 ± 2	<1
trans-**18**	193[b]	39 ± 1	41 ± 2	13 ± 2	7 ± 1	40 ± 1	21 ± 2	34 ± 2	4 ± 1
	214[b]	43 ± 2	38 ± 2	10 ± 2	9 ± 1	50 ± 2	14 ± 2	29 ± 2	7.5 ± 0.5
	228[b]	57 ± 3	22 ± 2	12 ± 2	8 ± 1	76 ± 4[c]	3 ± 1[c]	13 ± 2[c]	8 ± 2[c]

a. Based on triplicate determinations of relative product yields at maximum conversion. Solution phase irradiations employed 0.05-M solutions and were carried out to a maximum conversion of 5-8%, unless otherwise noted.
b. Maximum conversion 0.7-1.5%.
c. Concentration = 0.15 M.

The photolysates were also monitored by capillary gas chromatography as a function of irradiation time (or dose for those at 193-nm) to *ca.* 8% conversion. The slopes of concentration vs. time plots were linear up to about 5% conversion in most cases, although mild curvature was observed in some of the gas phase experiments and with *trans*-**18** in solution. These plots can be found in Appendix 1. The slight curvature in some of the plots suggests that secondary photolysis of the dienes occurs in these cases.

In order to accentuate any unobserved variations in the peak areas, the ring-opening to cycloreversion ratios (total yield of dienes relative to 2-butyne) and diene isomer ratios (i.e. *E,Z*-/*E,E*-**19** for *cis*-**18** and *E,E*-/*E,Z*-**19** plus *Z,Z*-/*E,Z*-**19** for *trans*-**18**) with 214-nm and 228-nm excitation, were plotted against percent conversion or irradiation time. These plots are shown in Figure 2.2 for *cis*-**18** and Figure 2.3 for *trans*-**18**. In each case (including that of **50**) the ring-opening to cycloreversion ratios (RO/CR) lines were constant over the conversion ranges monitored, suggesting that secondary irradiation has little effect on the total product yields. However, the plots of diene isomer ratios against conversion gave non-zero slopes in the irradiations of *cis*-**18** in the gas phase at 214-nm and *trans*-**18** at 228-nm in both the gas and solution phases. In one case (*trans*-**18**) the excitation at 228-nm in hexanes was repeated with a higher cyclobutene concentration (0.15 M), but the plots of relative diene isomer yields against conversion still had non-zero slopes.

Figure 2.2. Plots of product ratios vs percent conversion of the starting material for the irradiations of *cis*-**18** at 214-nm in 1 atm of SF_6 and in hexanes solution (0.05 M) (□: RO/CR, ● : *E,Z*-/*E,E*-**19**).

a) gas phase at 214-nm

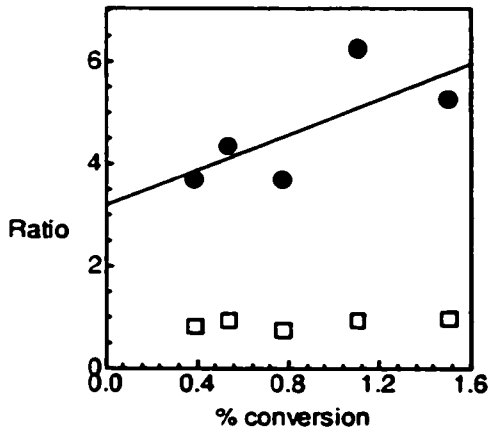

b) in hexanes at 214-nm

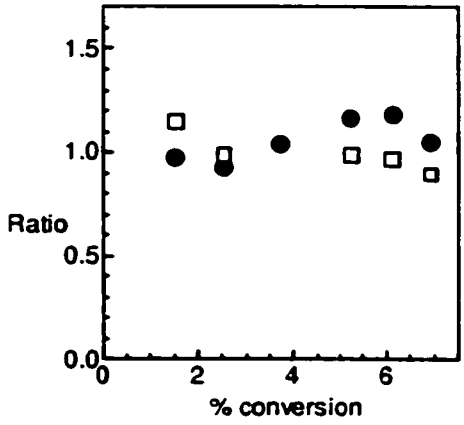

Figure 2.3. Plots of product ratios vs. percent conversion of the starting material for the irradiations of *trans*-**18** at 214-nm and 228-nm in 1 atm of SF_6 and in hexane solution (0.05 M).

a) 214-nm in SF_6 (open) and hexanes (filled). (● : *E,E*-/*E,Z*-**19**, ◆ : RO/CR)

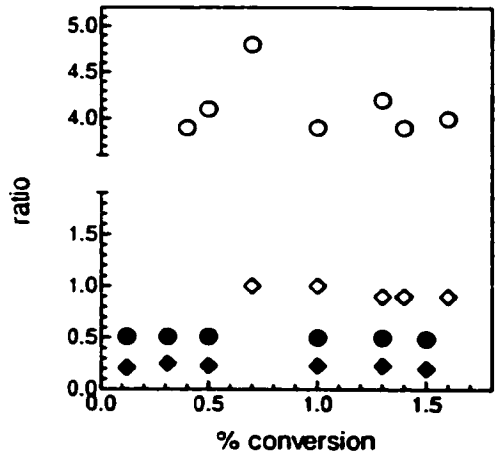

b) in SF_6 at 228-nm (○ : *E,E*/*E,Z*-**19**, ◊ : *Z,Z*/*E,Z*-**19**)

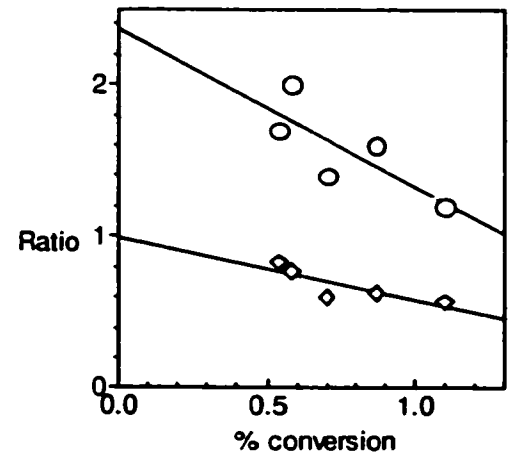

c) in hexanes (0.05 M) at 228-nm (● : *E,E*/*E,Z*-**19**, ◆ : *Z,Z*/*E,Z*-**19**)

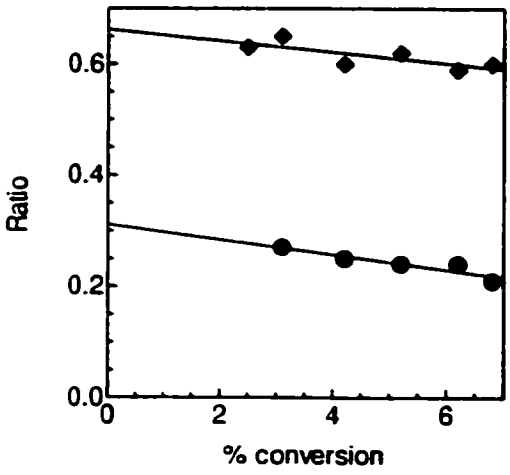

d) in hexanes (0.15 M) at 228-nm (● : *E,E*/*E,Z*-**19**, ◆ : *Z,Z*/*E,Z*-**19**)

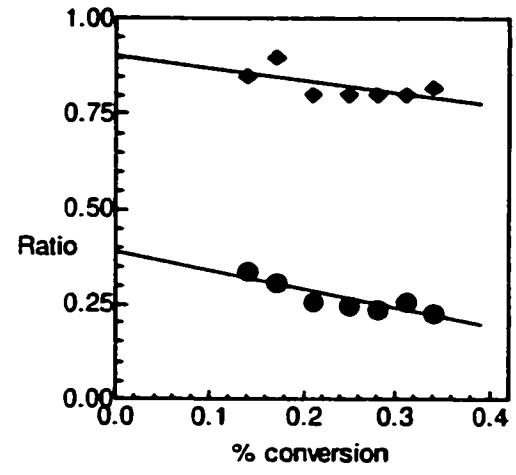

The relative diene isomer yields were taken as either the relative slopes from the concentration vs. time plots, or from the y-intercepts of the isomer ratio plots when the slopes of the former deviated significantly from zero. Tables 2.2 and 2.3 list the results of these photochemical experiments in the gas phase and in hydrocarbon solution, respectively. The data are summarized in the form of ring-opening / cycloreversion ratios (RO/CR), diene isomer ratios, and conrotatory / disrotatory ring-opening product ratios (CON/DIS; [*E,Z*-**19**] / [*E,E*-**19** + *Z,Z*-**19**] for *cis*-**18** and the inverse for *trans*-**18**).

The photostationary state of the 3,4-dimethyl-2,4-hexadienes (**19**) at 228-nm was determined in the gas phase and in solution. The ratios were determined by exhaustive photolysis of samples of *E,E*- and *E,Z*-**19**. These values are also included in Tables 2.2 and 2.3.

Table 2.2. Ring-opening/cycloreversion ratios (**53(19)/35(4)**) and isomeric diene distributions from the photolysis of **50** and **18** with 193-, 214- and 228-nm light in the gas phase (1 atm SF_6).

Cyclobutene	λ_{ex} (nm)	**53(19) / 35(4)**	E,E:E,Z:Z,Z	CON/DIS[a]
50	193	3.0	-	-
	214	2.4	-	-
	228	2.0	-	-
cis-**18**	193	1.6	1 : 2 : 0	2.0
	214	0.90	1 : 3.3 : 0	3.3
	228	0.82	<1 : >20 : 0	> 20
trans-**18**	193	1.6	6 : 2 : 1	3.5
	214	1.6	4.3 : 1 : 1.1	5.4
	228	1.3	2.4 : 1 : 1	3.0
pss	228	-	1 : 7 : 2	-

a. CON/DIS represents the ratio of conrotatory to disrotatory ring-opening products

Table 2.3. Ring-opening/cycloreversion ratios (**53(19)/35(4)**) and isomeric diene distributions from the photolysis of **50** and **18** with 193-, 214- and 228-nm light as deoxygenated 0.05 M solutions in isooctane or hexanes[a].

Cyclobutene	λ_{ex} (nm)	**53(19) / 35(4)**	E,E:E,Z:Z,Z	CON/DIS[b]
50	193	1.3	-	-
	214	0.92	-	-
	228	0.79	-	-
cis-**18**	193	1.9	1.6 : 1 : 0	0.63
	214	1.1[c]	1.1 : 1.0 : 0	1.0
	228	0.69	<1 : >20 : 0	> 20
trans-**18**	193	1.5	5.2 : 8.5 : 1	0.74
	214	0.80	2.2 : 4.2 : 1	0.76
	228	0.25[c]	1 : 2.6 : 2.3	1.3
pss	228	-	1 : 7.1 : 4.4	-

a. Irradiations of **50** were carried out in isooctane where those of **18** were in carried out in hexanes.
b. CON/DIS represents the ratio of conrotatory to dirotatory ring-opening products

A control experiment was performed with the goal of estimating the degree at which secondary photolysis occurs, and the initial diene ratios in the

photolysis of *trans*-**18** at 228-nm in solution. Using a syringe pump, a 1:1 mixture of *E,E*-**19** and *Z,Z*-**19** was slowly added to a solution of **50** in hexanes (0.15 M), while irradiating the solution at 228-nm. The rate of addition was set up as roughly equal to that of diene formation in the actual irradiation of *trans*-**18**. Even at the initial stages of the experiment (below *ca.* 0.2% conversion), GC analysis showed that *E,Z*-**19** was formed. The diene isomer ratios for the control experiment were plotted against time and are superimposed with those from the original photolysis of *trans*-**18** in Figure 2.4.a. Figure 2.4.b shows a plot of total dienes ([*E,E*- + *E,Z*- + *Z,Z*-**19**]) vs. time for both the control and the actual irradiations. This confirms that the rate of diene addition was adequately matched to that of formation from *trans*-**18** in the initial experiment. The experiment was repeated with a control solution of higher E,E/Z,Z ratio (1.6:1) and the data were treated in similar fashion. In this case the plots of diene isomer ratios against time (Fig. 2.5.a) were found to be much different than both the actual excitation of *trans*-**18** and the initial control. The total dienes vs. time plot is shown in Figure 2.5.b.

Figure 2.4. Plots of a) isomeric diene ratios and b) total dienes in solution vs. time for the photolysis of *trans*-**18** in pentane solution and the control experiment using a 1:1 mixture of *E,E*-/*Z,Z*-**19** (EZ/EE : ■ , EZ/ZZ : ● , Filled : photolysis of *trans*-**18**, Empty : control experiment).

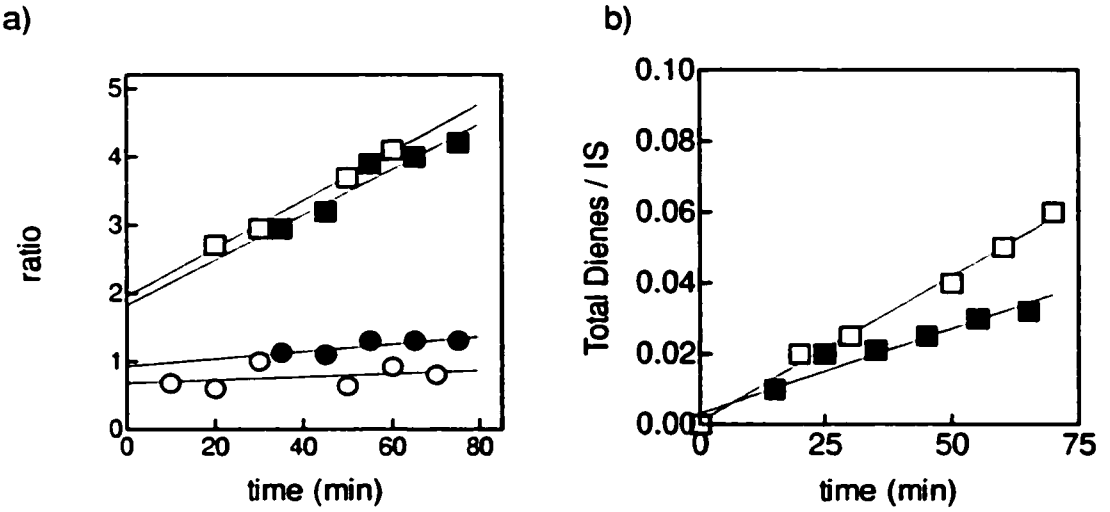

Figure 2.5. Plots of isomeric diene ratios (a) and total dienes in solution (b) vs. time for the photolysis of *trans*-**18** in pentane solution and the control experiment using a 1.6:1 mixture of *E,E*-/*Z,Z*-**19** (EZ/EE : ■ , EZ/ZZ : ● , filled : photolysis of *trans*-**18**, empty : control experiment).

a) b)

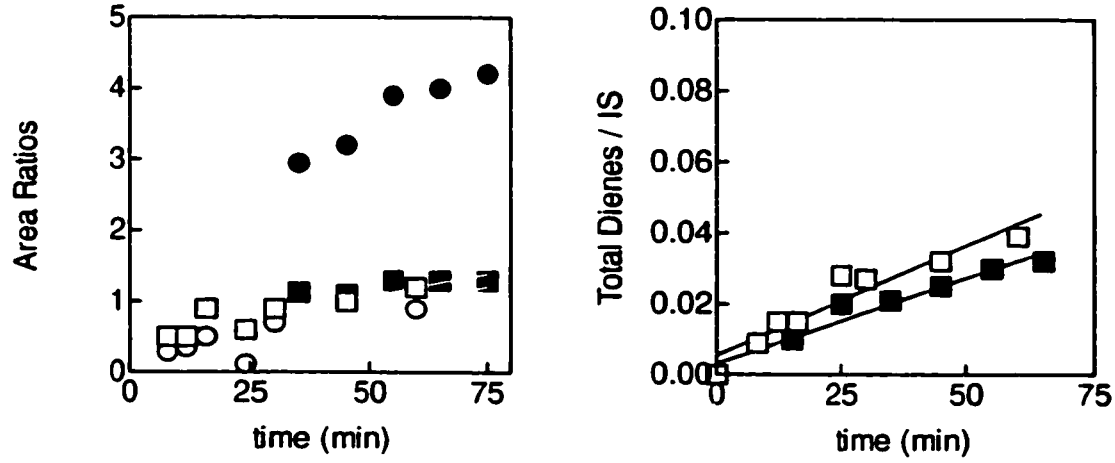

2.2.4. Irradiation of 1,2-Dimethylcyclobutene (**50**) in Methanol

1,2-Dimethylcyclobutene (**50**) was irradiated as a deoxygenated 0.05-M solution in methanol with both the 228-nm and 214-nm light sources. Three new products were observed by gas chromatography in addition to those of ring-opening and cycloreversion (eqn. 2.6, Table 2.4). The formation of 2-butyne (**35**) was obscured by the elution of methanol, but was implied by the detection of ethylene (**4**). The new products had similar GC retention times so it was difficult

to isolate them or determine their exact yields. Each compound was isolated as a mixture with the other two by semi-preparative gas chromatography (60-70% purity). The three compounds were tentatively identified as methanol adducts **77**- **80** on the basis of their ^{1}H-nmr and GC-MS data, and comparison with reported data from similar experiments with 1,2-dimethylcyclopentene.[85] Table 2.5 provides the relevant diagnostic ^{1}H-nmr resonances for the 1,2-cyclobutene methanol adducts along with those for the 1,2-dimethylcyclopentene (**60**) methanol adducts.

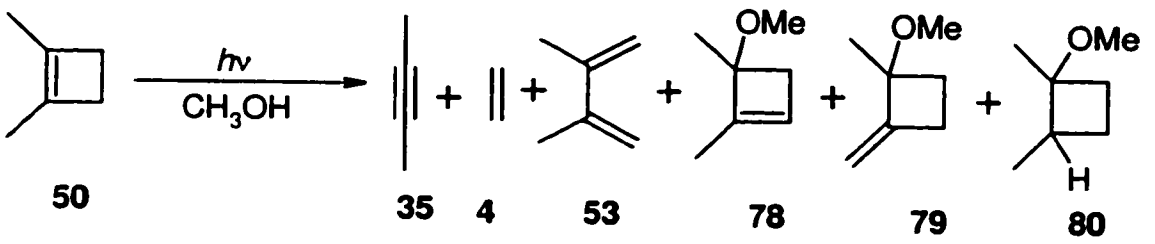

50 **35** **4** **53** **78** **79** **80**

[2.6]

Table 2.4. Product yields from the irradiation of **50** (0.05-M) in methanol at 214- and 228-nm.

λ_{exc}	**53**	**35+4**	**78**	**79**	**80**
214	36	20	14	17	13
228	12	7	25	28	25

Table 2.5. Diagnostic ^{1}H-nmr (200 MHz in $CDCl_3$) resonances of **78-80** compared to those of **61-63** (100 MHz in $CDCl_3$).[85]

Compound		δ (ppm), $-CH_3$	δ (ppm), $-OCH_3$	δ (ppm), =CHR
79	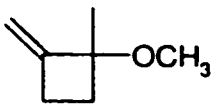	1.35	3.24	4.94
62	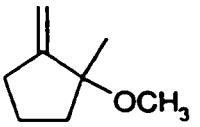	1.19	2.97	4.87
78	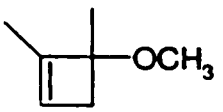	1.33	3.23	5.79
61	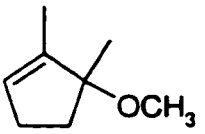	1.19	2.92	5.41
80	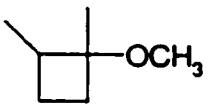	0.93 1.15	3.14	
63	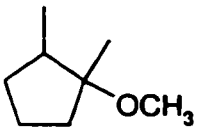	0.87 1.10	3.03	

2.3. Discussion

2.3.1. The Gas Phase UV Absorption Spectra of Alkylcyclobutenes

The UV spectrum of **50** in SF_6 (1atm) (Fig.2.1.a) shows the strong π,π^* absorption from 190-nm to 210-nm which is common to all aliphatic alkenes.[8,9,11] At longer wavelengths (210-nm to 230-nm), a weaker set of absorptions is observed that is assigned to the Rydberg π,R(3s) transition. The vibronic spacings of this band are similar to those of the π,R(3s) Rydberg transitions in other alkenes (Table 2.6).[11] As expected, the intensities of these absorptions are significantly reduced in the solution phase spectrum. The same transitions are displayed in the uv spectrum of *cis*-**18** although it appears as though the π,π^* absorption is stronger and extends from *ca.* 190-nm to 210-nm (Fig.2.1.b). With the *trans*-**18** isomer this phenomenon is even more apparent as it appears there is a third set of bands between 195-nm and 210-nm which is superimposed on the valence π,π^* band (Fig.2.1.c). This is tentatively assigned to the Rydberg π,R(3p) progression. It is possible that this transition is also the source of the increased absorptivity at short wavelengths for *cis*-**18** where it may be slightly shifted to the blue. Table 2.6 summarizes the vibronic spacings of the Rydberg transitions for **50** and *cis*- and *trans*-**18**.

Table 2.6. Positions and spacings of the vibronic band structures in the gas phase UV spectra of **50** and **18** (Fig. 2.1).

Cyclobutene	π,R(3p)		π,R(3s)	
	Position	Spacing	Position	Spacing
50	-		212-nm	1500cm^{-1}
			219-nm	
			226-nm	
cis-**18**	194-nm	1200cm^{-1}	212-nm	1500cm^{-1}
	199-nm		219-nm	
	203-nm		226-nm	
trans-**18**	199-nm	1200cm^{-1}	211-nm	1500cm^{-1}
	204-nm		218-nm	
			226-nm	

Each simple cyclobutene possesses a clear Rydberg π,R(3s) transition which is isolated from the valence π,π* transition and can be selectively excited at 228-nm. Therefore, the photochemistry of the Rydberg state can be studied without interference from the competing direct population of the π,π* excited state.

2.3.2. The Photochemistry of Monocyclic Alkylcyclobutenes in the Gas Phase and in Solution

The photochemistry of three alkylcyclobutene derivatives was studied at three different excitation wavelengths in the gas phase (1atm SF_6) and in hydrocarbon solution. In both the gas phase and solution, the ring-opening to cycloreversion ratio (RO/CR) decreases as the excitation wavelength is increased from 193-nm to 228-nm (Tables 2.2 and 2.3). The largest variation is observed in the irradiations of *trans*-**18** where the RO/CR in solution falls from 1.5 at 193-nm to 0.25 at 228-nm. This general observation is consistent with the hypothesis that the Rydberg state is largely responsible for the cycloreversion reaction.[15,89] However, the persistence of ring-opening at 228-nm was unexpected, and immediately suggests that the Rydberg state *also contributes to ring-opening*. This conclusion seems sound since the valence π,π^* state cannot be populated by direct light absorption at this wavelength.

The stereochemistry of the Rydberg state ring-opening reaction is quite different from that observed at lower wavelengths. *Cis*-**18** shows a remarkable increase in conrotatory stereospecificity in both the gas and solution phase. For instance, the CON/DIS ratio in solution increases from 0.63 to >20 upon increasing the excitation wavelength from 193-nm to 228-nm. The >20:1 ratio implies that the Rydberg excitation results in *stereospecific conrotatory* ring-opening in both the gas and solution phase. Incidentally, this is the first

observation of stereospecific photochemical ring opening of a cyclobutene. However, the trans isomer does not appear to react analogously. In both the gas and solution phase photolyses of *trans*-**18**, the CON/DIS ratio does not undergo a dramatic increase with a decrease in excitation wavelength, and remains relatively constant. The only notable difference is an increase in the yield of *Z,Z*-**19** relative to the other isomers upon excitation at 228-nm in solution. In fact, the ratio of diene isomers approaches that of the photostationary state, suggesting that secondary photolysis of the products is occurring.

One of the inherent difficulties in interpreting the results of these experiments at 228-nm, is the fact that the dienes have a much higher extinction coefficient than the cyclobutenes at this wavelength, and secondary irradiation poses a problem. Since *cis*-**18** only gives rise to one diene it obviously does not suffer from this effect. The plots of the product ratios vs. conversion in Figures 2.2 and 2.3, offer some insight into the degree that secondary photolysis is affecting the results. As expected, the plots of RO/CR ratios vs. conversion give zero-slopes in every case, indicating that secondary isomerization does not affect the *total* diene yield in an appreciable amount. However, the plots of diene isomer ratios vs. percent conversion for *trans*-**18** (Figure 2.3.b and 2.4.b) show quite clearly that the 228-nm irradiations are subject to this phenomenon. In both the gas phase and solution, these plots have marked negative slopes. Although the solution phase experiment is less problematic, the effect is quite

evident in the E,E/E,Z ratio, suggesting that the yield of *E,E*-**19** decreases at increased photolysis times by isomerization to *E,Z*-**19**.

Inspection of the photostationary states (pss) at 228-nm supports this explanation. A photostationary state can simply be considered as the photochemical equilibrium mixture of the components. The pss then depends on the relative extinction coefficients and quantum yields for interconversion of the components involved. For instance, with the 2,4-hexadienes (**19**) the pss can be represented by equation 2.8.

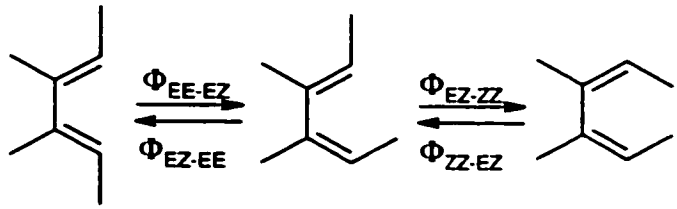

$$([E,E]:[E,Z]:[Z,Z])_{pss} = (\Phi_{EZ\text{-}EE}\varepsilon_{EZ})(\Phi_{ZZ\text{-}EZ}\varepsilon_{ZZ})/(\Phi_{EE\text{-}EZ}\varepsilon_{EE})(\Phi_{ZZ\text{-}EZ}\varepsilon_{ZZ})/(\Phi_{EZ\text{-}ZZ}\varepsilon_{EZ})(\Phi_{EE\text{-}EZ}\varepsilon_{EE}) \quad [2.8]$$

The 228-nm pss of E,E:E,Z:Z,Z=1:7.1:4.4 for the isomers of **19** indicates that the E,E isomer is most sensitive to secondary photolysis at this wavelength, while *E,Z*-**19** is least susceptible. If the Rydberg state ring-opening of *trans*-**18** is proceeding to give the conrotatory products only (*E,E*- + *Z,Z*-**19**), then it is clear that secondary photolysis will be more problematic than observed with the cis isomer (where the conrotatory product is *E,Z*-**19**).

A control experiment was designed to mimic this effect and aid in determining the initial product distribution of the ring opening of *trans*-**18**. A 1:1 mixture of *E,E*- and *Z,Z*-**19** was slowly added to a solution of **50** (0.15-M) while it was being irradiated at 228-nm (eqn. 2.9). Care was taken to ensure that the rate of addition was as close as possible to that of total diene formation in the actual photolysis of *trans*-**18** (Fig. 2.4.b). Even at the lowest conversion analyzed (*ca.* 0.2%), *E,Z*-**19** was present in significant amounts (*ca.* 50%) suggesting that secondary irradiation in the original photolysis is pronounced. The plots of the diene isomer ratios vs. time for the control experiment do not match that of the original exactly, but they are very close (Figure 2.4.a). Thus the experiment was repeated with a diene mixture of *E,E*/*Z,Z*-**19** of 1.6:1 (Figure 2.5). In this case, *E,E*-**19** is present in much higher amounts than the other isomers throughout the experiment and there is no reasonable match between the diene isomer ratios of the control and the original. The results of the two experiments indicate that the true, primary ratio of *E,E*/*Z,Z*-**19** is slightly larger than 1:1, and the primary diene composition is roughly E,E:E,Z:Z,Z = 1:0:1. It is concluded that both *cis*- and *trans*-**18** undergo stereospecific *conrotatory* ring-opening upon 228-nm excitation in solution.

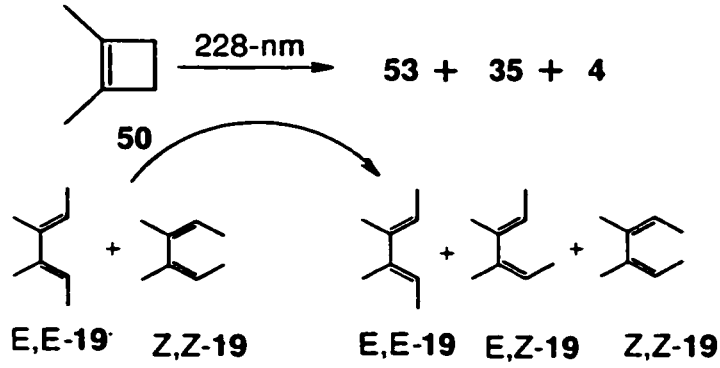

[2.9]

It is now clear that both the π,π^* and Rydberg π,R(3s) excited states give rise to ring-opening. However, the component of the reaction that results from the Rydberg state clearly proceeds with *conrotatory stereospecificity*. Understanding the contribution of the Rydberg state reaction to the ring-opening at shorter wavelengths (where the two states are overlapped) becomes of utmost importance since it could affect the interpretation of the results in support of an adiabatic mechanism.

Two possible mechanisms for the Rydberg state ring-opening can be proposed. The first possibility is that the Rydberg state offers an efficient avenue for internal conversion to the ground state where thermal (conrotatory) ring-opening occurs from upper vibrational levels of the S_0 surface. This will be referred to as the "hot ground state" mechanism. The second possibility is that a cyclobutene in the Rydberg state can undergo direct ring-opening, possibly due to its radical cation character.

The photolysis of **50** in methanol shows that the Rydberg state of alkylcyclobutenes has analogous character to those of other tetraalkyl substituted alkenes.[84-86] The electron deficient cyclobutene is subject to nucleophilic attack, and the observed adducts **78-80** are the expected products of methanol addition to the cationic site followed by free radical hydrogen abstraction or disproportionation (eqn. 2.10).

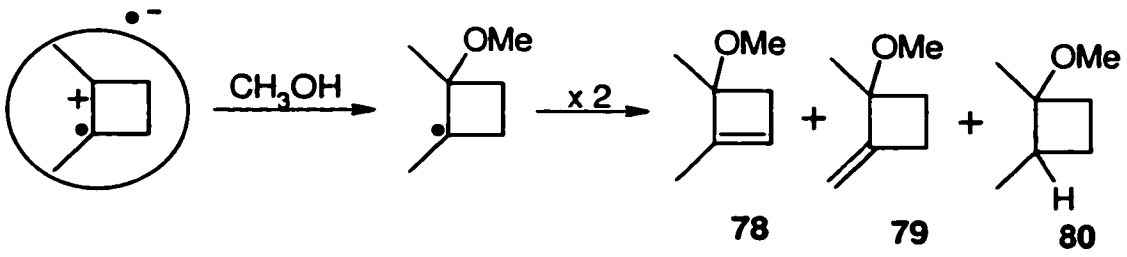

78 **79** **80**

[2.10]

As expected, the yields of these reactions are lower at 214-nm than they are at 228-nm where the π,R(3s) state is exclusively populated (Table 2.4). However, the formation of products from both cycloreversion and ring-opening is still observed under these conditions at both wavelengths.

Johnston and coworkers have studied the reactivity of diene radical cations with various nucleophiles by time-resolved laser flash photolysis.[93] The radical cations of simple dienes such as **15** , **25**, and **17**, react with methanol with rate constants of 1.8×10^8 $M^{-1}s^{-1}$, 4.8×10^6 $M^{-1}s^{-1}$ and 4.3×10^7 $M^{-1}s^{-1}$,

respectively. Unfortunately, there is a lack of kinetic data for the reaction of methanol with alkyl substituted alkene radical cations.

15

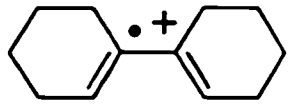

25

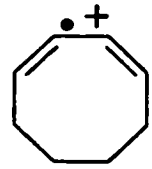

17

The rate of reaction between the Rydberg state of **50** and methanol can be estimated from the current results in order to compare it to those of the diene radical cations. If it is assumed that the lifetime of the Rydberg state is analogous to that of 2,3-dimethyl-2-butene (<100 ps)[94,95] then the reaction of the excited **50** with methanol must occur near the diffusion controlled rate ($1x10^{11}$ $M^{-1}s^{-1}$) in order to form the three adducts in such significant yields. Although this rate is somewhat faster than that observed with the diene radical cations, one might expect that simple alkene radical cations would have an enhanced rate of reaction with nucleophiles due to the lack of any resonance stabilization.

Chapter 3.

Investigation of Hot Ground State Reactivity in the Photochemistry of Alkylcyclobutenes : Quantum Yields and Theoretical Rate Constants for Thermal Ring-Opening

3.1. Introduction

In solution, most photochemical reactions are the result of uni- or bimolecular bond cleavage/formation processes which begin on the excited state potential energy surface. The efficiency of the reaction reflects the ratio of the excited state reaction relative to those of other deactivation pathways,[96] such as internal conversion, i.e. S_1 to S_0 radiationless decay. One normally considers internal conversion (IC) as a process that leads to non-productive excited state decay, although this is not always the case.[13] Internal conversion from S_1 initially places the molecule in a high vibrational level of S_0. Normally, the molecule will quickly redistribute the absorbed energy via intramolecular vibrational-energy

redistribution (IVR),[97] and then relax to the v=0 level by collisional deactivation with the solvent. For instance, using time-resolved spectroscopy, the decay of vibrationally excited cycloheptatriene in heptane (eqn. 3.1) was determined to occur with a pseudo first order rate constant of $k_{rel} = 1x10^{11}s^{-1}$.[98]

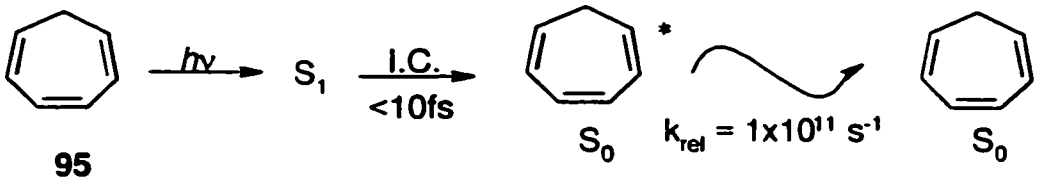

95

[3.1]

However, if there is a ground state reaction available to the molecule which proceeds at a similar rate to collisional deactivation, then products of thermal reaction can result from photochemical excitation.[12,13,96,98-101] Such photochemical reactions are termed "hot ground state" reactions.

A popular model for depicting this type of reactivity is that in which thermal reaction can occur at each vibrational level as the molecule deactivates in stepwise fashion.[98,100,102] As a result of the loss in energy, the rate of thermal reaction systematically decreases to a point where the competition is overwhelmingly in favour of deactivation, and reaction is no longer observed. In the gaseous state where collisions with buffer gas and reactants are much less frequent, it is believed that the deactivation is sufficiently slow that the thermal reaction can successfully compete with deactivation in a large number of

cases.[98,100,103,104] As the pressure of the buffer gas is increased, the rate of collisional deactivation increases, and the formation of thermal products decreases in efficiency. However, save a few minor examples,[105-111] it is believed that in condensed phases such as solvents and glasses, hot ground state reactivity cannot compete with the exceedingly fast collisional deactivation of excess energy.[102,112] A representation of the cyclobutene ring-opening reaction within this model is given in Figure 3.1.

Figure 3.1. The stepladder model for collisional deactivation of vibrationally excited molecules.

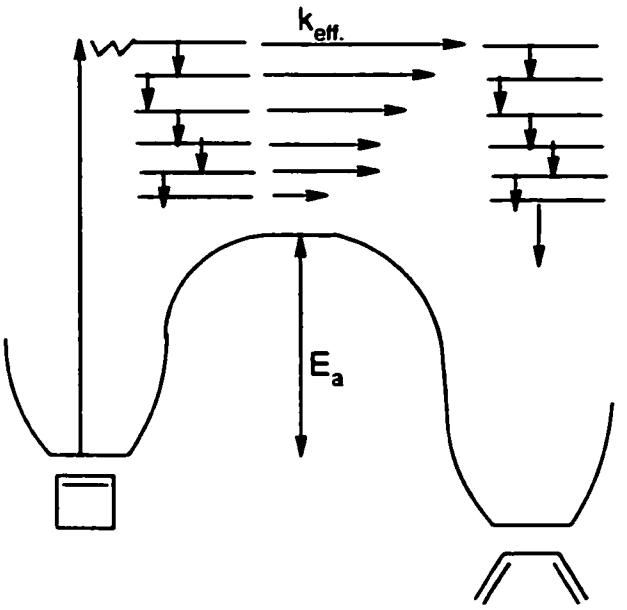

In order to examine the possibility that the conrotatory ring-opening of cyclobutenes at 228-nm occurs by the hot ground state mechanism, quantum yields for ring-opening have been determined for a series of alkylcyclobutenes and compared to values estimated from calculated rate constants for ground state ring-opening at the energy corresponding to that associated with the excitation wavelength. Both experimental and theoretical data have been obtained for a series of four monocyclic cyclobutenes of increasing molecular weight, including 1,2-dimethylcyclobutene (**50**), *cis*- and *trans*-1,2,3,4-tetramethylcyclobutene (**18**), and hexamethylcyclobutene (**22**). The data for *cis*- and *trans*-tricyclo[6.4.0.$0^{2,7}$] dodec-1-ene (**24**) were also compared since these derivatives are of equal molecular weights but have very different activation parameters for thermal ring-opening. By systematically varying these parameters, and the propensity for vibrational-energy redistribution (molecular weight and vibrational degrees of freedom), the efficiency of hot ground state reactivity will be affected.

3.2. Results

3.2.1. Preparation of the Cyclobutenes and their Photoproducts

The same monocyclic cyclobutenes (**50**, and **18**) were studied as in Chapter 2 with the addition of hexamethylcyclobutene (**22**). The latter compound

was prepared by the route shown in equation 3.2 and purified by semi-preparative gas chromatography. The synthetic intermediate (**81**) was kindly provided by Dr. J.A. Postigo.

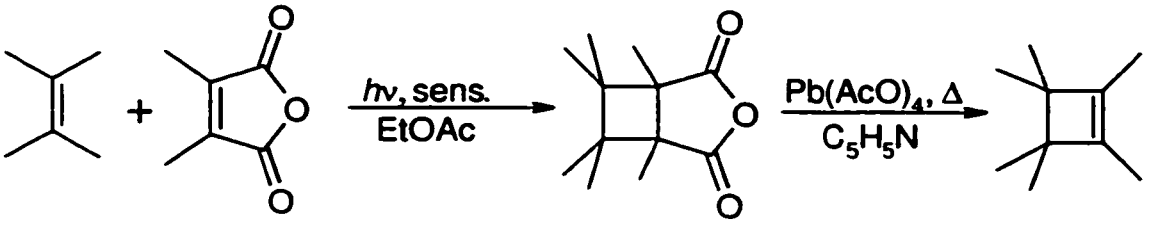

6 **74** **81** **22**

[3.2]

2,3,4,5-Tetramethyl-2,4-hexadiene (**23**) was prepared by reductive coupling of 3-methyl-2-butanone (**82**), followed by dehydration with propionic anhydride.(eqn. 3.3) Purification was accomplished by radial chromatography.

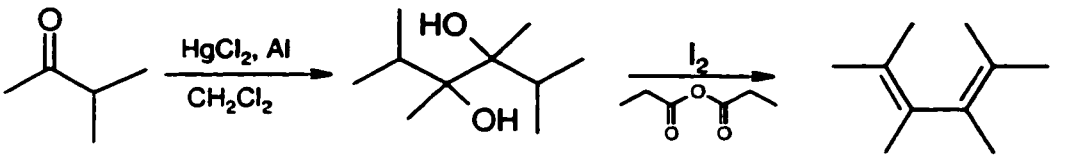

82 **83** **23**

[3.3]

cis-Tricyclo[6.4.0.0]dodec-1^2-ene (*cis*-**24**) was prepared in three steps from cyclohexanone (**84**) (eqn. 3.4).[32] First, 1,1'-bis(hydroxy)bicyclohexane (**85**)

was synthesized by reductive coupling of **84** with $HgCl_2$ and aluminum foil.[113] Dehydration with dilute sulfuric acid provided 1,1'-bicyclohexenyl (**25**) which was converted to *cis*-**24** by triplet sensitized isomerization.[32] Separation from **25** and purification was accomplished using semi-preparative gas chromatography.

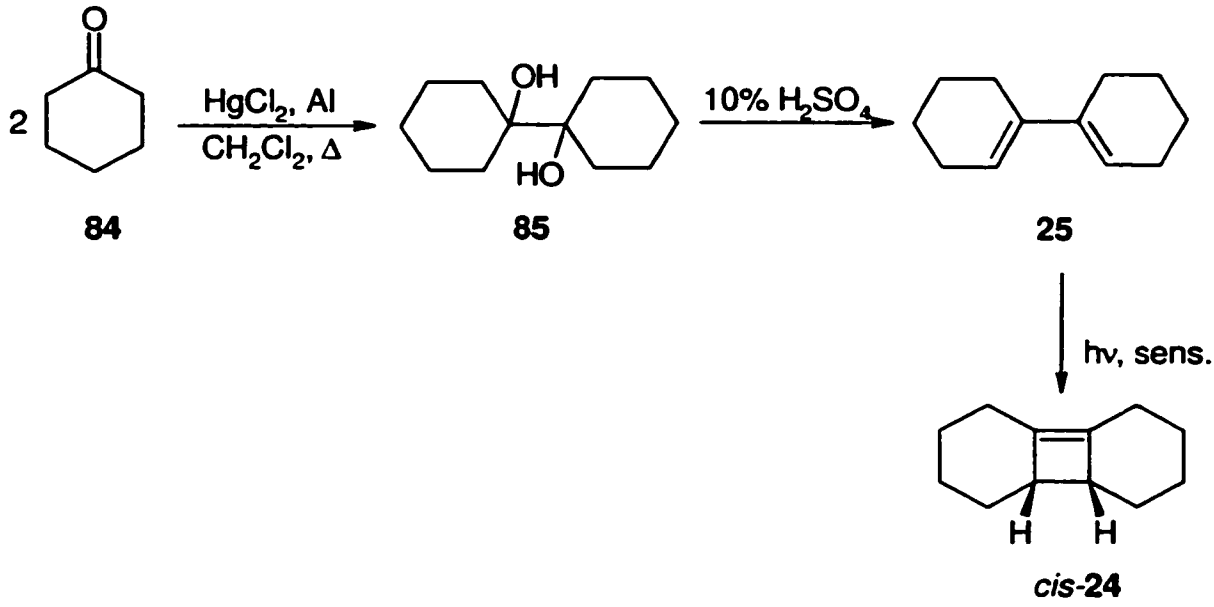

84 **85** **25** *cis*-**24**

[3.4]

trans- Tricyclo[6.4.0.0]dodec-1^2-ene (*trans*-**24**) was prepared following the synthetic scheme shown[32,147] in equation 3.5. Purification was accomplished by column chromatography to remove small amounts of **25** which arise due to the thermal instability of the cyclobutene. After chromatography the cyclobutene was 99.8% pure with 0.2% diene present.

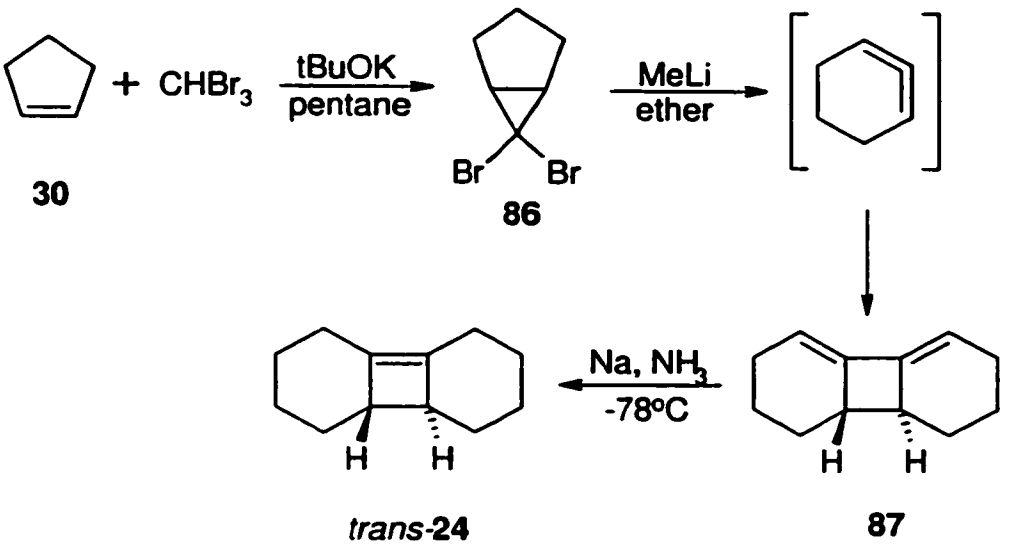

30 **86** *trans*-**24** **87**

[3.5]

The cycloreversion products of *cis*- and *trans*-**24**, (*E*- and *Z*-**28**, respectively), were isolated by preparative scale irradiations of the appropriate cyclobutene isomers.

3.2.2. Quantum Yield Determinations for **50**, **18**, **22**, and **24**

The quantum yields for ring opening (RO) of the series of alkylcyclobutenes were measured at 228-nm. In all cases, products from ring-opening and cycloreversion were observed and identified by GC co-injection with authentic samples. The appropriate reactions are given in equation 3.6.

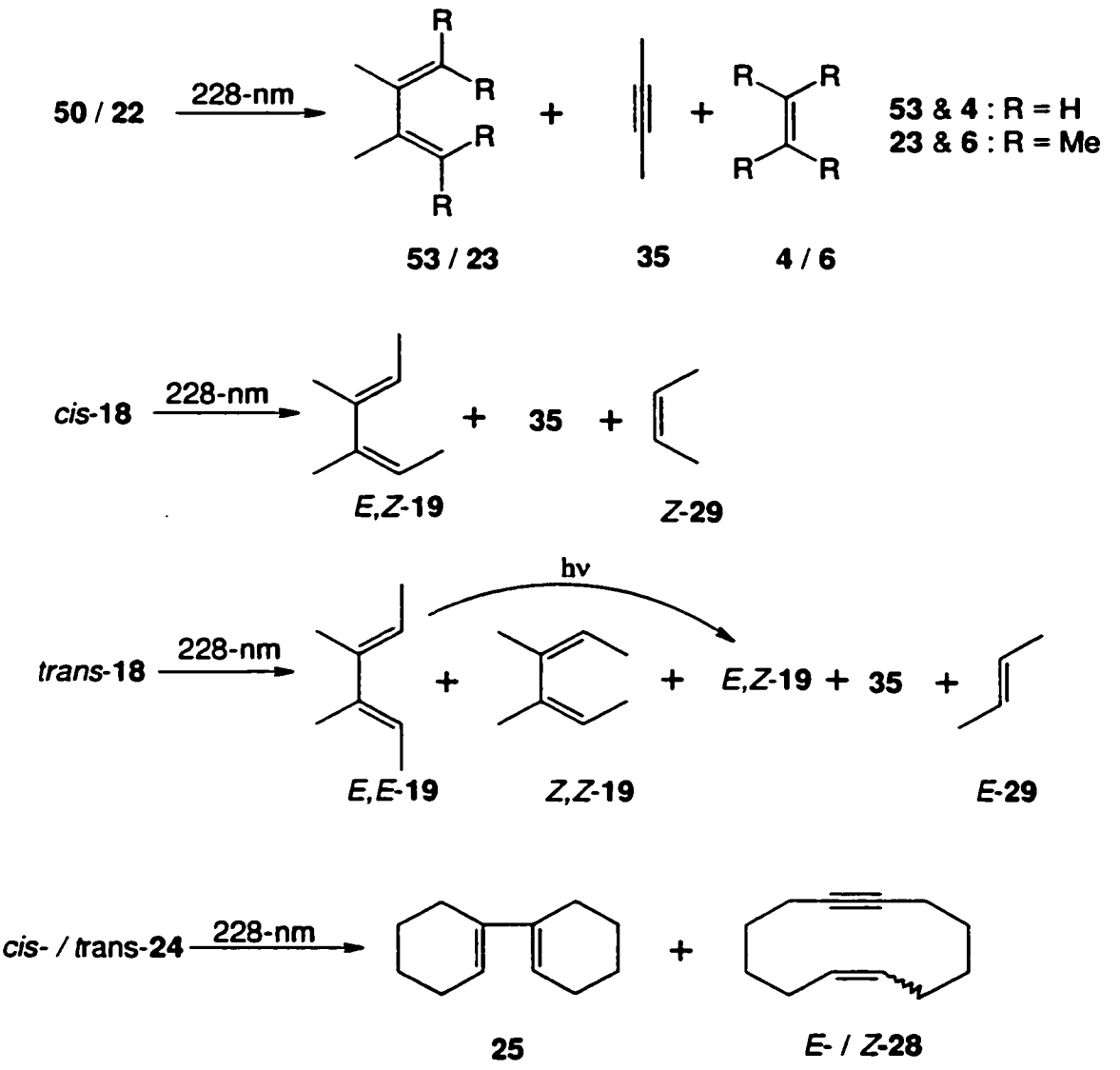

[3.6]

The quantum yield for ring-opening (Φ_{RO}) of **50** at 228-nm in isooctane (0.06 M) was determined in quadruplicate by uranyl oxalate actinometry following the procedure outlined by Eaton.[114] The product yields from **50** were determined by gas chromatography at less than 4% conversion to ensure that the single

point determinations were obtained before secondary irradiation of **53** occurred. The quantum yields for ring-opening of **18**, **22** and **24** were determined using **50** as a secondary actinometer from the relative slopes of concentration vs. time plots. A complete set of these plots can be found in Appendix 2. Separate samples of **50**, and the desired cyclobutene were irradiated at 228-nm on a merry-go-round apparatus. In the case of *trans*-**18**, the quantum yield for ring-opening was determined as the sum of all the diene isomers since secondary irradiation was known to affect the isomer ratios. All values were obtained from triplicate determination of these experiments in hexanes (0.06 M) using cyclohexane as an internal standard, and corrected for the FID response with calibration curves. Figure 3.2 shows typical plots for *cis*- and *trans*-**18**. Ring-opening to cycloreversion ratios (RO/CR) were also obtained from the relative slopes of concentration vs. time plots. In addition, plotting RO/CR against time provided straight lines with slopes indistinguishable from zero. This suggests that secondary photolysis of the products was negligible over the conversions examined (< 5%). Typical plots for the quantum yield determinations of *cis*- and *trans*-**24** at both 214-nm and 228-nm are shown in Figure 3.3. The quantum yields for ring-opening of **50**, **18**, and **22** at 228-nm are listed in Table 3.1 along with RO/CR ratios. The corresponding data for *cis*- and *trans*-**24** at both 214- and 228-nm are also listed in Table 3.1.

Figure 3.2. Quantum yield determinations for the ring-opening of a) *cis*-**18** and b) *trans*-**18** with 228-nm excitation in hexanes using **50** as an actinometer (■ : formation of **53** from **50**, ● : formation of *E,Z*-**19**, ▼ formation of *E,E*-**19**, ◆ : formation of *Z,Z*-**19**).

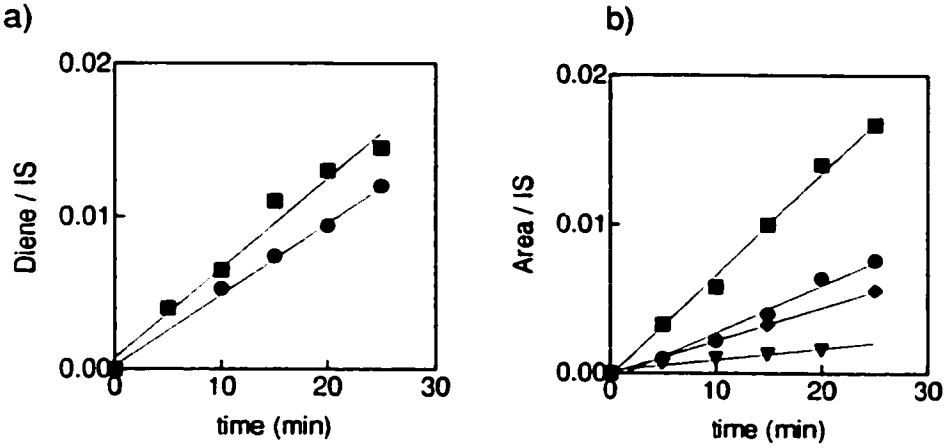

Figure 3.3. Quantum yield determinations for the ring-opening of *cis*- and *trans*-**24** at a) 214-nm and b) 228-nm in hexanes using **50** as an actinometer. (■ : formation of **53** from **50**, ● : formation of **25** from cis-**24**, ▼ : formation of **25** from trans-**24**).

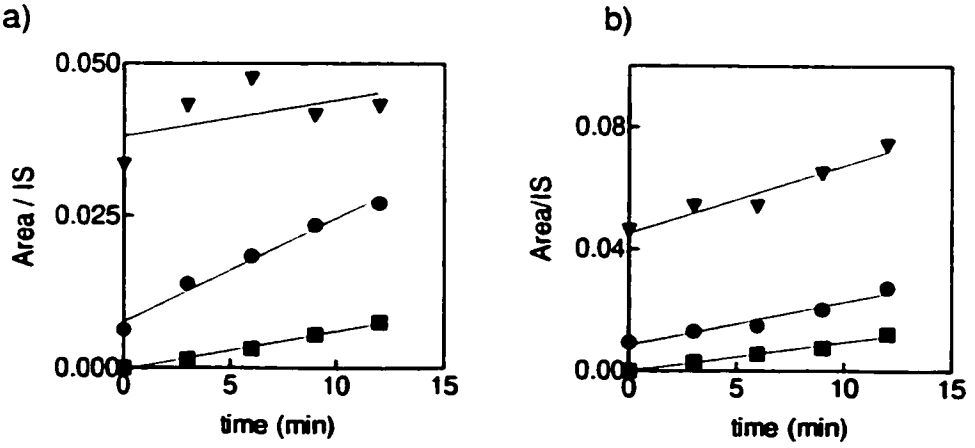

Table 3.1. Ring-opening / cycloreversion ratios (RO/CR) and quantum yields for ring-opening for **50**, **18**, **22**, and **24**.

Compound	214-nm		228-nm	
	RO/CR[a]	Φ_{RO}[b]	RO/CR[a]	Φ_{RO}[b]
cis-**24**	2.7±0.2	0.15±0.02	2.6±0.03	0.13±0.02
trans-**24**	0.27±0.02	0.06±0.02	0.39±0.02	0.20±0.04
50	-	-	0.79±0.09	0.09±0.02
cis-**18**	-	-	0.69±0.09	0.08±0.01
trans-**18**	-	-	0.25±0.04	0.08±0.01
22	-	-	0.52±0.05	0.11±0.02

a. Based on the relative slopes of concentration vs. time plots.
b. Errors taken as the standard deviation of triplicate determinations.

3.2.3. Calculated Rate Constants for Thermal Ring-Opening of the Cyclobutenes

Rate constants for thermal ring-opening of **50**, **18**, and **22**, at the energy associated with a 228-nm photon were determined using RRKM theory.[115] Those for *cis*- and *trans*-**24** were calculated using a more approximate procedure. First, the vibrational spectra of **50**, **18**, **22**, and **24** were calculated using Gaussian 94.[116] The geometries of all the cyclobutenes were optimized

with the 6-31G(d) basis set. The vibrational frequencies of **50**, **18**, and **22** were obtained using B3LYP/6-31G(d) calculations. Those of **24** were calculated with the 3-21G basis set after it was found that similar effective temperatures (*vide infra*) were obtained for **50** using either method. A complete listing of the calculated vibrational frequencies can be found in Appendix 4. A correction factor of 0.98 or 0.91 was applied to the vibrational frequencies obtained from the B3LYP and 3-21G calculations, respectively.[117]

RRKM calculations using the predetermined vibrational frequencies were performed by Profs. W.J. Leigh (McMaster University) and R. Walsh (Reading University). Figure 3.4 shows plots of log k(E) vs. energy (E) determined for **50**, **18**, and **22**, from these calculations. Rate constants for thermal ring-opening were thus obtained for the energy of a 228-nm photon (43,860cm^{-1}) and that of a 214-nm photon (46,729cm^{-1}), k_{228} and k_{214}, respectively. Values of k_{228} and k_{214} were determined for the ring-opening of *trans*-**18** to both *E,E*- and *Z,Z*-**19** by this method. Since the activation energy for the ring opening to *Z,Z*-**19** is unknown, it was estimated using theoretical prediction factors put forth by Rondan and Houk.[118]

Figure 3.4. Plots of log k(E) against energy (E) for the thermal ring-opening of **50, 18,** and **22** as determined by RRKM theory (▼ : **50**, ■ : *cis*-**18**, ○ : *trans*-**18** to *E,E*-**19**, ◊ : *trans*-**18** to *Z,Z*-**19**, ▲ : **22**).

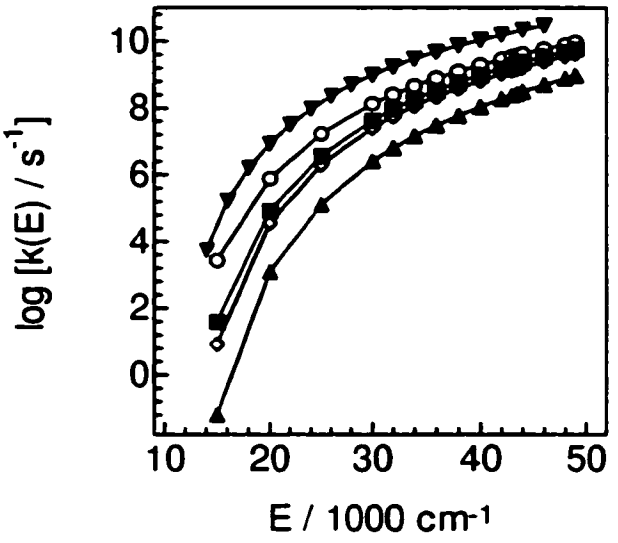

The molecular weights of *cis*- and *trans*-**24** exceed the practical limit for accurate RRKM calculations, so k_{228} was determined using the published Arrhenius parameters for ring-opening,[28,29] and effective temperatures calculated using statistical thermodynamics. Using the calculated vibrational frequencies, a plot of energy (E) vs. temperature (T) was constructed from equation 3.7.[119] Figure 3.5 shows this plot for *cis*-**24**. That of *trans*-**24** is almost exactly analogous since the vibrational frequencies and zero-point energies are very similar at the level of theory used. The effective internal temperatures (T_{eff}) of the cyclobutenes corresponding to an internal energy equal to that of a 228-nm

photon were then estimated from the graph. The k_{228} values were calculated using the thermal activation parameters in Table 3.2. Rate constants calculated in the same fashion for **50** and **18** were similar to those from RRKM theory.

$$\langle E \rangle = \frac{1}{2}h\nu + \sum\left[\frac{h\nu_i}{\exp(\frac{h\nu_i}{kT})} - 1\right] \qquad [3.7]$$

Figure 3.5. A plot of energy vs. temperature for *cis*- and *trans*-**24** as determined from equation 3.7 using the calculated vibrational frequencies.

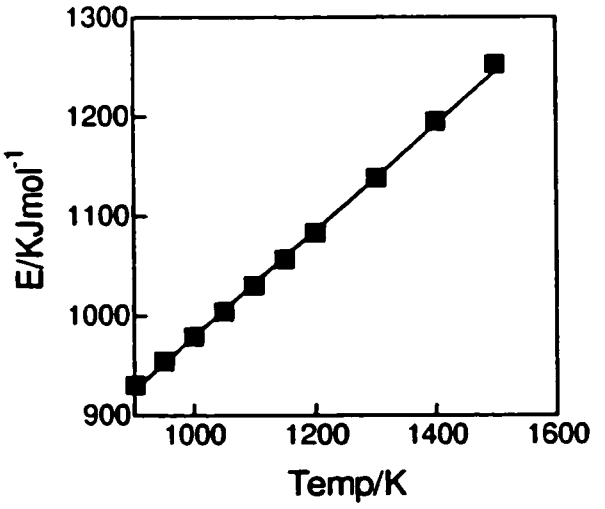

Table 3.2 summarizes the values for Φ_{RO}, k_{228}, and T_{eff}, for **50**, **18**, **22**, and **24** along with the published Arrhenius activation parameters for thermal ring-opening.

Table 3.2. Quantum yields for ring-opening, calculated k_{228} values, and effective temperatures (T_{eff}) for **50**, **18**, **22**, and **24**, along with the known Arrhenius activation parameters.

Compound	Φ_{RO}^{228}	k_{228}[b] ($10^7 s^{-1}$)	T_{eff}[c] (K)	Ea[d] (kcal/mol)	log(A)[d]
50	0.09	2000	2340	36.0	13.84
cis-**18**	0.08	251	1970	37.4	13.32
trans-**18** : *E,E*	0.04[a]	398	1815	33.6	13.25
trans-**18** : *Z,Z*	0.04[a]	158	-	42.0[e]	-
22	0.11	32	1515	40.0	14.95
cis-**24**	0.13	5.5[c]	1490	44.2[28]	14.2[28]
trans-**24**	0.20	230[c]	1495	28.9[28]	13.6[28]

a. Estimated based on the 1:1 ratio of formation of *E,E*- and *Z,Z*-**19** from *trans*-**18** with 228-nm excitation.
b. Determined using RRKM theory unless otherwise noted.
c. Determined using equation 3.7.
d. From reference 29 unless otherwise noted.
e. Estimated as indicated in reference 118.

3.2.4. Calculation of Approximate Ring-Opening Quantum Yields from RRKM-Derived Rate Constants

In order to estimate an expected value for the quantum yield of cyclobutene ring-opening via the hot ground state mechanism, it was assumed that after absorption of a photon (214- or 228-nm) internal conversion to the ground state occurs with unit efficiency, i.e. $\Phi_{ic}=1$. This leads to an upper estimate for the quantum yield for hot ground state ring-opening. The quantum yield was then calculated from equation 3.8, where Φ_{CR} is the quantum yield for cycloreversion from the Rydberg state, k_{RO} is the calculated rate constant for ring-opening with the energy from the photon, and k_{rel} is the rate constant for collisional deactivation of the vibrationally excited cyclobutene. Luther and coworkers have determined the rate constant for collisional deactivation of vibrationally excited cycloheptatriene in heptane to be $k_{rel}=1x10^{11}s^{-1}$.[120,121] Since the cyclobutenes studied are of similar molecular weight and composition, this value of k_{rel} was adopted. The calculated Φ_{calc} values are in Table 3.3.

$$\Phi_{calc} = (1 - \Phi_{CR}) \frac{k_{RO}}{k_{RO} + k_{rel}} \qquad [3.8]$$

The estimated quantum yields for ring-opening at 214-nm, were only determined for those cyclobutenes where the stereochemistry can be traced, since hot ground state ring-opening will only lead to the conrotatory products. In these cases it is assumed that the π,π^* state contributes to the photochemistry by giving rise to disrotatory ring-opening. To account for this loss of efficiency, the Φ_{calc}^{214} was scaled by a factor of $(1-\Phi_{allowed})$ as opposed to $(1-\Phi_{CR})$.[35] The resulting values are listed in Table 3.3.

Table 3.3. Calculated quantum yields for thermal ring-opening along with the experimental values for **50**, **18**, and **22**, at 214-nm and 228-nm.

Compound	$\Phi_{calc}^{228\ a}$	Φ_{RO}^{228}	$\Phi_{calc}^{214\ c}$	Φ_{RO}^{214}(con)[d]
50	0.15	0.09	NA	NA
cis-**18**	0.022	0.08	0.032	0.10
trans-**18** to *E,E*	0.026	0.04[b]	0.046	0.089
trans-**18** to *Z,Z*	0.011	0.04[b]	0.021	0.029
22	0.003	0.1	NA	NA
cis-**24**	0.0005	0.13	NA	NA
trans-**24**	0.012	0.2	NA	NA

a. Calculated from equation 3.8.
b. Estimated based on the 1:1 ratio of *E,E*- and *Z,Z*-**19** formed from irradiation of *trans*-**18** at 228-nm.
c. Calculated from equation 3.8 but scaled by a factor of $(1-\Phi_{allowed})$.
d. From reference 35.

3.3. Discussion

3.3.1. Hot Ground State Reactivity

There is precedent for hot ground state reactivity in the photochemistry of small hydrocarbons. Irradiation of cyclohexene (**31**) vapour at 185-nm or 214-nm results in the formation of three minor rearrangement products (**88, 89, 90**), along with cycloreversion (or retro-Diels Alder reaction) to yield butadiene (**2**) and ethylene (**4**) (eqn. 3.9).[105,122] The quantum yield is substantially affected by changes in pressure and ranges from 0.85 at 5 torr, to 0.4 at 30 torr. When the irradiation is conducted in solution, the cycloreversion products cease to be formed. Excitation of *cis*-4,5-dimethylcyclohexene under similar conditions results in the formation of 1,3-butadiene and Z-2-butene.[106] The high degree of stereospecificity observed in this case, and the pronounced pressure dependence on the quantum yield provide very strong evidence that cycloreversion occurs via a hot ground state mechanism. The ground state reaction occurs with Arrhenius activation parameters of E_a = 65 kcal/mol, and log(A) = 14.93.[123]

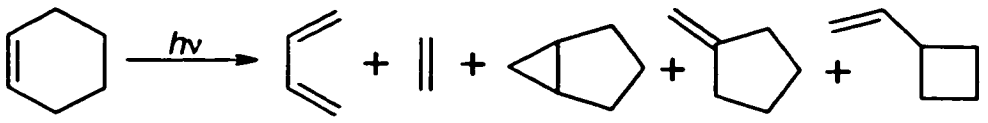

31 **2** **4** **88** **89** **90**

[3.9]

Excitation of norbornadiene (**91**) in the gas phase at 254-nm results in the formation of toluene (**92**) and the products of retro-Diels Alder reaction, cyclopentadiene (**93**) and acetylene (**3**) (eqn. 3.10).[107,108] The quantum yields for the formation of **3** and **93** are essentially independent of pressure over the 4 to 31 mmHg range, and remains at 0.4-0.5 as the buffer gas is varied.[108] Irradiation of **91** in hydrocarbon solution results in the formation of quadricyclane (**94**) as the major product.[107] The formation of toluene is suppressed completely while the quantum yields for **93** and **3** are decreased by a factor of four in comparison to the gas phase values. The Arrhenius activation parameters for this cycloreversion reaction are E_a = 50.2 kcal/mol and log(A) = 14.6.[124]

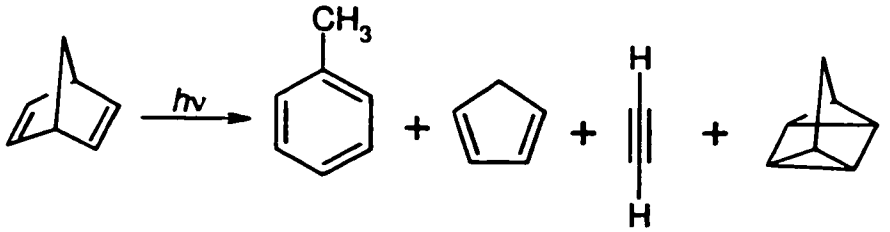

91 **92** **93** **3** **94**

[3.10]

Since the alkylcyclobutenes studied here are generally of similar molecular weight to cyclohexene and norbornadiene, and the thermal ring-opening occurs with much lower activation barriers[125] than the reactions discussed above, it seemed very likely that the ring-opening from the Rydberg state could be due to hot ground state reactivity. The approach used to evaluate this mechanistic possibility involved correlating the experimentally determined quantum yields for ring-opening with expected values, calculated from computed ring-opening rate constants and experimental kinetic data for the vibrational relaxation of highly excited molecules in solution.

3.3.2. Comparison of the Experimental and Calculated Quantum Yields for Ring-Opening

The data for *cis*- and *trans*-**24** provide an interesting perspective in this analysis since the two derivatives possess very different activation parameters for thermal ring-opening, but identical molecular composition (note that $T_{eff.}$ is the same for both compounds). When switching from 214-nm to 228-nm excitation and progressing into the Rydberg absorption band, both the Φ_{RO} and RO/CR values increase for *trans*-**24** (Table 3.1). This may be expected with a hot ground state mechanism, since *trans*-**24** undergoes thermal ring-opening with Ea=29.2 and log(A)=14.23. However, *cis*-**24** (Ea = 41.6. log (A) = 12.96) would be expected to show the opposite effects if this mechanism was involved. There

is, in fact, no change in the Φ_{RO}, or RO/CR values for *cis*-**24** as the excitation wavelength is varied. In addition, the Φ_{RO}^{228} values for the two isomers are nearly the same within experimental error. The difference between the calculated values of k_{228} (corresponding to the energy of a 228-nm photon) is very large, however, with the value of *trans*-**24** being 25 times greater than that of the cis isomer. The lack of any effect on the photochemistry due to the large difference in Arrhenius activation parameters of these derivatives, is inconsistent with a hot ground state mechanism.

As indicated in Table 3.1, the experimental quantum yields for ring-opening at 228-nm (Φ_{RO}^{228}) for the cyclobutenes **50, 18,** and **22,** are the same within experimental error (*ca.* 0.1). In contrast, the calculated rate constants for thermal ring-opening at the energy of a 228-nm photon vary over four orders of magnitude, from 5×10^7 s^{-1} to 2×10^{10} s^{-1} (for **22** and **50**, respectively, Table 3.2). The difference is also reflected in the $T_{eff.}$ values which are calculated using statistical thermodynamics. The smallest derivative, 1,2-dimethylcyclobutene (**50**), possesses an internal temperature of 2340 K where that of hexamethylcyclobutene (**22**) is 1515 K. Once again, the absence of any correlation between the experimentally determined quantum yields *and* the calculated thermal parameters, suggests that hot ground state reactivity is not a substantial contributor to the conrotatory ring-opening of these cyclobutenes.

However, a direct comparison between experimental and calculated quantum yields for ring-opening allows an estimation of the degree to which hot

ground state reactivity may contribute to the photochemistry. The theoretical quantum yields were determined as a ratio of the calculated rate constant for ring opening at the photon energy, and the sum of the rate constants for the processes which deplete the vibrationally excited state (eqns. 3.8 and 3.11). Table 3.3 compares the calculated and experimental quantum yields for ring opening at 228-nm.

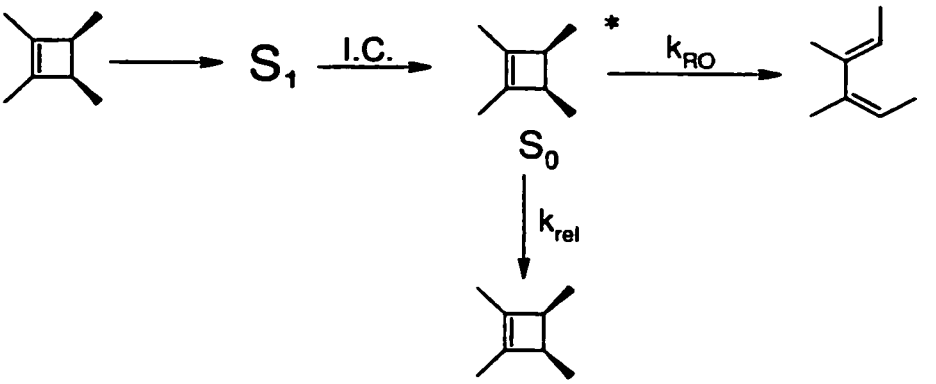

[3.11]

It was possible to calculate separate rate constants for the ring-opening of *trans*-**18** to each of *E,E*-**19** and *Z,Z*-**19**. The activation energy for the ring opening to *Z,Z*-**19** was approximated to be 42 kcal/mol using the additive factors determined by Rondan and Houk.[118] Their theoretical predictions suggest that the inward motion of a -CH_3 substituent adds +3 to the activation energy whereas the outward motion subtracts -1. The difference then, between the E_a to *Z,Z*- or *E,E*-**19**, is 2[+3-(-1)] = 8 kcal/mol. Therefore, the rate constants, k_{228},

were calculated using $E_a(E,E)$ = 33.6 kcal/mol and $E_a(Z,Z)$ = 41.6 kcal/mol for *E,E*- and *Z,Z*-**19**, respectively (eqn. 3.12).

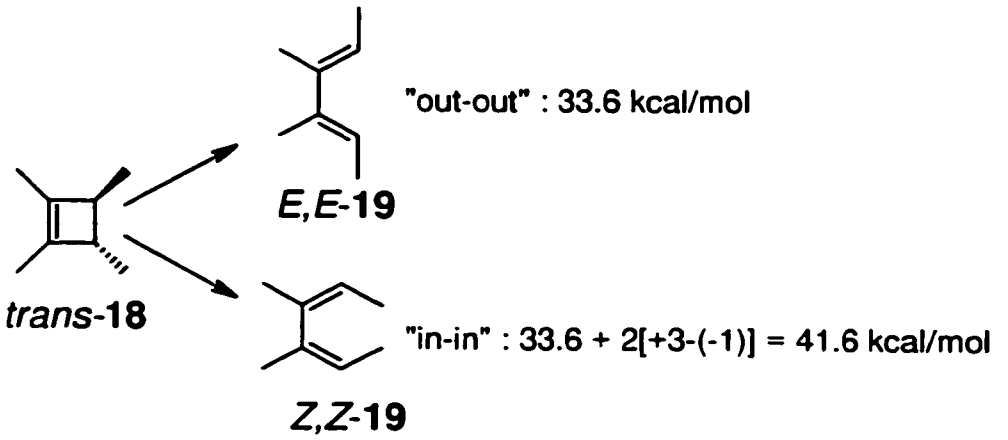

[3.12]

The data in Table 3.3 suggest that hot ground state reactivity is a definite possibility in the photochemistry of **50**, as the calculated quantum yield can account for 100% of the observed Φ_{RO}[228]. However, with the remainder of the cyclobutenes only the *trans*-**18** to *E,E*-**19** reaction has a Φ_{calc}[228] value which is comparable to the actual value. In fact, with **22**, the calculated value is negligible in comparison to the experimental quantum yield. These observations are reflected in Figure 3.6 where the calculated quantum yields for hot ground state ring-opening are plotted against the experimental values for 228-nm excitation.

Figure 3.6. Calculated quantum yields for hot ground state ring-opening against experimentally determined quantum yields with 228-nm excitation.

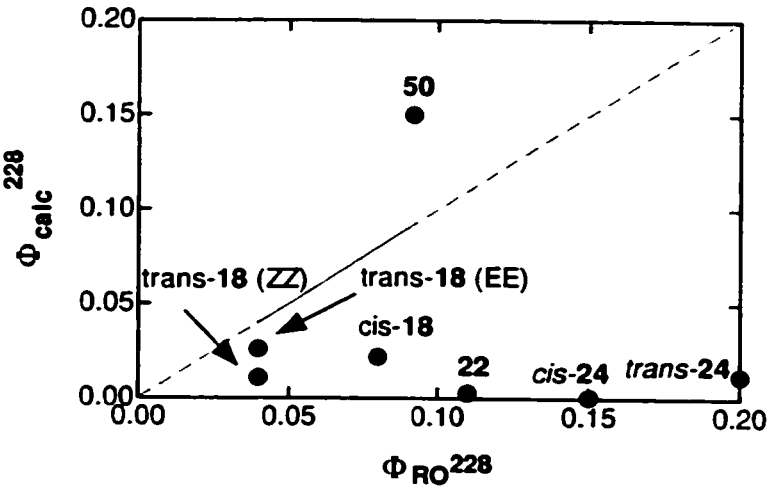

Additional evidence to suggest that hot ground state reactivity is unimportant comes from comparing the actual and calculated *E,E/Z,Z*-**19** ratios from ring-opening of *trans*-**18**. It was defined in Chapter 2 that *trans*-**18** produces an initial mixture of *E,E/Z,Z*-**19** that is approximately 1:1 at 228-nm.[17] The relative Φ_{calc}^{228} values suggest that the lower limit of the expected ratio from hot ground state ring-opening should be E,E/Z,Z = 2.4:1. Note that this ratio is a *minimum* value since it would be expected to increase as the system loses energy. Figure 3.4 shows quite clearly that the rate constant for ring-opening to *Z,Z*-**19** decreases more quickly than that for formation of *E,E*-**19**.

Excitation of the cyclobutenes at 214-nm (46729 cm^{-1}) populates an even higher vibrational level of the ground state after internal conversion. However, analysis of the quantum yield data at this wavelength provides similar conclusions (Table 3.3). According to the Φ_{calc}^{214} values, hot ground state reaction can only account for ~30% of the conrotatory ring-opening component of *cis*-**18**. In addition, only 60% of the *E,E*-**19** and 70% of the *Z,Z*-**19** from *trans*-**18** can be produced by hot ground state reactivity at 214-nm.

Although some of the calculated values are suspiciously close to the actual Φ_{RO} , the majority of evidence is against hot ground state involvement in the photochemical conrotatory ring opening of cyclobutenes. This is especially evident in the cases of **22** and **24**, where the Φ_{calc} values are a small fraction of the actual quantum yields (Figure 3.6). At most, a portion of the observed ring-opening can be derived from thermal reaction, but there must be another mechanism which leads to these products. The implications of this conclusion can be carried further into organic photochemistry. For instance, if photochemical cyclobutene ring opening in solution is not subject to hot ground state reaction then it is very unlikely that the cycloreversion of norbornadiene (**91**) occurs by the hot ground state mechanism in solution since the reaction has a higher activation energy. Indeed, the RRKM analysis of the cycloreversion reaction of **91** revealed that only 9% of the quantum yield in solution can be accounted for by hot ground state reactivity.[126] Realistically, due to the extremely low activation energy associated with cyclobutene ring opening and

the results of this work, the possibility of observing such a reaction is minimal. This conclusion has been alluded to by Troe during their studies of vibrational deactivation of organic molecules in the gas phase and solution.[102] Both the current study and that by Troe, rely on RRKM theory in the interpretations. In using RRKM theory to describe the reaction dynamics, it is assumed that the ring-opening is ergodic.[115] Herek and coworkers have recently demonstrated that if the rate of reaction at high energies is faster than IVR, nonergodic behaviour can be observed.[127] However, one might expect much larger quantum yields for ring-opening if the present system were actually nonergodic in nature.

Chapter 4.

The Effect of Central Bond Torsional Restrictions on the Rydberg State Ring-Opening of Alkylcyclobutenes

4.1. Introduction

With the possibility of hot ground state reactivity from the Rydberg excited state excluded as a major contributor to the conrotatory stereospecificity in the photochemical ring-opening of cyclobutenes, another reasonable mechanism is still required. A viable alternative is a mechanism in which ring-opening proceeds directly from the Rydberg π,R(3s) state. As mentioned earlier in Chapter 1, it has been shown that the Rydberg states of alkenes possess radical cation characteristics as they are susceptible to nucleophilic attack and skeletal rearrangements analogous to those of carbocations. [3,85,86,128] Previous work,[14,15] including that in Chapter 2, has demonstrated that alkylcyclobutenes behave in similar fashion. However, cyclobutene radical cations have also been shown to undergo ring-opening to produce the 1,3-butadiene radical cation. This reaction has been studied both experimentally and computationally, and there is evidence

to suggest that it occurs with conrotatory stereospecificity in such a way that the resulting diene is formed in the s-*trans* conformation (eqn. 4.1).[129-131]

[4.1]

If ring-opening from the Rydberg state occurs with similar characteristics, a marked influence of torsional flexibility about the central bond would be expected. Consequently, the photochemistry of bicyclic cyclobutenes **44-46** was studied at 214- and 228-nm to examine the effects of systematic variation in the degree of incipient torsional strain on the central bond of the system.

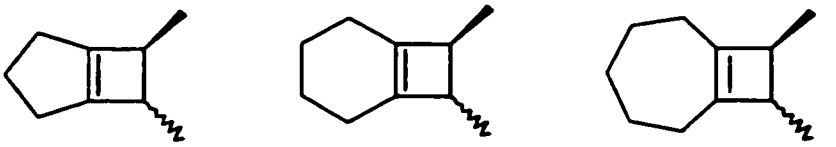

44 **45** **46**

4.2. Results

4.2.1. Preparation of the Cyclobutenes and their Isomeric Dienes

The bicyclic cyclobutenes (or dimethylbicyclo[*n*.2.0]alk-(*n*+2)-enes), **44-46**, and their diene photoproducts (**47-49**) were prepared as described by Leigh and Postigo.[16] The reaction sequence involved three steps including the zirconocene mediated (**98**) synthesis of 1,2-bis(ethylidene)cycloalkanes as developed by Negishi[132] and Nugent.[133] The resultant E,E dienes were easily purified by radial chromatography. Direct irradiation of a deoxygenated hexane solution of the E,E diene (0.1 M) resulted in a mixture of products including the desired cis and trans cyclobutenes, along with the E,Z diene isomer and small amounts of the Z,Z isomer (eqn. 4.2).

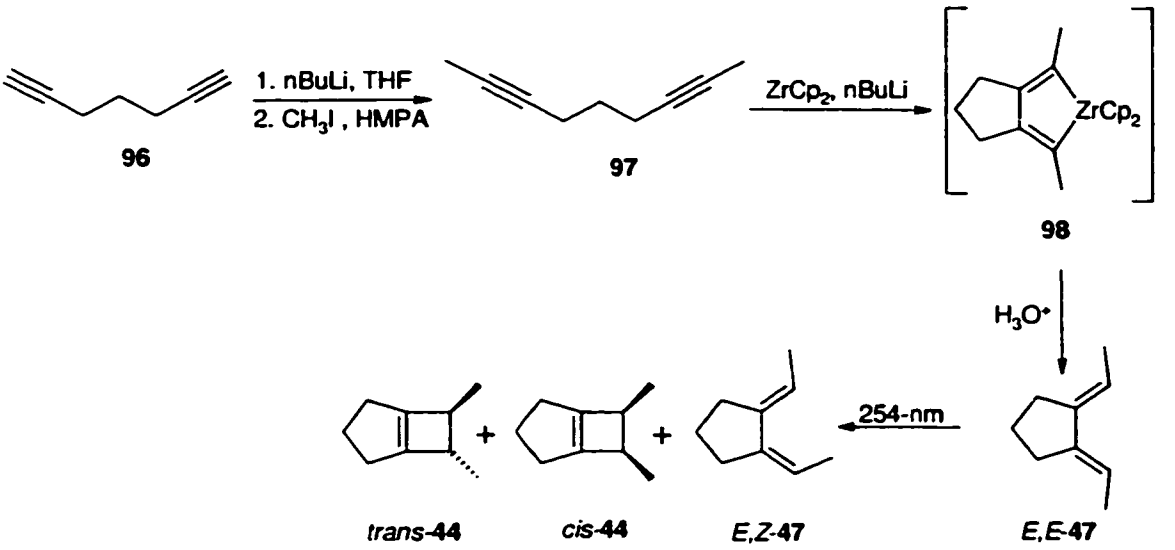

96 97 98

trans-44 *cis*-44 *E,Z*-47 *E,E*-47

[4.2]

The cyclobutenes and E,Z diene isomers were isolated and purified by semipreparative gas chromatography. Further purification of the cyclobutenes by column chromatography was required to remove small amounts of diene contaminants. An alternative route to the E,Z and Z,Z diene isomers was used in some cases. Triplet sensitized irradiation of the E,E isomer provided a good yield of the E,Z diene and also allowed identification of the Z,Z isomer by gas chromatography and GC-MS.

The uv absorption spectrum of *cis*-**45** was obtained in the gas phase at *ca.* 2 torr and is shown in Figure 4.1.

Figure 4.1. The UV absorption spectrum of *cis*-**45** in the gas phase (*ca.* 2 torr).

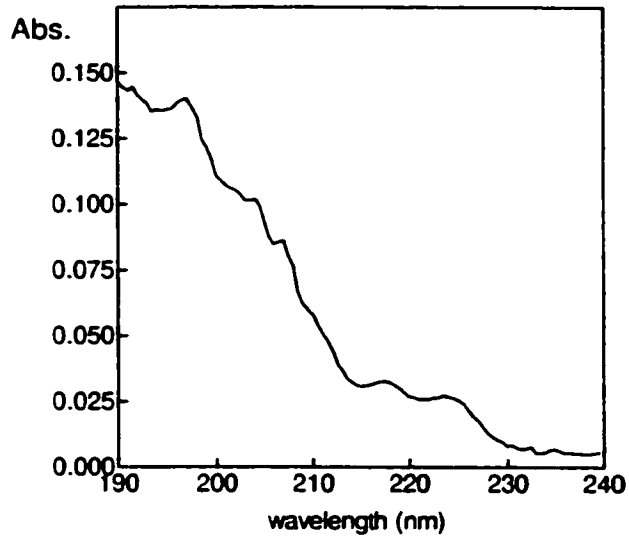

4.2.2. Irradiation of Dimethylbicyclo[*n*.2.0]alk-(*n*+2)-enes, **44-46**

Hexane solutions of **44-46** (*ca.* 0.05 M) containing a small amount of *n*-octane as an internal standard were irradiated at 214-nm and 228-nm with the light from a Zn and Cd resonance lamp, respectively. The photoproducts were identified by co-injection with authentic samples of the E,Z and E,E diene isomers of **47-49** (eqn. 4.3). In most cases, the Z,Z isomer was not observed since the irradiations were performed at very low conversions (*ca.* 1-2 %) in order to minimize secondary irradiation of the initially produced mixture of diene isomers. However, the Z,Z isomers could be detected in photolyses carried out to higher conversions. The Z,Z isomer only appeared to be formed as a primary product in the 228-nm excitation of *trans*-**46**. *Z,Z*-Bis(ethylidene)cycloheptane

(*Z,Z*-**49**) was tentatively identified based on its GC retention time and GC-MS data, relative to that of the other isomers of **49**. For instance, *Z,Z*-**49** elutes before the other two diene isomers and the M+ and mass spectral fragmentation pattern from GC-MS analysis were similar to those of *E,Z*- and *E,E*-**49**. Analogous results corresponding to the signal of *Z,Z*-**49** were obtained from both the direct and sensitized irradiation of *E,E*-**49**, as well as the direct irradiation of **46** at 228-nm.

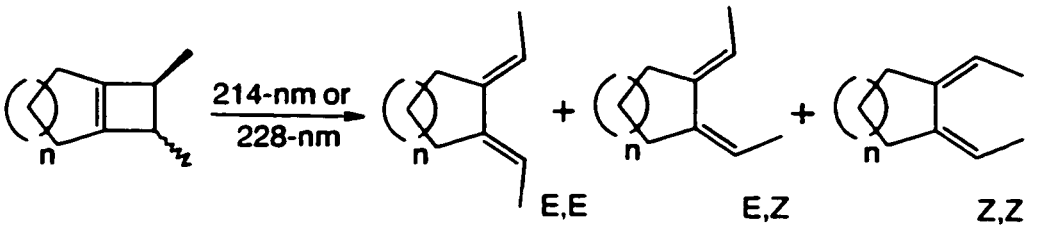

44 : n=1
45 : n=2
46 : n=3

47 : n=1
48 : n=2
49 : n=3

[4.3]

The production of the diene isomers was followed by GC analysis. Plots of concentration vs. time for all of the irradiations can be found in Appendix 3. Differences due to the GC-FID response were corrected by calibration curves for the diene isomers. Plots of diene isomer ratios against time were constructed to accentuate the effects of secondary irradiation of the dienes. In most cases these plots gave slopes that were indistinguishable from zero except with cis-**44**

and *trans*-**45** with 228-nm excitation. Examples of both of these plots are shown in Fig. 4.2, where the ratios are given as CON/DIS ([E,E+Z,Z]/[E,Z] for the trans cyclobutenes and [E,Z]/[E,E+Z,Z] for the cis cyclobutenes). The CON/DIS values for the irradiations at 214-nm were similar to those published previously.[16] The results are summarized in Table 4.1 as CON/DIS ring-opening ratios as taken from the y-intercepts of these plots.

In the case of *trans*-**46** where all three isomers of **49** were formed from 228-nm excitation, the diene isomer ratios were also plotted as E,E/E,Z and Z,Z/E,Z to confirm that the Z,Z isomer was indeed a primary photochemical product, and that secondary irradiation was unimportant. These plots gave slopes which did not significantly deviate from zero, and are shown in Figure 4.3.

Fig 4.2. Plots of conrotatory / disrotatory diene isomer ratios for **44-46** in hexanes (0.05 M) with 228-nm excitation.

a) *cis*-**44**

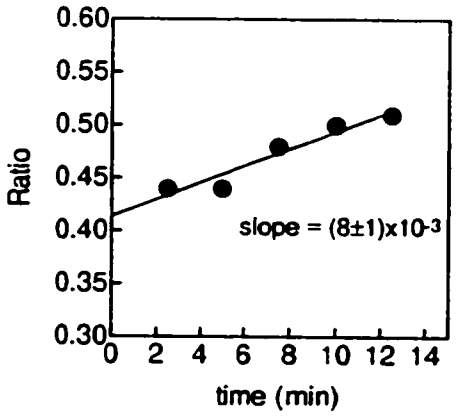

b) *trans*-**44**

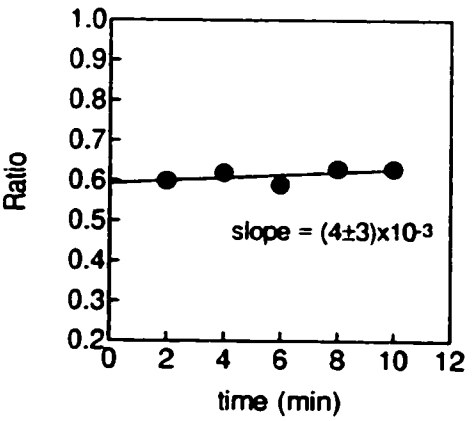

c) *cis*-**45**

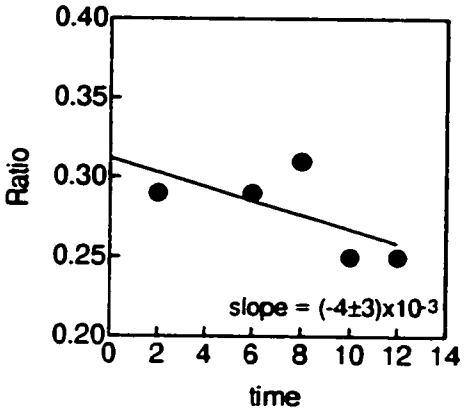

d) *trans*-**45**

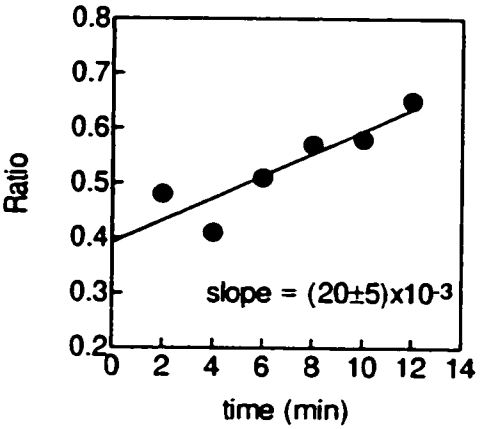

e) *cis*-**46**

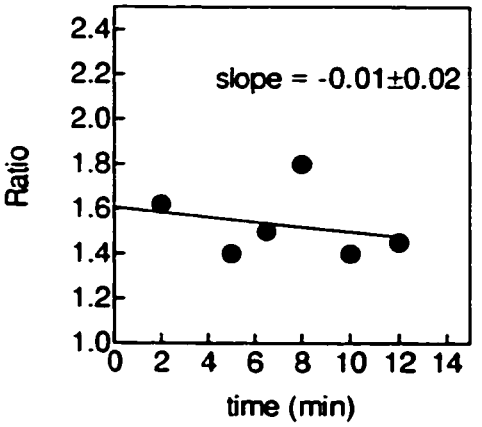

f) *trans*-**46**

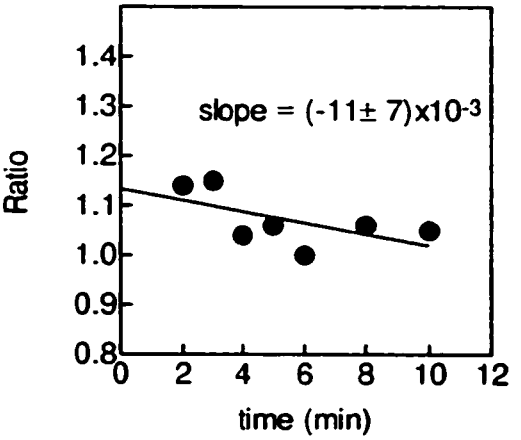

Figure 4.3. Plots of *E,Z*-/*E,E*-**49** and *E,Z*/*Z,Z*-**49** vs. time for the irradiation of *trans*-**46** at 228-nm (■ : *E,Z*/*E,E*-**49**, ● : *E,Z*/*Z,Z*-**49**).

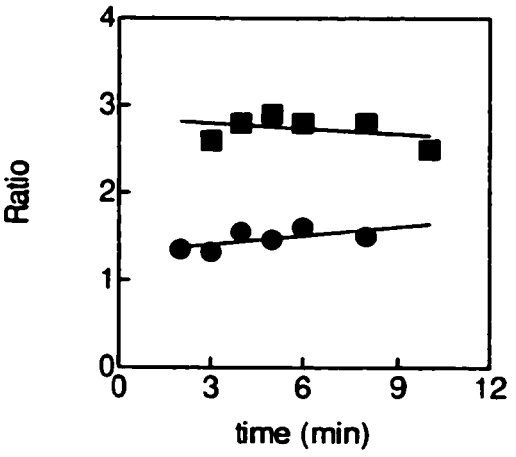

The photostationary states (PSS) of the various dienes were determined by monitoring the photolysis of the E,E isomer in hexanes at 228-nm over time until the diene isomer ratios remained unchanged for prolonged periods (*ca.* 2-5 hours). These values are also reported as CON/DIS ratios for each separate cyclobutene isomer in Table 4.1. For example, the PSS of **47** listed for *trans*-**44** is in the form of E,E/E,Z where that for *cis*-**44** is the inverse.

Table 4.1. Conrotatory to disrotatory ring-opening ratios[a] at 214-nm and 228-nm for **44**-**46** along with the photostationary state compositions at 228-nm for dienes **47**-**49** in hexanes.

Compound	CON / DIS		PSS (CON/DIS)
	214-nm	228-nm	228-nm
cis-**44**	0.52 ± 0.01	0.42 ± 0.01	0.8
trans-**44**	0.40 ± 0.05	0.57 ± 0.03	1.2
cis-**45**	0.24 ± 0.03	0.31 ± 0.03	0.8
trans-**45**	0.22 ± 0.01	0.39 ± 0.04	1.2
cis-**46**	0.15 ± 0.03	1.6 ± 0.2	1.8
trans-**46**	0.42 ± 0.04	1.1 ± 0.1	0.6

a. Taken as the y-intercepts from plots of diene ratios vs. time.

4.3. Discussion

4.3.1. The Ring-Opening of Cyclobutene Radical Cations

The ring-opening of cyclobutene radical cations has been studied both experimentally[129,134-139] and computationally.[37,130,131,140,141] Early computational results[130] from Bauld and coworkers demonstrated that a *nonelectrocyclic* pathway proceeding via a cyclopropyl carbinyl intermediate (**100**) was favoured over the presumed electrocyclic reaction pathway (eqn. 4.4).[134,135,141] Although both pathways were shown to proceed with conrotatory rotation of the termini, it was suggested that the nonelectrocyclic ring opening would favour production of the diene radical ion (**101**) in the s-*trans* conformation over the s-*cis*. The formation of the s-*trans* butadiene as a primary product has been suggested on numerous occasions in both theory and experiment.[129,131,139,140,142,143]

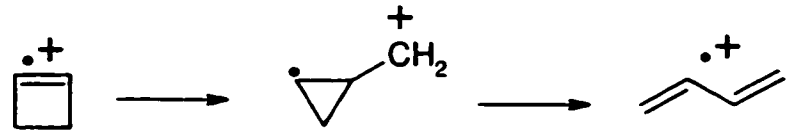

99 **100** **101**

[4.4]

Bally and coworkers have also produced both experimental[129,139] and computational[131,140,142] studies in the thermal and photochemical ring-opening of cyclobutene radical cations. Recent high-level *ab initio* calculations appear to have delineated the mechanistic intricacies of the ground state ring-opening of these species. These studies have shown that there are four reactants which can be interconnected on the potential energy surface; cyclobutene $\bullet+$ (**99**), s-*cis*-butadiene $\bullet+$ (s-*cis*-**101**), s-*trans*-BD $\bullet+$ (s-*trans*-**101**), and bicyclobutane $\bullet+$ (**102**). [131,140,143] The ring-opening reaction can proceed to the conrotatory product by one of two mechanisms. The first possibility is a concerted mechanism which proceeds along a C_1 symmetric pathway. The second is a stepwise reaction passing through a cyclopropylcarbinyl intermediate along a C_2 symmetric pathway. Interestingly, both processes are nonsynchronous and occur with *conrotatory* stereochemistry. These pathways are shown in equation 4.5. It was determined that a plateau exists on the PES in which the transition state geometry resembles the cyclopropyl carbinyl intermediate (**100**) proposed much earlier by Bauld.[130] The transition state in the plateau region connects all of the reactants along a C_2 symmetric pathway.

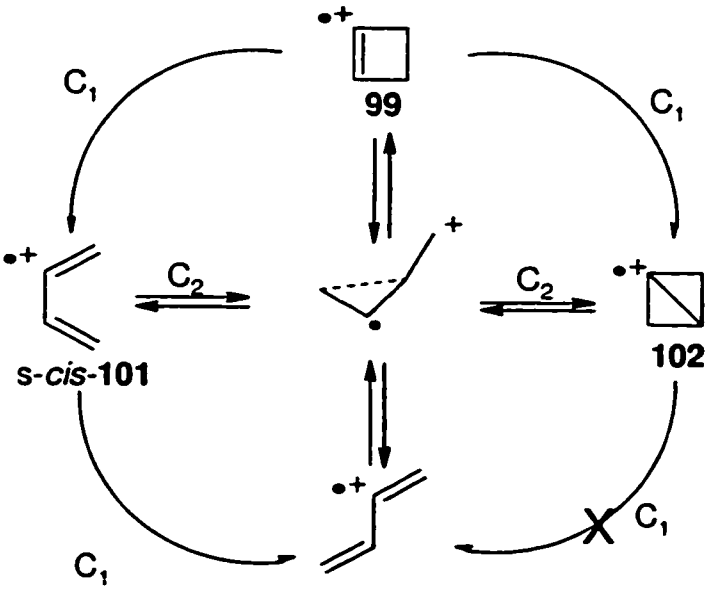

[4.5]

When solvent is accounted for in the calculations, the stepwise mechanism is favoured by at least 1 kcal/mol.[131] The $\Delta G^{\ddagger}$ for the concerted pathway (b) was found to be 21.2 kcal/mol, whereas that of the stepwise pathway (a) is 20.1 kcal/mol (eqn. 4.6). They have suggested that this difference is enough to introduce stereospecificity in the thermal reaction.

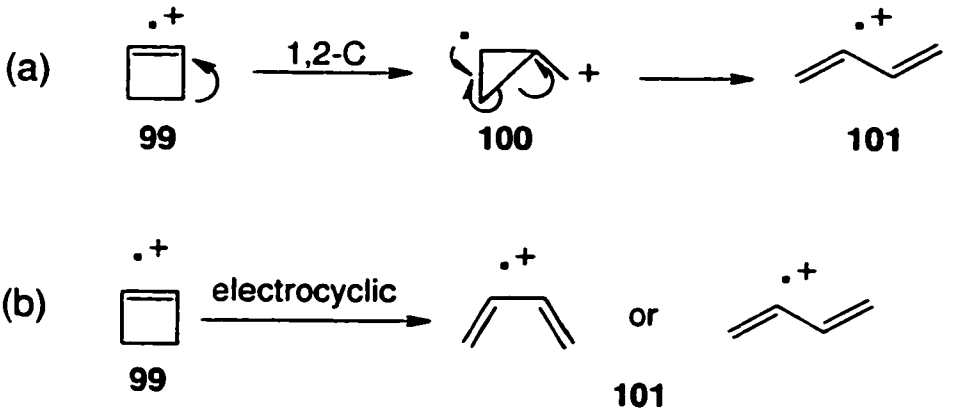

[4.6]

4.3.2. The Effect of Incipient C1-C2 Torsional Mobility on the Rydberg State Ring-Opening of Cyclobutenes

If the Rydberg state ring-opening of cyclobutenes is occurring in analogous fashion to the ring-opening of cyclobutene radical ions, the incipient torsional flexibility in the central bond ought to be important in the outcome of the reaction. In order to examine the effects of this torsional flexibility on the Rydberg state ring-opening, the same cyclobutenes which provided evidence in support of an adiabatic mechanism (**44-46**) were studied.[16,37] The UV spectra of these bicyclic derivatives were obtained in hexanes solution by Leigh, Postigo and Zheng.[16] The spectra are analogous to those observed with monocyclic alkylcyclobutenes, suggesting that the transition to the π,R(3s) Rydberg state occurs with similar efficiency. Previous evidence suggests that ring strain has no effect on the Rydberg state transitions of cycloalkenes such as cyclopentene,

cyclohexene, and cyclooctene.[11] The gas phase UV spectrum of *cis*-**45** (Fig. 4.1) confirms this, as the Rydberg transitions (as described in Chapter 2) are clearly visible between 220- and 230-nm.

The compounds were irradiated at both 214-nm and 228-nm in hexanes solution to compare the diene isomer ratios produced from the Rydberg state excitations to those obtained at a shorter wavelength. It was expected that increased strain on the central bond would significantly reduce the photochemical reactivity of the cyclobutene from the Rydberg state, since formation of the s-*trans* diene would be unfavourable. Equation 4.7 shows the Rydberg state ring-opening of **44**-**46** to the highly strained s-*trans* conformation of the dienes.

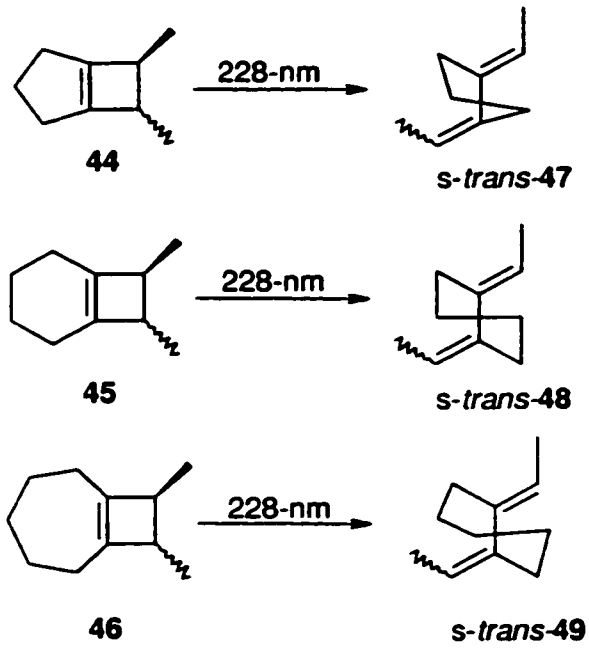

[4.7]

The results of this study show a trend which appears to be related to the incipient torsional flexibility of the central bond of the cyclobutene. The photochemical ring-opening of **44** and **45** with 228-nm excitation does not favour conrotatory ring-opening as the monocyclic derivatives, *cis*- and *trans*-**18**, do. In fact, the excitations yield mixtures of diene isomers that are similar to those obtained with 214-nm excitation (Table 4.1). Although with *cis*-**44** and *trans*-**45** there is some detectable secondary isomerization with 228-nm excitation, (Figures 4.2.a and d, respectively) the effect is unimportant since the CON/DIS ratio is *less* than that observed in the photostationary state. If **44** and **45** were opening with conrotatory stereospecificity and undergoing secondary isomerization, the observed CON/DIS ratio would be equal to, or *greater* than the PSS value. For instance, as secondary irradiation ensued the diene isomer ratio could only decrease until it reached the PSS. Equation 4.8 depicts the observed product ratios of a) the actual 228-nm photolysis of *cis*-**45** and b) the minimum CON/DIS ratio (the PSS) which would result from secondary photolysis of *E,Z*-**48**.

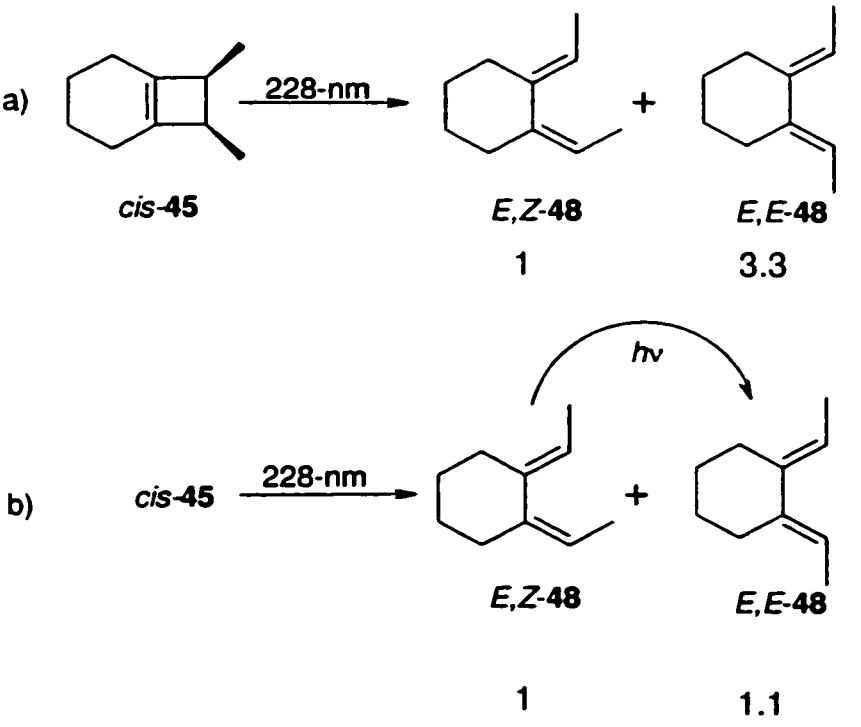

[4.8]

In contrast, mixtures enriched in the conrotatory ring-opening product are observed upon 228-nm excitation of *cis*- and *trans*-**46** (Table 4.1). Although the ring-opening of these derivatives does not appear to occur with the same degree of conrotatory stereospecificity as *cis*- and *trans*-**18**, there is an important trend observed in the photolysis of **44-46**. The derivatives with small ancillary rings, and increased incipient torsion about the central bond, produce similar diene isomer ratios from the Rydberg state ring-opening as they do from the π,π^* state. As the size of the ancillary ring is increased (and the incipient torsional strain is decreased), an increase in conrotatory ring-opening is observed. The

importance of the incipient torsional strain on the central bond in the photochemical ring-opening of these cyclobutenes strongly suggests that the ring-opening from the Rydberg state occurs with a similar mechanism to the ring-opening of cyclobutene radical cations, and produces the s-*trans* diene conformer as the initial product.

Another intriguing aspect of the Rydberg excited state reactivity is revealed in this study. One might expect that if the Rydberg state ring-opening were impossible, i.e. the torsion on the central bond is too high, that internal conversion to the ground state would predominate. This is obviously not so, as ring-opening is observed in all cases. In fact, the difference between the CON/DIS ratios at the two wavelengths (Table 4.1) for the smaller derivatives (**44-45**) is very small, whereas the CON/DIS ratios of the larger derivatives (**46**) change markedly. The fact that the ratios for the ring-opening of **44** and **45** remain constant between the two excitation wavelengths indicates that there must be a crossing between the π,π^* and π,R(3s) excited states when there is little flexibility in the central bond. When the flexibility increases (as in *cis*- and *trans*-**46**) the reactivity changes towards that displayed by the "pure" Rydberg state (stereospecific conrotatory ring opening)[17] suggesting that the crossing becomes less important (eqn. 4.9).

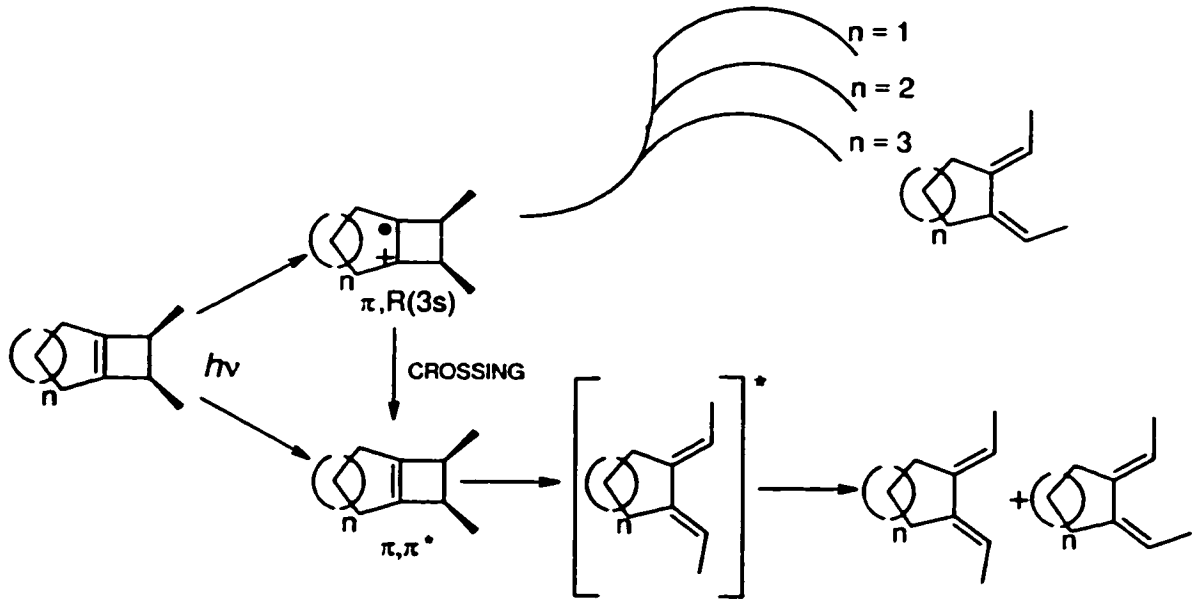

[4.9]

Since the π,R(3s) state lies below the π,π* in tetraalkyl substituted alkenes,[11,12] a surface crossing between these two states requires either an increase in the energy of the Rydberg state or a decrease in energy of the π,π* state. A similar crossing between these states which occurs with an increase in the Rydberg state energy, has been proposed for the twisting of singlet ethylene.[144] The fact that monocyclic cyclobutenes open with conrotatory stereospecificity (Chapter 2) suggests that it is also possible to avoid the crossing to the π,π* state surface completely. This implies that restricting torsional mobility about the central bond of the incipient diene results in an energy barrier for ring-opening on the potential energy surface of the π,R(3s) state. Derivatives with free rotation can progress along the Rydberg state

potential energy surface with little or no barrier to ring-opening, and without crossing to the valence state surface. For cyclobutenes with more hindered rotation, a barrier is met which causes the Rydberg state PES to rise in energy and cross with that of the π,π^* state. As the cyclobutene begins to climb along this pathway, it crosses with the π,π^* state manifold and follows the new surface to product formation. An illustration of this concept is presented in Figure 4.4.

Figure 4.4. A reaction coordinate diagram depicting possible π,π^* state and π,R(3s) state ring-opening pathways.

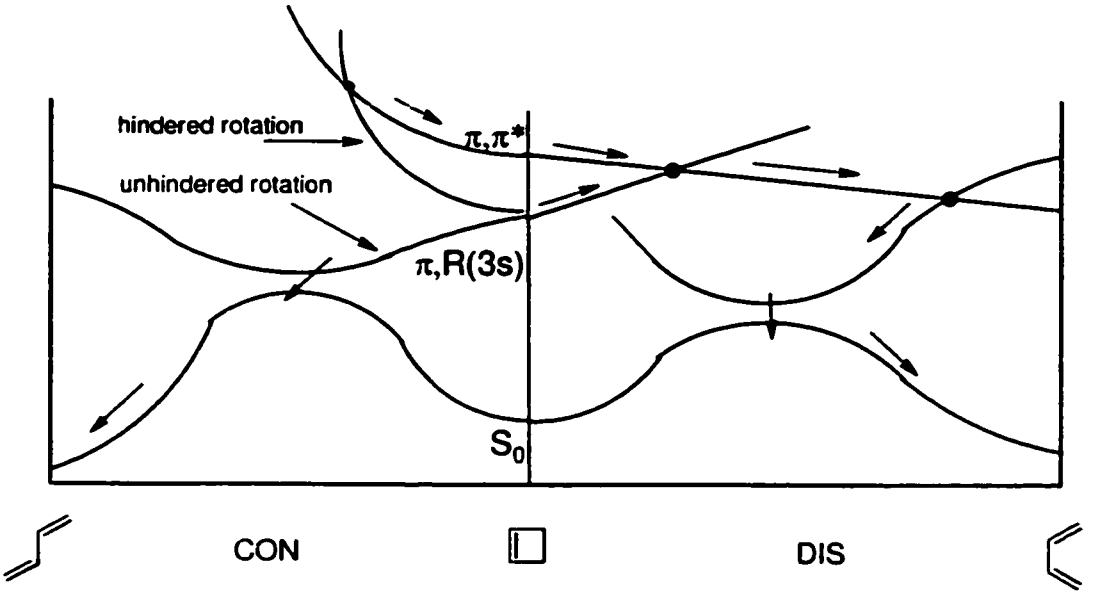

In this two-dimensional depiction of the reaction coordinate diagram, disrotation leads to the s-*cis* conformer of the diene, whereas conrotation provides the s-*trans*. The π,π^* excited state reaction occurs adiabatically, and produces the s-cis diene in the excited state. The ground state is accessed along the potential energy surface of the diene. When the Rydberg state potential energy surface is followed, disrotatory ring-opening to the s-*cis* diene is unfavoured, and the crossing to the ground state occurs along the pathway to the s-*trans* diene. As stated earlier, this pathway is likely preceded by a small energy barrier for cyclobutenes which open to dienes with free central bond rotation, but a large barrier for cyclobutenes in which the incipient central bond rotation is hindered. In the latter cases, a state crossing is encountered which leads to the π,π^* state surface and products of adiabatic ring-opening are obtained.

Perhaps of predominant importance these data also support an adiabatic ring-opening mechanism from the π,π^* state. The contribution of the Rydberg state is limited to systems in which there is facile rotation about the incipient central bond. It follows that the initial investigations into the adiabatic ring-opening involving cyclobutenes **44** and **45**[6,50] were observed in the absence of the Rydberg state ring opening and the results were thus indicative of the valence π,π^* state reactivity.

Chapter 5

Conclusions and Contributions of this Research

The most fundamental conclusion that can be made from this research is that the reactivity of cyclobutene Rydberg π,R(3s) excited states is not limited to cycloreversion. This work has shown that the Rydberg state contributes to the photochemical ring-opening of cyclobutenes. This new ring-opening reaction occurs in similar fashion to that which is proposed for cyclobutene radical cations, likely due to the electron deficient core of cyclobutenes in the Rydberg state.[13,84] The stereochemical course of the process is dependent on the degree of incipient torsional strain about the central bond. For instance, with cyclobutenes which give rise to dienes with free rotation about this bond, the π,R(3s) state opens with conrotatory stereospecificity. When rotation about this bond is restricted due to torsional strain, the observed ring-opening is analogous to that of the valence π,π^* state. This suggests that there exists a surface crossing between the Rydberg and π,π^* states which is accessed when there is significant torsional strain about the central bond in the diene products. From this result, it can be concluded that the previously proposed adiabatic ring

opening mechanism from the π,π^* state is valid.[16,20,39,50] The photochemical ring-opening of alkylcyclobutenes in the π,π^* state proceeds via the orbital symmetry-allowed pathway to yield the disrotatory diene isomer in the excited state. The excited diene then yields a mixture of isomers as it relaxes to the ground state through excited state *E,Z*-isomerization.

This research has also shown that hot ground state reactivity is unimportant in the photochemistry of cyclobutenes despite their low molecular weight (and vibrational degrees of freedom) and activation energies for thermal ring-opening. This is indicated by the lack of a correlation between experimental quantum yields for conrotatory ring-opening at 228-nm and those calculated from theoretical rate constants. The nonstereospecific ring-opening of **44-46** with 228-nm excitation verifies this conclusion.

Chapter 6.

Experimental Details

6.1. General

^{1}H nmr and ^{13}C nmr spectra were recorded on a Bruker AM200 (200MHz) spectrometer, and are reported in parts per million downfield from tetramethylsilane. Mass spectra were obtained by GC/MS, using a Hewlett-Packard 5890 gas chromatograph equipped with a HP-5971A mass selective detector and a DB-5 microbore capillary column (15m x 0.2mm; Chromatographic Specialties, Inc.). Ultraviolet absorption spectra were recorded on a Perkin-Elmer Lambda 9 or a Cary 50 spectrometer. Gas chromatographic analyses were carried out on a Hewlett-Packard 5890 gas chromatograph equipped with a flame ionization detector, a Hewlett-Packard 3396 integrator and one of three different columns. Analyses for experiments with **50**, *cis*- and *trans*-**18**, and **22** were performed on a DB-1 megabore capillary column (30m x 0.53mm ID). Experiments with *cis*- and *trans*-**24** were performed on a DB-17 megabore capillary column (15m x 0.22mm ID), while those for the dimethylbicyclo[*n*.2.0]alk-(*n*+2)-enes, **44-46**, were performed on a DB-1

microbore capillary column (15m x 0.22mm ID). Relative peak areas of the products were corrected for the FID response with calibration curves.

Semi-preparative gas chromatographic separations were performed on a Varian gas chromatograph equipped with a thermal conductivity detector and one of four columns : a) 20% β,β-oxy-bis(dipropionitrile) (ODPN) on 80/100 Chromosorb PNAW (20' x 0.25", stainless steel; Chromatographic Specialties), b) 3.8% UC W982 on 80/100 Supelcort (24' x 0.25", stainless steel; Supelco), c) 20% TCEP on 80/100 Chromosorb PNAW (6' x 0.25", stainless steel; Chromatographic Specialties), or d) 15% Carbowax on 80/100 Chromosob PNAW (12' x 0.25", stainless steel; Chromatographic Specialties).

Irradiations employed one of six light sources; a) an ArF excimer laser (unfocused, operated at an output power of *ca.* 80 mJ and a repetition rate of 1 Hz), b) a 16-W Philips 93106E zinc resonance lamp (unfiltered), c) a 16-W Philips 93107E cadmium resonance lamp (unfiltered), d) RPR 253.7-nm lamps, e) RPR 300.0-nm lamps, or f) a 100 W Hanovia medium pressure mercury lamp with a Vycor filter.

6.2. Commercial Reagents

Hexanes, isooctane, cyclohexane (all BDH Omnisolv), pentane, ethyl acetate, 2-propanol and dichloromethane were used as received. Tetrahydrofuran, ether, and benzene were distilled over sodium prior to use.

Hexamethylphosphoramide (Aldrich) was dried over 4A molecular sieves, and pyridine (Aldrich) was dried over KOH pellets. 2,3-Dimethyl-1,3-butadiene, 2,3-dimethylmaleic anhydride, acetophenone, *cis*- and *trans*-2-butene, 2-butyne, bromoform, cyclopentene, potassium *tert*-butoxide, lithium aluminum hydride, octane, n-decane, n-butyllithium, methyllithium, bis(cyclopentadienyl) zirconium dichloride, methyl iodide, lead (IV) tetraacetate, mercuric chloride, 2-butanone, cyclohexanone and 3-methyl-2-butanone were all used as received from Aldrich Chemical Co. Ammonia was used as received from Liquid Air™. 1,6-Heptadiyne, 1,7-octadiyne, and 1,8-nonadiyne were used as received from Lancaster Inc., as were uranyl sulfate (Alfa Inorganics) and ceric ammonium nitrate (Fischer Scientific CO.). Sodium oxalate (J.T. Baker Chemical Co.) was recrystallized from water prior to use.

6.3. Preparation of Cyclobutenes

6.3.1. 1,2-Dimethylcyclobutene (**50**)

A solution of 2,3-dimethyl-1,3-butadiene (**53**) (2.1g, 0.026 mol) in pentane (50 mL) was placed in four 12.5 mL quartz tubes, sealed with rubber septums and deoxygenated with a stream of dry argon for 20 min. The samples were irradiated in a Rayonet reactor for *ca.* 36hrs with eight 253.7-nm lamps. The sample was concentrated by distillation of the solvent to a volume of *ca.* 2.5 mL.

Purification was accomplished by semi-preparative gas chromatography on column (a), to a purity of >99% as determined by GC. The compound was identified as **50** by spectral data similar to those previously published.[24]

^{1}H nmr ($CDCl_3$) δ : 1.56 (s, 6H), 2.22 (s, 4H).

6.3.2. *cis*- and *trans*-1,2,3,4-Tetramethylcyclobutene (**18**)

Dimethylmaleic anhydride (**74**; 3.8g, 0.03 mol) and acetophenone (1.5 mL) were dissolved in ethyl acetate (0.35 L) and placed in a 1 L immersion well fitted with a water cooled jacket. The solution was deoxygenated with a stream of dry nitrogen for 20 minutes and cooled to -78°C. Approximately 25 mL of condensed 2-butene was then poured into the vessel. The solution was irradiated for 6 hours with a Hanovia medium pressure mercury lamp and the solvent was removed under reduced pressure. The product was purified by vacuum distillation (50 °C, 0.5 mmHg) of the residue, affording a yellow oil identified as **75** on the basis of similar spectral data to those determined previously.[91] The purity of the compound was estimated to be 90% by GC.

^{1}H nmr ($CDCl_3$) δ : 0.95 (d, 6H), 1.24 (s, 6H).

A sample of **75** (2.0 g, 0.011 mol) was dissolved in 20 mL of dry pyridine in a three-necked 100 mL round bottom flask fitted with a vigreux column connected to three cooled traps (-78 °C). The reaction mixture was oxygenated

with a stream of oxygen for 20 minutes. Lead (IV) tetraacetate (5.5 g, 0.015 mol) was added to the mixture, and the reaction vessel was placed in a preheated oil bath (*ca.* 65 °C). When the evolution of CO_2 was observed to cease, the temperature was increased to *ca.* 90 °C. The reaction mixture was stirred at this temperature for 8 hours while the cold traps were maintained at –78 °C, in order to collect the volatile products. After the allotted time, the traps, connecting tubes, and column were rinsed several times with pentane, the washings were combined and neutralized with 10% HCl, washed with water (2x10 mL), dried with $MgSO_4$ and filtered. The sample was then concentrated to *ca.* 1 mL by distillation. Separation and purification of the two major products was accomplished by semi-preparative gas chromatography on column (b). The isolated compounds were identified as *cis*- and *trans*-**18** on the basis of spectral data consistent with those previously reported.[14]

cis-1,2,3,4-Tetramethylcyclobutene (*cis*-**18**: 99% pure by GC) : ^{1}H nmr ($CDCl_3$) δ : 0.9 (d, 6H), 1.49 (s, 6H), 2.5 (m, 2H); MS m/e (I) : 110 (1), 108 (36), 93 (100), 91 (72), 77 (75), 65 (16), 53 (20), 39 (35), 27 (28).

trans-1,2,3,4-Tetramethylcyclobutene (*trans*-**18** : 98% pure by GC) : ^{1}H nmr ($CDCl_3$) δ : 1.0 (d, 6H), 1.50 (s, 6H), 1.99 (m, 2H); ^{13}C nmr : δ = 10.97, 16.62, 45.2, 138.6; MS m/e (I) : 110 (32), 95 (100), 79 (14), 67 (71), 55 (40), 41 (38), 27 (35).

6.3.3. Hexamethylcyclobutene (**22**)

A sample of **82** (5.0 g, 0.023 mol; obtained from Dr. J.A. Postigo) was dissolved in dry pyridine (50 mL). The procedure was identical to that used for the transformation of **75** to **18**. Separation and purification of the product were accomplished by semipreparative gas chromatography on column (b). It was identified as **22** (99% pure by GC) on the basis of the following spectral data.[35]

^{1}H nmr ($CDCl_3$) δ : 1.0 (s, 12H), 1.16 (s, 6H); MS m/e (I) : 138 (15), 123 (100), 107 (6), 95 (31), 91 (17), 81 (81), 67 (31), 55 (17), 53 (16), 41 (34), 39 (25), 27 (12).

6.3.4. *cis*-Tricyclo[6.4.0.0]dodec-1^2-ene (*cis*-**24**)

Shredded aluminum foil (6.0 g) and dichloromethane (200 mL) were placed in a 500 mL two-necked round bottom flask equipped with a condenser, an addition funnel and magnetic stirrer. Mercuric chloride (12.0 g, 0.044 mol) was dissolved in cyclohexanone (40.18 g, 0.41 mol) and placed in the addition funnel. Approximately 2 mL of this solution was added to the mixture and the flask was heated until a reaction was observed by the evolution of gas. The rest of the solution was added over 45 minutes and the mixture was stirred for 6 hours at 30 °C. The reaction was then quenched with distilled water (*ca.* 15 ml) resulting in the precipitation of a large amount of solid material. The solid was

filtered off and the solution was extracted with ether (3x30 mL). The combined ether layers were washed with distilled water, dried over $MgSO_4$, and filtered. The ether was removed under reduced pressure to leave a solid material which was recrystallized from petroleum ether / ethylacetate (1:1) to yield fine colourless needles of **84** (5.7 g, 20%; m.p = 126 ^{o}C).[145]

^{1}H nmr ($CDCl_3$) δ : 1.1 (m, 12H), 1.3-1.45 (cm, 4H), 1.5-1.7 (cm,2H), MS m/e (I) : 198 (1), 180 (1), 137 (3), 110 (2), 99 (100), 81 (67), 67 (9), 55 (30), 53 (11).

Compound **84** (2.5 g, 0.014 mol) was weighed into a 50 mL round bottom flask. Sulfuric acid (10%, 25 mL) was added to the flask all at once and the mixture was heated (90 ^{o}C) with stirring for 5 hours. Approximately 10 mL of ether was added, followed by sufficient 5% $NaHCO_3$ to neutralize the solution. The mixture was extracted with ether (3x20 mL). The combined ether layers were washed with 5% $NaHCO_3$ (10 mL) and water (10 mL), and then dried with $MgSO_4$ and filtered. The ether was removed under reduced pressure to yield a colourless liquid. The crude material was purified by radial chromatography with pentane, and identified as **25** (1.2 g, 7.4 mmol, 53%, 98% pure by GC) on the basis of the following spectral data.[145,146]

^{1}H nmr δ : 1.51-1.66 (cm, 8H), 2.12 - 2.19 (m, 8H), 5.76 (bs, 2H); MS m/e (I) : 162 (63), 147 (9), 133 (29), 199 (34), 91 (100), 79 (77), 65 (13), 53 (10), 41 (23), 27 (12).

A portion of the sample of **25** (1.0g, 6.2 mmol) and acetophenone (2.0 g, 16 mmol) were dissolved in distilled benzene (0.8 L), and placed in a 1.0 L quartz immersion well equipped with a Vycor filter. The solution was deoxygenated with a stream of dry nitrogen for 20 minutes and then irradiated with a medium pressure mercury lamp for 8 hours. The product and remaining **25** were separated from the acetophenone by radial chromatography with pentane, and then concentrated by distillation to *ca.* 1mL. The product was isolated by semi-preparative gas chromatography on column (d). It was identified as *cis*-**24** (99% pure by GC) based on the following spectral data.[34]

^{1}H nmr ($CDCl_3$) δ : 1.16 (bs, 8H), 1.53-1.77 (cm, 8H), 2.20-2.39 (cm, 2H); MS m/e (I) = 161 (1), 120 (30), 105 (100), 77 (60), 63 (2), 51 (17), 43 (6), 27 (1).

6.3.5. *trans*-Tricyclo[6.4.0.0]dodec-1^2-ene (*trans*-**24**)

Potassium *tert*-butoxide (12 g, 0.1 mol) was weighed into a flame-dried, two-necked 250 mL round bottom flask fitted with a nitrogen inlet and an addition funnel. A mixture of cyclopentene (6.8 g, 0.1 mol) in pentane (50 mL) was added and the solution was cooled to –15 °C. A solution of bromoform (30 g, 0.12 mol) in pentane (50 mL) was added drop-wise over 30 minutes via the addition funnel, while the reaction was vigorously stirred. The reaction mixture turned into a brown slurry. After four hours the reaction was quenched with water (50 mL), causing the solution to become orange and clear. The layers

were separated and the aqueous fraction was extracted with hexanes (3x25 mL). The combined organic extracts were washed with water and dried over $MgSO_4$. The drying agent was filtered off and the hexanes were removed under reduced pressure. Distillation of the product (45 °C, 0.1 mmHg) afforded a clear colourless liquid (12.2 g, 0.051 mols, 51%) which was identified as **86** (95% pure by GC) by the following spectral data.[147]

^1H nmr ($CDCl_3$) δ : 1.65 - 2.06 (cm, 6H), 2.22 (t, 2H); MS m/e (I) : 240 (4), 199 (32), 161 (22), 131 (4), 119 (4), 79 (100), 51 (27), 39 (27), 27 (21).

A three-necked, 500 mL round bottom flask fitted with a condenser, a rubber septum, and a nitrogen inlet was flame-dried under a stream of dry nitrogen. Dry ether (200 mL) was introduced and 30 mL of methyl lithium in ether (1.0 M) was added with a syringe. A sample of **86** (5.6 g, 0.024 mol) in dry ether was then added drop-wise with a syringe to the stirring solution over 45 minutes. The reaction was refluxed for 45 minutes and then quenched with water (20 mL). The layers were separated and the aqueous fraction was extracted with ether (3x30 mL). The combined organic fractions were washed with water (2x10 mL) and dried over $MgSO_4$. The drying agent was filtered off and the ether was removed under reduced pressure. The product was purified by radial chromatography from pentane to obtain a clear colourless liquid (2.3 g, 0.013 mol, 54%). It was identified as **87** based on the following spectral data.[147]

^{1}H nmr ($CDCl_3$) δ : 1.5-2.0 (cm, 12H), 2.2 (m, 2H), 5.4 (bs, 2H); MS m/e (I) : 182 (1), 154 (1), 139 (1), 123 (14), 110 (70), 95 (100), 81 (10), 67 (25), 56 (40), 39 (25), 27 (17).

A 250 mL, two-necked round bottom flask was set up with a dry ice condenser, placed under a nitrogen atmosphere and flame-dried. The trap was cooled to -78 °C with a CO_2/2-propanol bath. A sample of **87** (2.0 g, 0.013 mol) was added to the flask and also cooled to -78 °C. Ammonia was introduced via the gas inlet until *ca.* 125 mL had collected as a liquid. Solid sodium was added until the solution turned blue (0.9 g, 0.04 mol). The cold bath was then removed from beneath the flask and the reaction was refluxed for 45 minutes. The reaction was quenched with ethanol until the blue colour disappeared and then NH_4Cl (2g) was added. After allowing the excess ammonia to evaporate, the product was extracted from the flask with pentane (3x30 mL). The combined organic fractions were washed with water (3x15 mL) and dried with $MgSO_4$. The drying agent was filtered off and the pentane was removed under reduced pressure to yield a clear colourless oil. Purification by semi-preparative gas chromatography on column (d) resulted in *trans*-**24** (0.1 g, 6.2 mmol, 5% yield, 97% pure by GC). Further purification to remove trace amounts of 1,1'-bicyclohexenyl (**25**) was accomplished by column chromatography with silica doped with $AgNO_3$ (20% w/w). The product was identified as *trans*-**24** based on the following spectral characteristics.[34,147]

^{1}H nmr ($CDCl_3$) δ : 1.0-1.4(cm, 4H), 1.4-2.1 (cm, 4H), 2.22 (m, 2H); ^{13}C nmr ($CDCl_3$) δ : 20.14, 25.30, 27.07, 31.91, 46.53, 136.68; MS m/e (I) : 162 (90), 147 (12), 133 (37), 199 (44) 105 (45), 91 (100), 79 (75), 65 (15), 53 (12), 39 (16), 27 (7).

6.3.6. *cis*- and *trans*-6,7-Dimethylbicyclo[3.2.0]hept-1^{5}-ene (44)

A three-necked 250 mL round bottom flask fitted with a nitrogen inlet, an addition funnel, and a magnetic stirrer, was flame dried under a steady stream of dry nitrogen and cooled to –78 °C. The vessel was charged with 5.0 g (0.054 mol) of 1,6-heptadiyne and dry THF (100 mL). *n*-Butyl lithium (65 mL, 0.1 mol) was added drop-wise through the addition funnel to the stirring solution. After the addition was complete, the reaction was allowed to stir for one hour while the cold bath was maintained. A mixture of methyl iodide (14.2 g, 0.1 mol) and dry HMPA (25 mL) was then added drop-wise to the reaction over 25 minutes. When this addition was complete the cold bath was removed and the reaction was allowed to slowly warm to room temperature and then stirred for an additional 5 hours. The reaction was quenched with water (15 mL) and extracted into pentane (3x25 mL). The pentane fractions were combined and washed with water (15 mL) and saturated brine (15 mL), then dried over $MgSO_4$ and filtered. The pentane was removed under reduced pressure. Vacuum distillation (85 °C,

60 mmHg) provided a clear colourless liquid which was identified as 2,7-nonadiyne (5.7 g, 0.048 mol, 88%, 98% pure by GC).[133]

^{1}H nmr δ : 1.60 (t, 2H), 1,73 (s, 6H), 2.1-2.3 (cm, 4H); MS m/e (I) : 120 (2), 105 (100), 91 (40), 79 (28), 65 (22), 51 (18), 39 (38), 27 (21).

Bis(cyclopentadienyl) zirconium dichloride (4.3 g, 0.015 mol) was weighed into a flame dried three-necked 250 mL round bottom flask equipped with an addition funnel and magnetic stirrer, and kept under a steady stream of dry nitrogen. The flask was cooled to –78°C and dry THF (100 mL) was added. *n*-Butyl lithium (20 mL, 0.03 mol) was added drop-wise through the addition funnel and the reaction was allowed to stir for one hour at –78°C. A portion of 2,7-nonadiyne (4.3 g, 0.015 mol) was mixed with 20 mL of dry THF and added drop-wise through the addition funnel over 20 minutes. After the addition was complete the reaction was slowly allowed to warm to room temperature and then stirred for 5 hours. The reaction was quenched with 6 M HCl (8-mL) and extracted into pentane (3x25 mL). The pentane fractions were combined and washed with water (3 x 15 mL) and saturated brine (10 mL), dried over $MgSO_4$ and filtered. The pentane was removed by distillation. Radial chromatography with pentane provided 1.2 g of a clear colourless liquid which was identified as *E,E*-**47** (1.2 g, 0.01 mol, 67%, 99% pure by GC).[16]

^{1}H nmr ($CDCl_3$) δ : 1.25 (m, 2H), 1.65 (d, 6H), 5.70 (m, 2H); MS m/e (I) : 122 (35), 107 (30), 93 (60), 91 (66), 79 (100), 77 (48), 65 (16), 51 (15), 39 (30), 27 (12).

A portion of *E,E*-**47** (1.0 g, 0.01 mol) was dissolved in 25 mL of hexanes (Omnisolv) and poured into two 12.5 mL quartz tubes fitted with rubber septums. The solutions were deoxygenated with a stream of dry argon for 20 minutes and then irradiated in a Rayonet reactor with eight 253.7-nm lamps for 15 hours. The hexanes were removed by distillation to leave a volume of *ca.* 2 mL. Semi-preparative gas chromatography on column (c) allowed isolation of *cis*- and *trans*-**44** as identified based on the following spectral data.[16] Further purification by column chromatography on silica doped with $AgNO_3$ (20% w/w) removed small amounts of *E,E*-**47** and resulted in *cis*- and *trans*-**44** in 99% purity by GC.

cis-6,7-Dimethylbicyclo[3.2.0]hept-1^5-ene (*cis*-**44**) ^{1}H nmr δ : 0.99 (d, 6H), 1.94-2.24 (cm, 6H), 2.85 (m, 2H); ^{13}C nmr δ : 14.08, 26.31, 29.75, 38.66, 153.88; MS m/e (I) : 122 (32), 107 (32), 93 (75), 91 (70), 79 (100), 77 (45), 65 (10), 53 (8), 39 (15), 27 (7).

trans-6,7-Dimethylbicyclo[3.2.0]hept-1^5-ene (*trans*-**44**) ^{1}H nmr δ : 1.12 (d, 6H), 2.0 (cm, 2H), 2.19-2.30 (cm, 6H); ^{13}C nmr δ : 17.66, 26.22, 29.76, 44.66, 152.75;

MS m/e (I) : 122 (56), 107 (42), 93 (84), 91 (70), 79 (100), 77 (45), 65 (10), 53 (8), 39 (15), 27 (12).

6.3.7. *cis*- and *trans*-7,8-Dimethylbicyclo[4.2.0]oct-1^6-ene (**45**)

The procedure was identical to that used for **44** except that the starting material was 1,7-octadiyne (4.3 g, 0.041 mol). The spectral characteristics of the synthetic intermediates and the products were similar to those previously reported.

2,8-Decadiyne :[133] yield : 2.7 g, 0.02 mols, 49% (99% pure by GC) bp : 120 °C, 70 mmHg; ^{1}H nmr ($CDCl_3$) δ : 1.53 (m, 4H), 1.75 (s, 6H), 2.1 (bs, 4H); MS m/e (I) : 134 (1), 133 (8), 119 (62), 106 (45), 91 (100), 79 (45), 67 (20), 53 (55), 39 (45), 27 (45).

E,E-1,2-Bis(ethylidene)cyclohexane:[16]: yield : 2.0 g, 0.015 mols, 74%, 98% pure by GC; ^{1}H nmr ($CDCl_3$) δ : 1.26 (m, 4H), 1.58 (d, 6H), 2.19 (bs, 4H); MS m/e (I) : 136 (58), 121 (22), 107 (63), 91 (46), 79 (100), 63 (21), 53 (18), 39 (41), 27 (32).

cis-7,8-Dimethylbicyclo[4.2.0]oct-1^6-ene:[16] (99% pure by GC) ^{1}H nmr ($CDCl_3$) δ : 0.94 (d, 6H), 1.58 (m, 4H), 1.80 (m, 4H), 2.79 (m, 2H); MS m/e (I) : 136 (41), 121

(26), 107 (72), 105 (11), 93 (50), 91 (46), 79 (100), 77 (31), 67 (29), 53 (16), 39 (32), 27 (21).

trans-7,8-Dimethylbicyclo[4.2.0]oct-1^6-ene:[16] (99% pure by GC) ^{1}H nmr ($CDCl_3$) δ : 1.04 (d, 6H), 1.65 (m, 4H), 1.80 (m, 4H), 2.18 (m, 2H); MS m/e (I) : 136 (14), 121 (11), 107 (26), 93 (54), 91 (70), 79 (100), 77 (54), 67 (21), 65 (22), 53 (23), 51 (24), 41 (25), 39 (50), 27 (25).

6.3.8. *cis*- and *trans*-8,9-Dimethylbicyclo[5.2.0]non-1^7-ene (**46**)

The procedure was identical to that used for **44** except that the starting material was 1,8-nonadiyne (3.7 g, 0.03 mol). The spectral characteristics of the synthetic intermediates and the products were similar to those previously reported.

2,9-Undecadiyne:[133] Yield : 3.1 g, 0.02 mols, 66%, 98% pure by GC; bp : 120 °C, 40 mmHg; ^{1}H -nmr ($CDCl_3$) δ : 1.45 (bs, 6H), 1.75 (t, 6H), 2.1 (bs, 4H); MS m/e (I) : 147 (1), 133 (18), 119 (20), 105 (100), 91 (53), 79 (40), 67 (33), 53 (60), 39 (66), 27 (48).

E,E-1,2-Bis(ethylidene)cycloheptane:[16] Yield : 1.1 g, 7.2mmol, 36%, 99% pure by GC; ^{1}H nmr ($CDCl_3$) δ : 0.95 (cm, 2H), 1.2-1.3 (cm, 4H), 1.55 (t, 6H), 2.15 (m,

4H); MS m/e (I) : 151 (3), 150 (35), 135 (14), 121 (35), 107 (34), 93 (91), 79 (100), 67 (42), 53 (38), 39 (72), 27 (40).

cis-8,9-Dimethylbicyclo[5.2.0]non-1^{7}-ene:[16] (99% pure by GC) ^{1}H nmr ($CDCl_3$) δ : 0.90 (d, 6H), 1.53-1.65 (cm, 6H), 1.88-1.99 (m, 4H), 2.55 (m, 2H), MS m/e (I) : 151 (1), 150 (12), 135 (10), 121 (21), 107 (34), 93 (92), 91 (85), 79 (100), 67(40), 53 (40), 39 (85), 27 (50).

trans-8,9-Dimethylbicyclo[5.2.0]non-1^{7}-ene:[16] (99% pure by GC) ^{1}H nmr ($CDCl_3$) δ : 1.00 (d, 6H), 1.53 (bs, 10H), 1.93 (m, 2H); MS m/e (I) : 121 (25), 107 (40), 93 (90), 91 (92), 79 (100), 77 (75), 67 (50), 53 (40), 39 (82), 27 (58).

6.4. Preparation of Photoproducts

6.4.1. *E,Z*- and *E,E*-3,4-Dimethyl-2,4-hexadiene (19)

Shredded aluminum foil (8.03 g) was placed in a 500 mL two-necked round bottom flask containing 200 mL of dichloromethane equipped with a condenser, an addition funnel, and a magnetic stirrer. Mercuric chloride (13.73 g, 0.05 mol) was dissolved in 2-butanone (**76**) (35.62 g, 0.5 mol) and added to the addition funnel. Approximately 2 mL of this solution was added to the flask and the mixture was heated until a reaction was observed by the evolution of

gas. The rest of the solution was added drop-wise over 30 minutes. The reaction was stirred while refluxing for approximately 6 hours. The solution was quenched with water (15 mL) resulting in the precipitation of a large amount of solid material. The solid was filtered off and the solution was extracted with ether (3x25 mL). The combined ether fractions were washed with water (15 mL) and dried with $MgSO_4$. The drying agent was filtered off and the ether was removed under reduced pressure to give a colourless oil. The product was distilled under reduced pressure (120 °C, 40 mmHg) to give a clear colourless liquid which was identified as **77** based on the following spectral data.[92]

^{1}H nmr δ : 0.93 (t, 6H), 1.10 (d, 6H), 1.92 (bs, 2H).

A portion of the sample of **77** (8.8 g, 0.06 mol) was weighed into a 25 mL round bottom flask fitted with a reflux condenser. The solid was dissolved in propionic anhydride (15 mL) and a crystal of iodine was added. The reaction was heated at *ca.* 90 °C and stirred for 6 hours. The solution was neutralized with 5% $NaHCO_3$ and extracted into pentane (3x25 mL). The combined pentane layers were washed with water (2x15 mL), dried over $MgSO_4$ and filtered. The sample was concentrated by distillation and the products were purified by radial chromatography with pentane, followed by semi-preparative gas chromatography on column (b) to give clear colourless liquids which were identified as *E,E*- and *E,Z*-**19** based on the following spectral data.[14]

E,Z-3,4-Dimethylhexadiene (*E,E*-**19**) : ^{1}H nmr ($CDCl_3$) δ : 1.52 (d, 3H), 1.60 (d, 3H), 1.72 (s, 6H), 5.17 (m, 2H)

E,E-3,4-Dimethylhexadiene (*E,Z*-**19**) : ^{1}H nmr ($CDCl_3$) δ : 1.69 (d, 6H), 1.75 (d, 3H), 5.60 (q, 2H)

The Z,Z isomer of **19** was prepared by irradiation of a solution of *E,Z*-**19** in hexanes (Omnisolv) (0.05 M). The solution was added to a 12 mL quartz tube and sealed with a rubber septum. After deoxygenating for 20 minutes with a stream of dry argon, the sample was irradiated with eight RPR 253.7-nm lamps in a Rayonet Reactor for 24 hrs. Gas chromatographic analysis showed all three diene isomers (*E,Z*-**19** being the major constituent) along with minor amounts of *cis*- and *trans*-**18**. *Z,Z*-**19** was isolated using semi-preparative gas chromatography on column (b) and identified based on the following spectral data.[14]

Z,Z-3,4-Dimethylhexadiene (*Z,Z*-**19**) : ^{1}H nmr ($CDCl_3$) δ : 1.41 (d, 3H), 1.49 (s, 6H), 5.22 (q, 2H)

6.4.2. 2,3,4,5-Tetramethylhexadiene (**23**)

Shredded aluminum foil (3.2 g) was placed in a 500 mL two-necked round bottom flask containing 200 mL of dichloromethane equipped with a condenser, an addition funnel, and a magnetic stirrer. Mercuric chloride (5.6 g, 0.021 mol) was dissolved in 3-methyl-2-butanone (**82**) (20.5g, 0.21 mol) and added to the addition funnel. Approximately 2 mL of this solution was added to the flask and the mixture was heated until a reaction was observed by the evolution of gas. The rest of the solution was added over 45 minutes. The reaction was stirred for 6 hours while being heated at 40 °C and then quenched with distilled water (30 mL). The solution was extracted with dichloromethane (3x30 mL), the combined organic fractions were washed with water (15 mL) and then aqueous NH_4Cl (10 mL), and dried over $MgSO_4$. The drying agent was filtered off and the solvent was removed under reduced pressure to afford a clear colourless liquid. The product was purified by distillation at 60 °C (0.7 mmHg) to give **83** (3.34 g, 0.02 mol, 9%) in 97% purity by GC. The product was identified based on the following spectral data.[148]

^1H nmr ($CDCl_3$) δ : 0.97 (d, 12H), 1.12 (s, 12H), 2.05 (m, 2H).

A portion of the sample of **83** (1.0 g, 6 mmol) was weighed into a 25 mL round bottom flask fitted with a reflux condenser and magnetic stirrer. The solid was dissolved in propionic anhydride (10 mL) and a crystal of iodine was added.

The reaction was heated at *ca.* 90 °C and stirred for 6 hours. The solution was neutralized with 5% $NaHCO_3$ and extracted into pentane (3x25 mL). The combined pentane layers were washed with water (2x15 mL), dried over $MgSO_4$ and filtered. The sample was concentrated by distillation and the major product was purified by radial chromatography with pentane, followed by semi-preparative gas chromatography on column (b) to yield a clear colourless liquid (0.05 g, 0.4mmol, 6%). The product was identified as **23** (99% pure by GC) based on the following spectral characteristics.[35]

^1H nmr ($CDCl_3$) δ : 1.46 (s, 6H), 1.60 (s, 12 H); ^{13}C nmr ($CDCl_3$) δ : 17.08, 19.30, 20.83, 122.10, 131.61; MS m/e (I) : 138 (55), 123 (84), 107 (6), 95 (37), 91 (18), 81 (100), 79 (22), 67 (46), 55 (32), 41 (67), 39 (45), 27 (27).

6.4.3. Methanol Adducts of 1,2-Dimethylcyclobutene

The irradiation of **1** (0.41 g, 5.0 mmol) in deoxygenated methanol (50 mL) was carried out with the 228-nm light source in a Suprasil quartz immersion well equipped with a magnetic stirrer, reflux condenser, and nitrogen inlet. Monitoring of the products at low conversions by capillary gc revealed the formation of **3**, **5** and three new products, which eluted with longer retention times and were just well-enough resolved to determine that they were formed in equal yields. Irradiation was continued to ~80% conversion of **1** (14 days), with no change in the relative yields of the five photoproducts. The mixture was extracted with

pentane (4 x 25 mL), and the combined pentane extracts were then concentrated by distillation to a volume of *ca.* 1.0 mL. Semi-preparative gas chromatography on column (b) allowed fractionation of the three major components of the mixture, which each consisted of one major component (70-80%) contaminated with small amounts of one or both of the others. The major components of each fraction were identified as **78-80** (in the order of their elution from the gc column), on the basis of the following ^{1}H nmr and gc/ms evidence:

3-Methoxy-2,3-dimethylcyclobutene (**78**): ^{1}H nmr δ : 1.33 (s, 3H), 1.59 (s, 3H), 2.15-2.59 (m, 2H), 3.23 (s, 3H), 5.79 (s, 1H); MS m/e (I) : 112 (27), 111 (12), 97 (100), 86 (33), 79 (37), 72 (68), 67 (30), 59 (21), 53 (28), 43 (84), 41 (52), 39 (42), 29 (21).

1-Methoxy-1-methyl-2-methylenecyclobutane (**79**). ^{1}H nmr δ : 1.35 (s, 3H), 2.39-2.15 (m, 4H), 3.24 (s, 3H), 4.86-4.94 (d, 2H); MS m/e (I) : (5), 111 (11), 97 (79), 86 (21), 72 (100), 53 (19), 43 (69), 42 (41), 41 (26), 39 (39).

1-Methoxy-1,2-dimethylcyclobutane (**80**): ^{1}H nmr, δ : 0.93 (d, 3H), 1.15 (s, 3H), 1.56-2.00 (m, 5H), 3.14 (s, 3H); MS m/e (I) : 97 (3), 86 (87), 72 (100), 71 (42), 55 (22), 43 (44), 42 (37), 41 (25), 39 (23).

6.4.4. 1,1'-Bicyclohexenyl (**25**)

As indicated in section 6.3.4.

6.4.5. *cis*-Cyclododeca-7-enyne (*cis*-**28**)

A solution of 0.1 g (0.6 mmol) of *cis*-**24** in hexanes (5 mL) was placed into a 5 mL quartz tube, sealed with a rubber septum, and deoxygenated with a stream of dry argon for 15 minutes. The tube was hung in front of a medium pressure mercury lamp and irradiated for 40 hrs. GC analysis showed the presence of **25** and one other product. The sample was concentrated by distillation to *ca.* 1 mL. The second product was purified by semi-preparative gas chromatography on column (d) to 99% purity by GC. It was identified as *cis*-**28** based on the following spectral data.[34]

^{1}H nmr ($CDCl_3$) δ : 1.56 (m, 8H), 2.1-2.25 (m, 8H), 5.4 (t, 2H); MS m/e (I) : 161 (1), 147 (5), 133 (15), 119 (25), 105 (42), 91 (100), 79 (75), 67 (26), 53 (25), 39 (64), 27 (26).

6.4.6. *trans*-Cyclododeca-7-enyne (*trans*-**28**)

A solution of 0.1 g (0.6 mmol) of *trans*-**24** in hexanes (5 mL) was placed in a 5 mL quartz tube and sealed with a rubber septum. The solution was then

deoxygenated with a stream of dry argon for 15 min. The sample was hung in front of a medium pressure mercury lamp and irradiated for 40 hrs. GC analysis showed the production of **24** and one other product. After irradiation, the sample was concentrated by distillation to *ca.* 1 mL. The second product was purified by semi-preparative gas chromatography on column (d) and identified based on the following spectral data.[34] The purity was estimated to be 99% by GC.

^{1}H nmr ($CDCl_3$) δ : 1.58 (m, 8H), 1.95 (bs, 4H), 2.1 (m, 4H), 5.7 (bs, 2H); ^{13}C nmr ($CDCl_3$) δ : 19.15, 26.56, 28.49, 30.15, 82.11, 130.82; MS m/e (I) : 161 (1), 147 (9), 133 (20), 119 (34), 105 (48), 91 (100), 79 (71), 67 (21), 53 (18), 39 (38), 27 (15).

6.4.7. *E,Z*-1,2-Bis(ethylidene)cyclopentane (*E,Z*-**47**)

A solution of *E,E*-**47** (1.2g) was added to pentane (10 mL) in a 12 mL quartz tube and sealed with a rubber septum. The solution was deoxygenated with dry argon for 30 minutes. The sample was irradiated in a Rayonet Reactor with eight RPR 253.7-nm lamps for 48 hours. GC analysis showed a mixture of 4 major components including *E,E*-**47** along with *cis*- and *trans*-**44**. After concentration by distillation, semi-preparative gas chromatography on column (c) allowed isolation of the unidentified product in 98% purity by GC. It was identified as *E,Z*-**47** based on the following spectral data.[16]

^{1}H nmr ($CDCl_3$) δ : 1.50 (bs, 6H), 1.63 (d, 2H), 2.15-2.22 (m, 4H), 5.22 (m, 2H)

6.4.8. *E,Z*-1,2-Bis(ethylidene)cyclohexane (**48**)

A solution of *E,E*-**48** (0.6 g) and acetophenone (0.01 g) was added to pentane (10 mL) in a 12 mL quartz tube and sealed with a rubber septum. The solution was deoxygenated with dry argon for 30 minutes. The sample was irradiated in a Rayonet Reactor with eight 300-nm lamps for 15 hours. GC analysis showed a mixture of three components, one of which was *E,E*-**48**. After concentration by distillation, semipreparative gas chromatography on column (c) allowed the isolation of the major unknown product in 99% purity by GC. It was identified as *E,Z*-**48** based on the following spectral data.[16]

^{1}H nmr ($CDCl_3$) δ : 1.58 (d, 6H), 1.60 (cm, 4H) 2.2 (bs, 4H), 5.25 (q, 2H); MS m/e (I) : 136 (45), 121 (20), 107 (54), 91 (47), 79 (100), 67 (27), 53 (20), 39 940), 27 (22).

6.4.9. *E,Z*- and *Z,Z*-Bis(ethylidene)cycloheptane (**49**)

A solution of *E,E*-**49** (0.1g, 0.7 mmol), acetophenone (0.010g) and pentane (10 mL) was added to a 12 mL quartz tube and sealed with a rubber septum. The solution was deoxygenated with dry argon for 30 minutes. The

sample was irradiated in a Rayonet Reactor with eight RPR 300-nm lamps for 10 hours. GC analysis showed three major components, one of which was *E,E*-**49**. After concentration by distillation, semi-preparative gas chromatography on column (c) allowed isolation of the major product in 98% purity by GC. It was identified as *E,Z*-**49** based on the following spectral data.[16]

E,Z-Bis(ethylidene)cycloheptane (*E,Z*-**49**): ^{1}H nmr ($CDCl_3$) : δ = 0.8 (m, 4H), 1.2 (m, 4H), 2.20 (m, 2H), 5.16 (q, 2H); MS m/e (I) : 150 (22), 121 (30), 105 (30), 93 (92), 91 (99), 79 (100), 67 (40), 65 (44), 53 (42), 39 (70), 27 (60).

The second product was not formed in great of enough yield to isolate, and was identified as *Z,Z*-**49** based on the following mass spectral data and its relative GC retention time to the other isomers of **49**.

Z,Z-Bis(ethylidene)cycloheptane (*E,Z*-**49**) MS m/e (I) : 150 (17), 135 (10), 121 (25), 107 (36), 93 (90), 91 (84), 79 (100), 77 (77), 67 (38), 65 (43), 53 (40), 41 (62), 39 (95), 27 (51).

6.5. Analytical Irradiations

6.5.1. Irradiations of **50** and **18** in the gas phase.

Gas phase samples for photolysis were prepared by placing 8 μL of the neat cyclobutene derivative and cyclohexane (0.05 μL as internal standard) in a 1 cm Suprasil cuvette which had been sealed with a septum and flushed for *ca.* 10 min. with a stream of SF_6. The samples were allowed to vapourize completely before beginning the experiments. Irradiations were accomplished with either a Zn (214-nm) or Cd (228-nm) lamp or an ArF Excimer laser (193-nm) and aliquots were taken for GC analysis at regular time intervals.

Gas phase samples for uv spectroscopy at 1 atm were prepared in analogous to those above fashion without the use of an internal standard. Samples for UV spectroscopy at reduced pressure were prepared with a vacuum line. The sample was introduced to a 10 cm cylindrical Suprasil cell from a cold finger.

6.5.2. Irradiations of **50**, **18**, **22** in solution.

The cyclobutene (*ca.* 10 μL) and cyclohexane as an internal standard (0.5 μL) was added to *ca.* 0.3 mL of solvent (either Omnisolv isooctane for **50**, or Omnisolv hexanes for **18**, and **22**) in a small Suprasil tube (*ca.* 0.5 mL) equipped

with a micro-stirbar and rubber septum. The sample was then deoxygenated with a stream of dry argon for 20 minutes. Irradiations were accomplished with either a Zn (214-nm) or Cd (228-nm) lamp or an ArF Excimer laser (193-nm) while being stirred, and aliquots were taken for GC analysis at regular time intervals.

6.5.3. Irradiations of **24** and **44-46** in solution.

The irradiations were identical to those above but employed decane (24) or octane (**44-46**) as an internal standard, and used only 214-nm and 228-nm light sources.

6.5.4. Quantum Yield Determinations.

The quantum yield determinations of **50** employed uranyl oxalate as the actinometer[149-152] and followed the procedure outlined by Eaton.[114] Uranyl oxalate was prepared by combining uranyl sulfate (0.43 g) with sodium oxalate (0.68 g) in 0.2N H_2SO_4 (950 mL) in the dark. Cesium sulfate was made by mixing ceric ammonium nitrate (5.70 g) in distilled water (15 mL) with concentrated ammonium hydroxide (150-mL). The precipitate was rinsed with water until neutral, and dissolved in hot H_2SO_4 (125 mL). After the solution cooled, it was diluted to 950 mL with water.

Samples of **50** in isooctane (0.05 M), and the uranyl oxalate were placed in 4 mL cylindrical Suprasil tubes, deoxygenated, and mounted on a merry-go-round apparatus. They were then irradiated with a Cd resonance lamp for *ca.* 30 minutes. The yield of **35** from **50** after this time was measured by gas chromatography and the conversion of uranyl oxalate was measured by uv spectroscopy. A sample of uranyl oxalate was also run in an identical Pyrex tube to test the effect of longer wavelength bands from the cadmium lamp. It was found that the contribution is negligible.

The quantum yield determinations for **18**, **22**, and **24** using **50** as the actinometer were carried out with similar samples to the analytical excitations (Section 6.5.2.) and were irradiated on a merry-go-round apparatus. The values were obtained by comparison of the slopes of concentration *vs* time plots for **50** and the analyte.

The quantum yields of *cis*- and *trans*-**24** were determined simultaneously as described above using **50** as the secondary actinometer. Those at 214-nm used the previously determined quantum yield for ring opening of **1** at 214-nm (Φ = 0.06).[35]

6.6. Photostationary State Determinations

6.6.1. 3,4-Dimethyl-2,4-hexadienes (19)

Photostationary state compositions for the isomers of **19** at 228-nm were determined by photolysing separate samples of *E,E*- and *E,Z*-**19** (7 μL in 1 atm SF_6 for gas phase experiments, or deoxygenated 0.05 M solutions in hexane), with periodic monitoring by GC, until common diene distributions were obtained (*ca.* 2-5 hours).

6.6.2. 1,2-Bis(ethylidene)cycloalkanes **47-49.**

The photostationary state compositions of **47-49** at 228-nm were determined by irradiating a stirred solution of the E,E isomer in hexanes (0.02 M). The progress of the excitation was monitored by GC until the diene distributions remained constant over prolonged periods of time (*ca.* 2-5 hours).

6.7. Control Experiments with *E,E*- and *Z,Z*-19.

A 1:1 mixture of *E,E*- and *Z,Z*-**19** was held in a 100 μL gas-tight syringe, set in a syringe-pump (Harvard Apparatus, Pump 22). The solution was added

at a rate similar to that of total diene formation in the 228-nm photolysis of *trans*-**18** to a stirring solution of **50** (0.15 M) in a 0.5 mL Suprasil tube being irradiated at 228-nm. Aliquots were taken at regular time intervals to be analyzed by GC.

6.8. Calculations of Vibrational Frequencies and Rate Constants

The geometries of **50**, **18**, **22**, and **24** were optimized using Gaussian 94.[116] All calculations with this program were performed on an Octane (Silicon Graphics) work-station. The optimizations were performed at the 6-31G+d restricted Hartree-Fock level using a z-matrix previously determined on HyperChem™ at the PM3 semi-empirical level. The frequency calculations for **50**, **18**, and **22** were performed at the B3LYP/6-31G(d) level where those for **24** were performed at the 3-21G level. A complete listing of the calulated vibrational frequencies can be found in Appendix 4. The resulting values were corrected by a factor of 0.98 for the B3LYP calculations or 0.91 for the 3-21G calculations.[117]

The RRKM calculations were performed by Dr. W.J. Leigh (McMaster University) and Dr. R. Walsh (Reading University) using the calculated vibrational frequencies. A plot of log(k) vs. Energy for the cyclobutenes **50**, **18**, and **22**, was fit as a third order polynomial for each compound. The rate constant at the energy of the desired photon wavelength was extracted from these plots. The statistical thermodynamic calculations on *cis*- and *trans*-**24** were performed on a Microsoft Excel spreadsheet using the equation for a canonical ensemble and

the calculated vibrational frequencies. The average energy was solved for a number of arbitrary T values. The temperature associated with the photon energy was extracted from a plot of energy vs. temperature. The rate constants were then determined from the Arrhenius equation using previously determined E_a and A values.[28]

Appendix 1

Figure A.1.1. Concentration vs. time plots for the irradiations of 1,2-dimethylcyclobutene (**50**) at 193-nm, 214-nm and 228-nm, in 1 atm of SF_6. (● 2,3-dimethyl-1,3-butadiene (**53**), ■ 2-butyne (**35**)

a) @ 193-nm (dmc193s2.pzm)

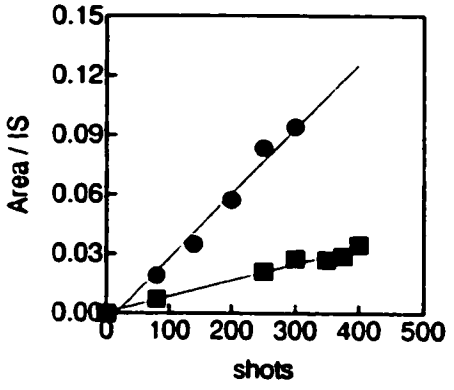

b) @ 214-nm (dmc214s1.pzm)

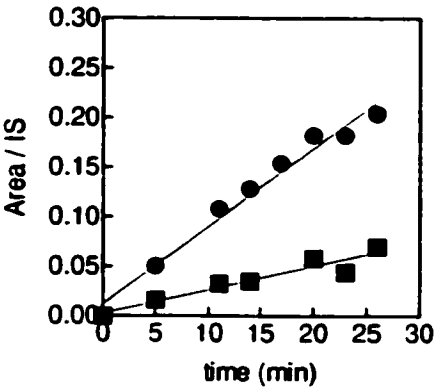

c) @ 228-nm (dmc228s1.pzm)

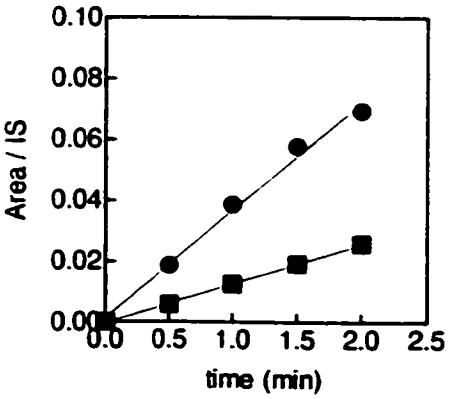

Figure A.1.2. Concentration vs. time plots for the irradiations of 1,2,-dimethylcyclobutene (**50**) at 193-nm, 214-nm and 228-nm in isooctane solution (0.06 M). (● 2,3-dimethyl-1,3-butadiene (**53**), ■ 2-butyne (**35**))

a) @ 193-nm (dmc193i1.pzm)

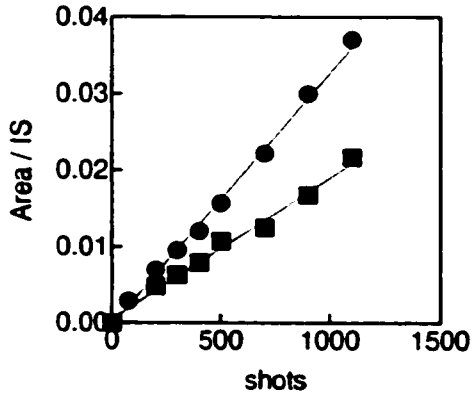

b) @ 214-nm (cbg214.pzm)

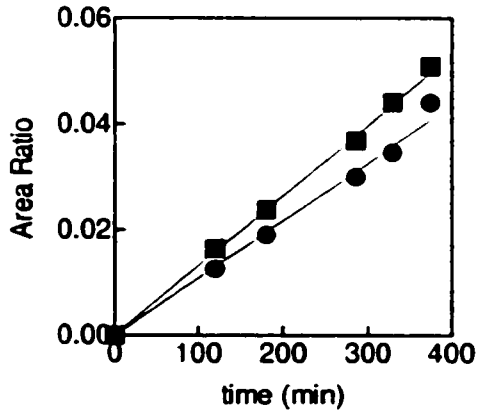

c) @ 228-nm (dmc228i1.pzm)

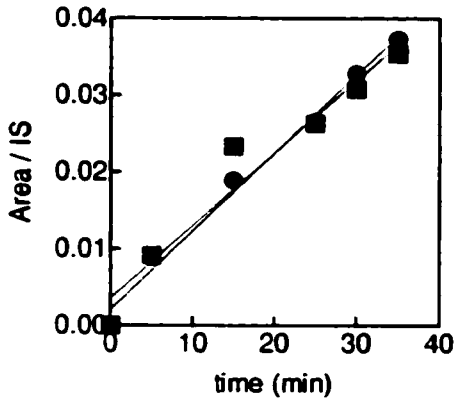

Figure A.1.3. Plots of concentration vs. time for the irradiations of cis-1,2,3,4-tetramethylcyclobutene (**18**) at 193-nm, 214-nm and 228-nm, in 1 atm of SF_6. (● *E,Z*-**19**,▼ *E,E*-**19**, ■ **35**)

a) @ 193-nm (ctm193s4.pzm)

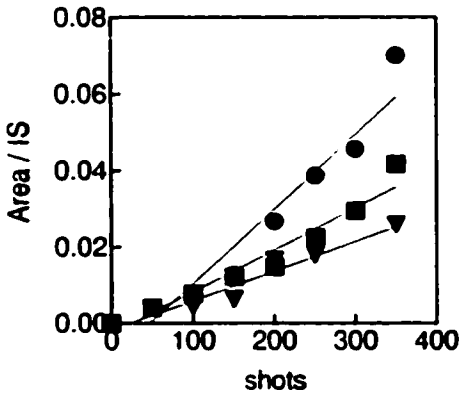

b) @ 214-nm (ctm214s2.pzm)

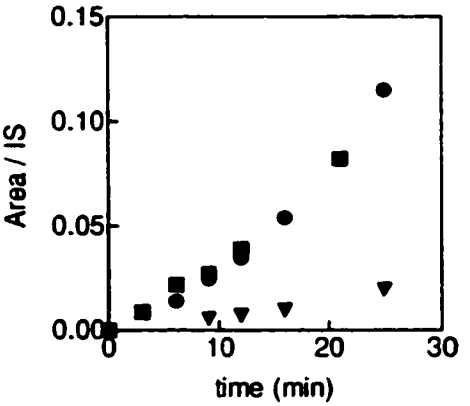

c) @ 228-nm (ctm228s1.pzm)

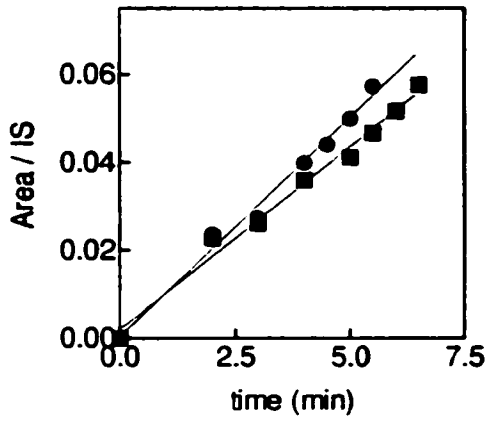

Figure A.1.4. Plots of concentration vs. time for the irradiations of cis-1,2,3,4-tetramethylcyclobutene (**18**) at 193-nm, 214-nm and 228-nm, in hexane solution (0.05 M). (● *E,Z*-**19**,▼ *E,E*-**19**, ■ **35**)

a) @ 193-nm (ctm193h1.pzm)

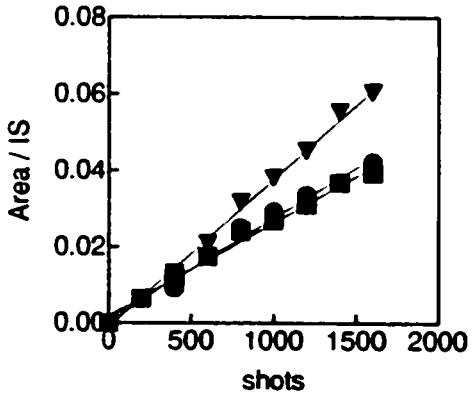

b) @ 214-nm (ctm214i1.pzm)

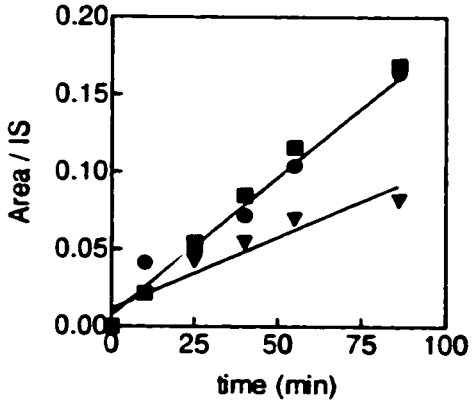

c) @228-nm (ctm228c1.pzm)

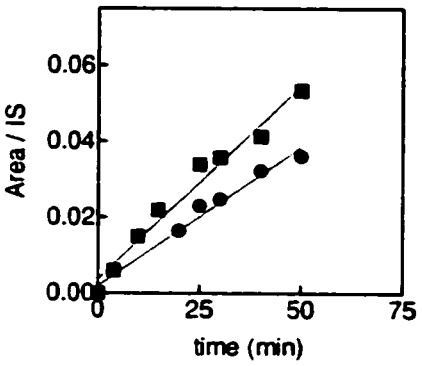

Figure A.1.5. Plots of concentration vs. time for the irradiations of *trans*-1,2,3,4-tetramethylcyclobutene (**18**) at 193-nm, 214-nm and 228-nm in 1 atm of SF_6. (● *E,Z*-**19**,▼ *E,E*-**19**,◆ *Z,Z*-**19**, ■ **35**).

a) @ 193-nm (ttm193s7.pzm)

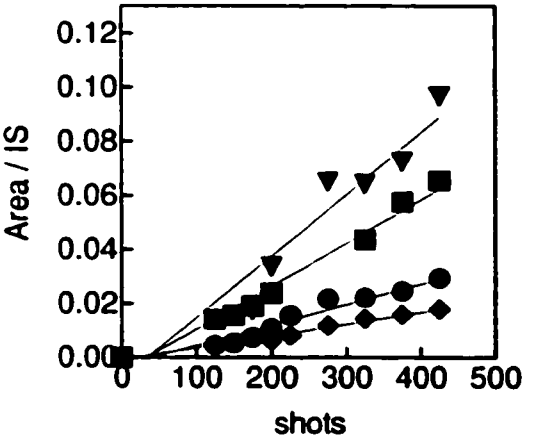

b) @ 214-nm (ttm214s2.pzm)

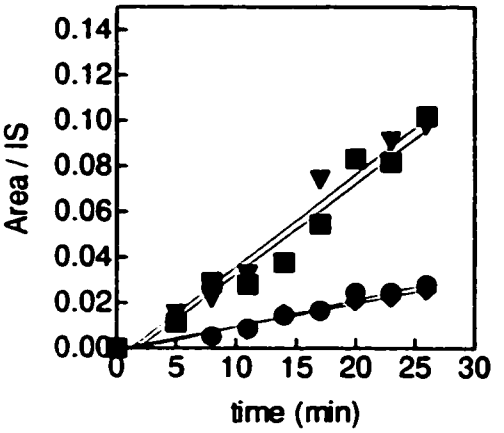

c) @ 228-nm (ttm228s3.pzm)

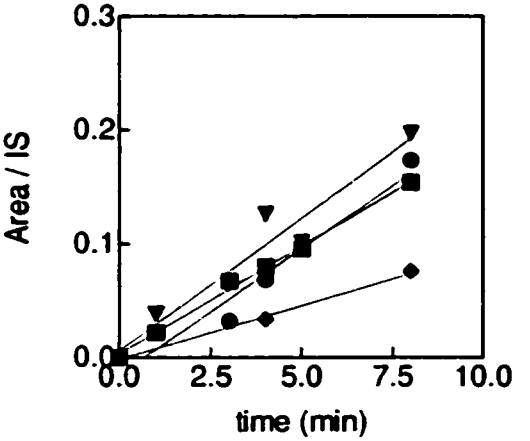

Figure A.1.5. Plots of concentration vs. time for the irradiations of *trans*-1,2,3,4-tetramethylcyclobutene (**18**) at 193-nm, 214-nm and 228-nm in hexane solution (0.05 M). (● *E,Z*-**19**,▼ *E,E*-**19**,◆ *Z,Z*-**19**, ■ **35**).

a) @ 193-nm (ttm193c1.pzm)

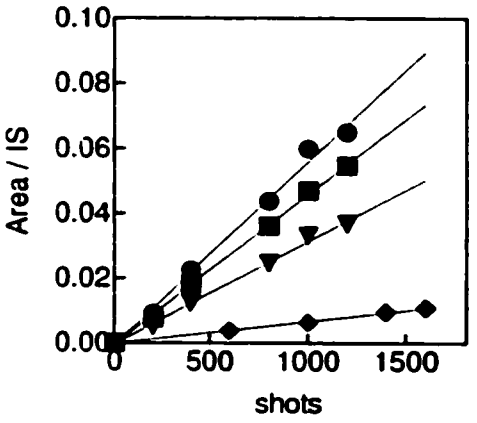

b) @ 214-nm (ttm214ch.pzm)

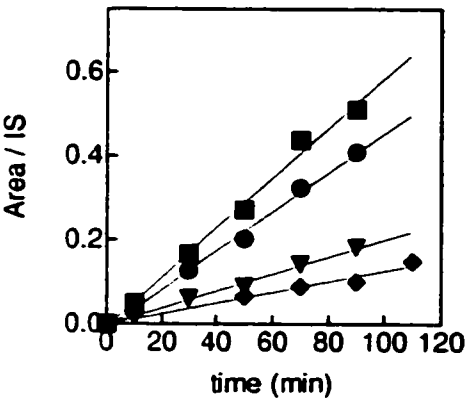

c) @ 228-nm (ttm228c1.pzm)

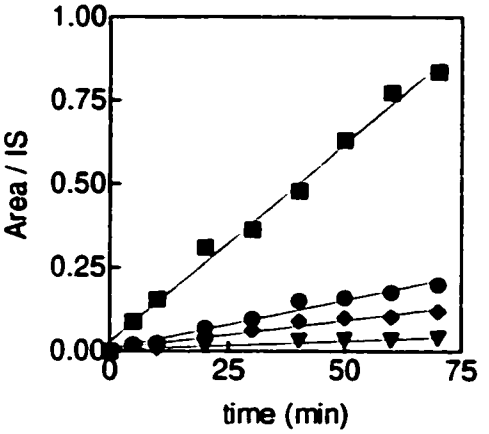

Appendix 2.

Figure A.2.1. Concentration vs. time plots for the irradiations of hexane solutions (0.05 M) of hexamethylcyclobutene (**22**) at 214-nm and 228-nm. (● 2,3,4,5-tetramethyl-2,4-hexadiene (**23**),■ 2-butyne (**35**)).

a) @ 214-nm (hm214h1.pzm) b) @ 228-nm (hm228h1.pzm)

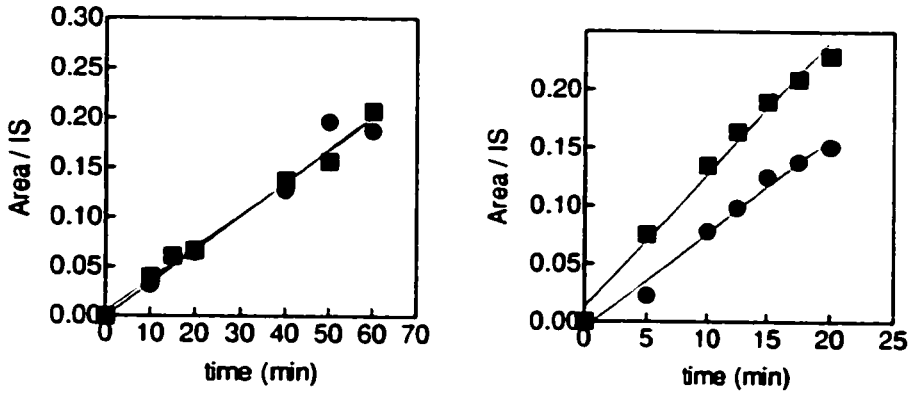

Figure A.2.2. Concentration vs. time plots for *cis*-tricyclododecene (**24**) in hexane (0.05 M) at 214-nm and 228-nm. (■ 1,1'-bicyclohexenyl (**25**),● enyne (**28**)).

a) @ 214-nm (cdd214h1.pzm) b) @ 228-nm (cdd228h1.pzm)

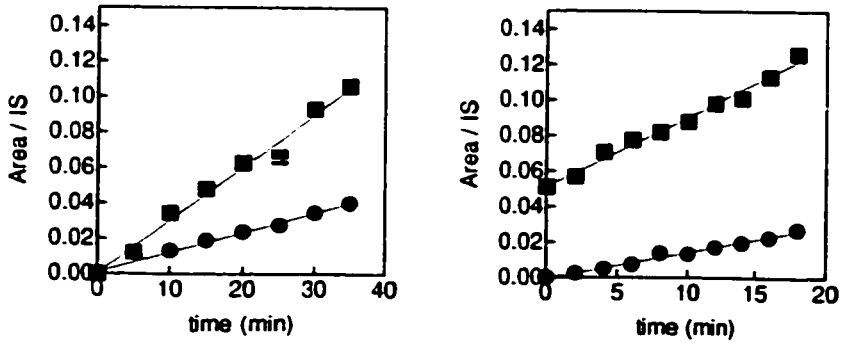

Figure A.2.3. Concentration vs. time plots for *trans*-tricyclododecene (**24**) in hexane (0.05 M) at 214-nm and 228-nm. (■ 1,1'-bicyclohexenyl (**25**),● enyne (**28**)).

a) @ 214-nm (tdd214h1.pzm)

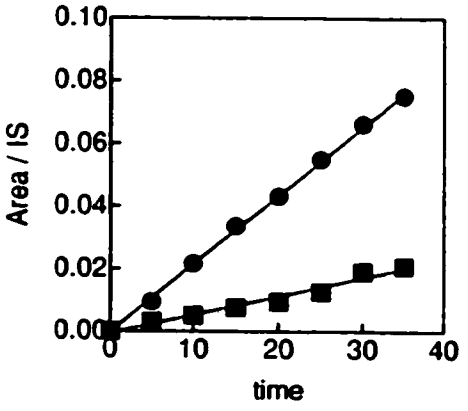

b) @ 228-nm (tdd228h3.pzm)

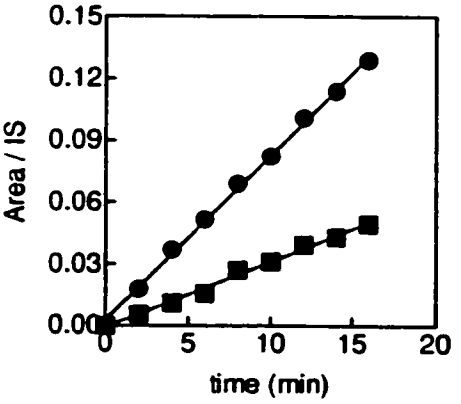

Appendix 3.

Figure A.3.1. Concentration vs. time plots for *cis*-bicyclo[3.2.0]heptene (**44**) in hexane solution (0.06 M) at 214-nm and 228-nm. (● :*E,Z*-**47**, ▼ : *E,E*-**47**)

a) @ 214-nm (cbch2141.pzm)

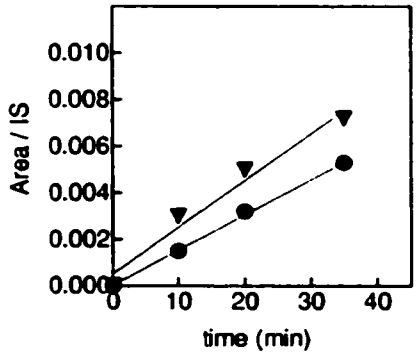

b) @ 228-nm (cbch2282.pzm)

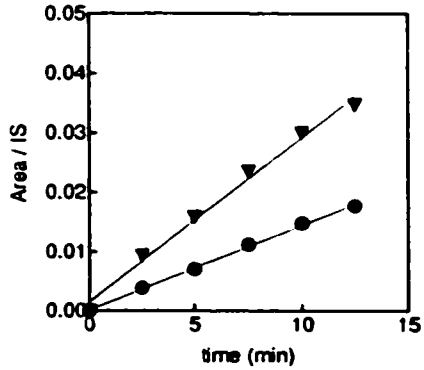

Figure A.3.2. Concentration vs. time plots for *trans*-bicyclo[3.2.0]heptene (**44**) in hexane solution (0.06 M) at 214-nm and 228-nm. (● :*E,Z*-**47**, ▼ : *E,E*-**47**)

a) @ 214-nm (tbch2141.pzm)

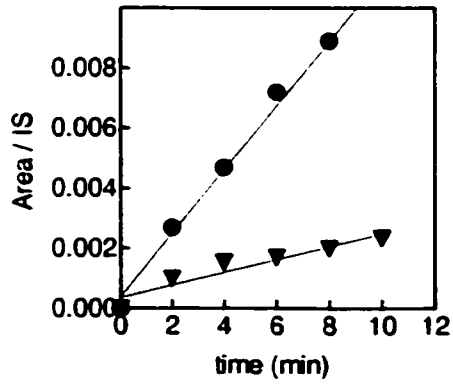

b) @ 228-nm (tbch2282.pzm)

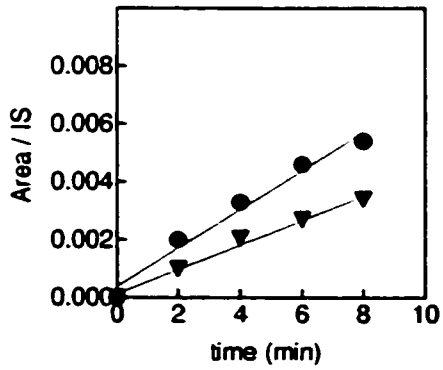

Figure A.3.3. Concentration vs. time plots for *cis*-bicyclo[4.2.0]octene (**45**) in hexane solution (0.06 M) at 214-nm and 228-nm. (● :*E,Z*-**48**, ▼ : *E,E*-**48**)

a) @ 214-nm (cbco2141.pzm)

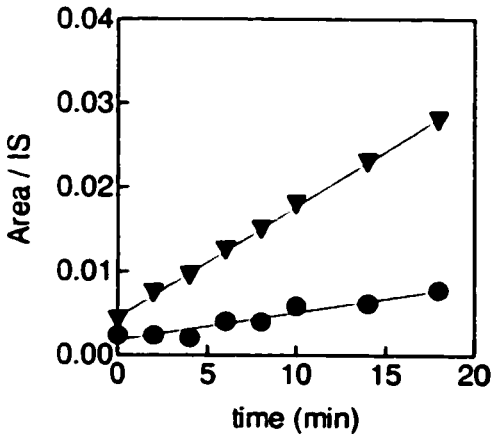

b) @ 228-nm (cbco2282.pzm)

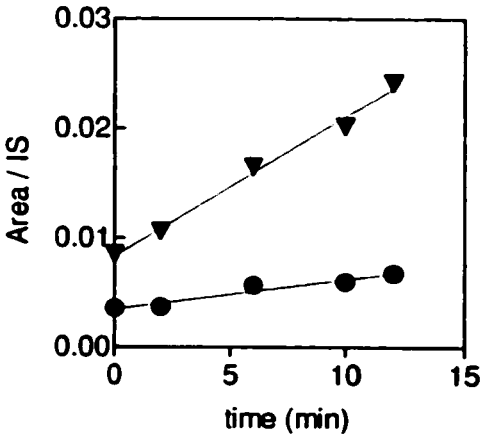

Figure A.3.4. Concentration vs. time plots for *trans*-bicyclo[4.2.0]octene (**45**) in hexane solution (0.06 M) at 214-nm and 228-nm. (● :*E,Z*-**48**, ▼ : *E,E*-**48**)

a) @ 214-nm (tbco2141.pzm)

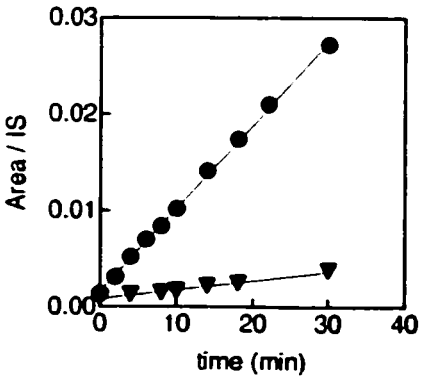

b) @ 228-nm (tbco2282.pzm)

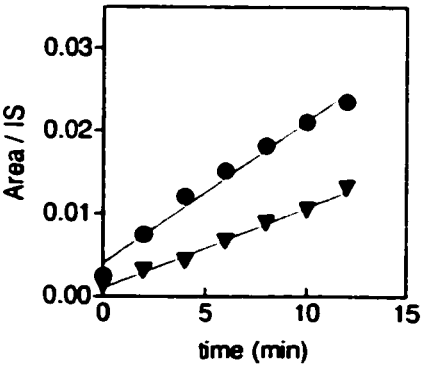

Figure A.3.5. Concentration vs. time plots for *cis*-bicyclo[5.2.0]nonene (**46**) in hexane solution (0.06 M) at 214-nm and 228-nm. (● :*E,Z*-**49**, ▼ : *E,E*-**49**)

a) @ 214-nm (cbcn2141.pzm)

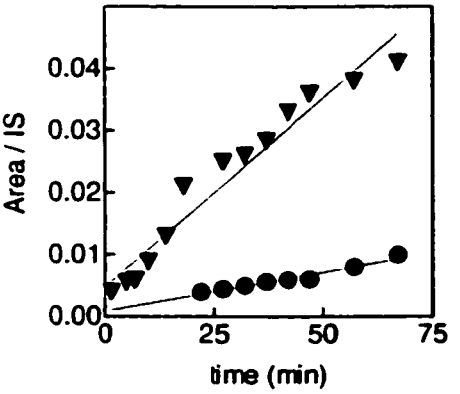

b) @ 228-nm (cbcn2284.pzm)

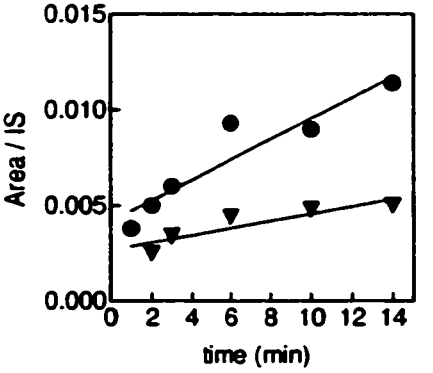

Figure A.3.6. Concentration vs. time plots for *trans*-bicyclo[5.2.0]nonene (**46**) in hexane solution (0.06 M) at 214-nm and 228-nm. (● :*E,Z*-**49**, ▼ :*E,E*-**49**, ♦ :*Z,Z*-**49**)

a) @ 214-nm (tbcn2141.pzm)

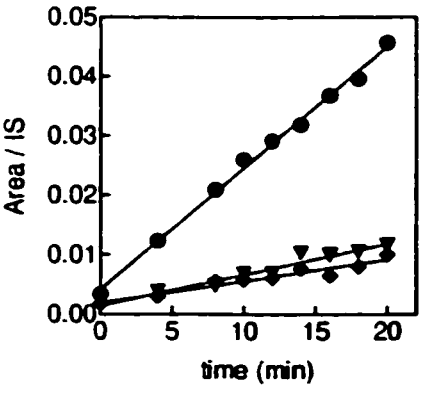

b) @ 228-nm (tbcn2281.pzm)

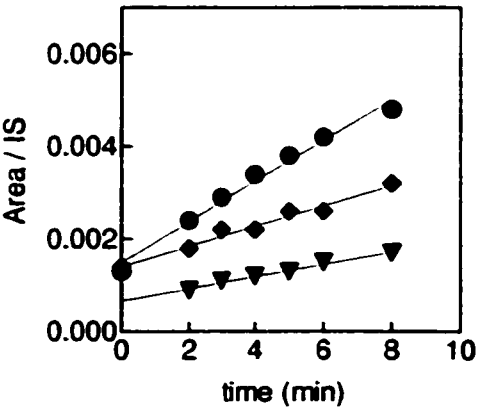

Appendix 4

A.4.1. Calculated Vibrational Frequencies of **50**

142.5337	165.0916	193.0562	225.6696	255.506	370.3935	473.3316	630.3847
686.7039	796.4174	885.078	900.4915	948.5993	983.6493	989.6661	1077.709
1112.427	1114.56	1153.077	1187.586	1194.169	1218.87	1306.019	1399.694
1405.155	1462.169	1469.499	1469.744	1475.613	1478.789	1484.245	1716.496
2958.112	2959.484	2965.673	2972.915	2997.685	3000.337	3000.942	3012.839
3037.503	3040.219						

A.4.2. Calculated Vibrational Frequencies of *cis*-**18**

87.32251	140.9351	163.9745	170.6863	204.77	207.6685	211.1023	229.8173
269.426	375.3315	429.9264	480.1746	550.9285	660.5992	672.109	746.4507
800.2365	913.639	978.4012	989.5499	1001.189	1015.164	1038.928	1067.424
1109.981	1117.725	1138.021	1198.287	1201.811	1217.188	1300.513	1334.793
1347.673	1392.335	1398.502	1400.923	1405.49	1469.448	1470.022	1477.263
1478.193	1481.141	1484.669	1494.139	1501.684	1716.031	2927.108	2940.639
2957.664	2959.205	2970.044	2975.173	2999.694	3000.562	3024.637	3028.18
3036.904	3037.824	3039.742	3047.16				

A.4.3. Calculated Vibrational Frequencies of *trans*-**18**

93.6049	140.221	162.6228	163.6884	195.0873	222.1375	226.1237	234.5958
241.4453	376.2922	402.8208	477.92	576.3648	604.9775	693.1451	796.4244

797.7494	913.9672	970.1009	990.5839	1007.197	1027.876	1034.232	1082.679
1083.848	1131.179	1137.791	1189.475	1205.245	1213.552	1294.631	1319.099
1355.946	1394.744	1396.458	1398.365	1404.754	1469.341	1470.121	1477.486
1478.065	1485.315	1487.217	1489.64	1489.908	1717.721	2937.975	2943.137
2957.845	2959.162	2965.368	2967.592	2999.545	3000.476	3025.095	3025.524
3029.891	3030.005	3036.806	3039.531				

A.4.4. Calculated Vibrational Frequencies of **22**

69.39625	135.7712	150.9168	160.1932	175.1636	192.9543	209.5653	210.9178
212.9307	230.49	245.3704	296.5798	325.3378	344.6637	379.7487	394.2726
457.5731	541.5279	554.1107	597.9985	606.935	706.0119	746.01	886.4161
923.3825	932.6139	933.0834	954.9721	985.3001	998.5773	1024.11	1052.926
1087.201	1105.704	1123.402	1125.58	1183.851	1213.716	1216.09	1283.551
1293.214	1382.688	1391.657	1397.159	1399.045	1402.889	1415.619	1467.839
1468.641	1469.87	1476.556	1477.527	1478.642	1483.704	1485.554	1495.072
1495.244	1502.864	1516.014	1722.834	2958.495	2959.889	2965.442	2969.138
2970.32	2977.767	3000.234	3001.395	3016.34	3019.933	3022.421	3026.096
3036.721	3039.609	3044.38	3046.421	3060.173	3061.07		

A.4.5.Calculated Vibrational Frequencies of *cis*-**24**

53.81612	54.16847	86.43089	198.9250	209.7186	266.5093	323.4748	369.2227
405.0085	433.9288	437.6958	475.0635	493.7923	525.5841	609.3779	653.7908
709.2655	722.4594	763.2238	787.6231	798.3471	817.7378	873.7005	877.4776
893.2642	897.2873	932.2046	959.7784	977.1318	1001.313	1008.220	1031.398
1040.963	1054.678	1110.516	1127.875	1163.789	1166.293	1174.648	1177.546

1214.539	1234.686	1263.894	1273.069	1284.021	1289.044	1290.826	1327.295
1330.841	1341.957	1343.352	1364.207	1368.411	1369.439	1373.430	1375.812
1378.678	1489.054	1492.286	1496.830	1506.359	1508.827	1510.943	1512.531
1524.354	1731.243	2904.967	2905.856	2911.025	2913.780	2915.725	2916.591
2917.508	2920.305	2934.436	2936.172	2936.279	2949.051	2950.823	2955.378
2957.228	2961.814	2965.294	2978.332				

A.4.6. Calculated Vibrational Frequencies of *trans*-**24**

92.11848	140.5135	140.5699	222.4132	231.4959	266.3004	279.7461	322.5309
384.8045	430.4954	437.5270	481.1339	482.2887	601.0542	621.1843	624.3686
705.2207	752.8769	766.7573	799.3054	809.9014	846.0026	854.5540	881.1966
886.0125	914.639	949.2089	959.1173	989.2899	1008.333	1009.015	1020.374
1023.108	1082.829	1089.855	1134.680	1143.421	1157.699	1177.081	1185.429
1214.046	1225.746	1265.512	1272.344	1277.436	1281.841	1283.603	1319.637
1338.773	1347.685	1348.440	1358.069	1361.908	1368.751	1368.786	1377.700
1378.709	1490.005	1491.947	1499.217	1499.979	1505.972	1506.236	1509.811
1510.586	1733.028	2901.458	2901.545	2901.901	2902.505	2908.009	2908.492
2913.132	2913.422	2929.283	2931.696	2940.421	2941.480	2946.729	2946.740
2952.266	2953.380	2959.953	2960.504				

References

1. Adam, W.; Oppenlander, T.; Zang, G. *J. Am. Chem. Soc.* **1985**, *107*, 3921.

2. Kropp, P. J.; Fravel, H. G.; Fields, T. R. *J. Am. Chem. Soc.* **1976**, *98*, 840.

3. Kropp, P. J. Photorearrangement and Fragmentation of Alkenes; In *CRC Handbook of Organic Photochemistry and Biology.* ; Horspool, W., ed. CRC Press: Boca Raton, 1996; pp 16-28.

4. Woodward, R. B.; Hoffmann, R. *The Conservation of Orbital Symmetry*; Verlag Chemie GmbH. Academic Press Inc.: Aschaffenburg, 1970.

5. Potts, W. J. Jr. *J. Chem. Phys.* **1955**, *23*, 65.

6. Loeffler, B. B.; Eberlin, E.; Pickett, L. W. *J. Chem. Phys.* **1958**, *28*, 345.

7. Sowers, B. L.; Arakawa, E. T.; Birkhoff, R. D. *J. Chem. Phys.* **1971**, *54*, 2319.

8. Watson, F. H.; Armstrong, A. T.; McGlynn, S. P. *Theor. Chim. Acta.* **1970**, *16*, 75.

9. Watson, F. H.; McGlynn, S. P. *Theor. Chim. Acta.* **1971**, *21*, 309.

10. Robin, M. B. *Higher Excited States of Polyatomic Molecules. Volume 1.*; Academic Press: New York, 1974; pp 1-100.

11. Robin, M. B. *Higher Excited States of Polyatomic Molecules. Volume 2.*; Academic Press: New York, 1975; pp 1-68.

12. Collin, G. J. Photochemistry of Simple Olefins: Chemistry of Electronic Excited States or Hot Ground States; In *Advances in Photochemistry*; Volman, D. H., Hammond, G. S., Gollnick, K., eds. John Wiley & Sons: New York, 1988; pp 135-176.

13. Michl, J.; Bonaic-Koutecky, V. *Electronic Aspects of Organic Photochemistry*; John Wiley & Sons: New York, 1990.

14. Clark, K. B.; Zheng, K.; Leigh, W. J. *Can. J. Chem.* **1990**, *68*, 1988.

15. Ma, J.; Werstiuk, N. H.; Nguyen, N.; Zheng, K.; Leigh, W. J. *J. Am. Chem. Soc.* **1991**, *113*, 4993.

16. Leigh, W. J.; Postigo, J. A.; Zheng, K. *Can. J. Chem.* **1996**, *74*, 951.

17. Leigh, W. J.; Cook, B. H. O. *J. Org. Chem.* **1999**, *64*, 5256.

18. Collin, G. J.; Deslauriers, H. *Can. J. Chem.* **1983**, *61*, 1510.

19. Robin, M. B.; Hart, R. R.; Kuebler, N. A. *J. Chem. Phys.* **1966**, *44*, 1803.

20. Leigh, W. J. *Can. J. Chem.* **1993**, *71*, 147.

21. Fonken, G. J. *Tetrahedron Lett.* **1962**, *13*, 549.

22. Marvell, E. N.; Caple, G.; Schatz, B. *Tetrahedron Lett.* **1965**, *7* , 385.

23. Gleiter, R.; Bohm, M. C. *Pure Appl. Chem.* **1983**, *55*, 237.

24. Crowley, K. J. *Tetrahedron* **1965**, *21*, 1001.

25. Srinivasan, R. *J. Am. Chem. Soc.* **1968**, *90*, 4498.

26. Frey, H. M.; Pope, B. M.; Skinner, R. F. *Trans. Faraday Soc.* **1967**, *63*, 1166.

27. Branton, G. R.; Frey, H. M.; Montague, D. C.; Stevens, I. D. R. *Trans. Faraday Soc.* **1966**, *62*, 659.

28. Criegee, R.; Reinhardt, H. G. *Chem. Ber.* **1968**, *101*, 102.

29. Criegee, R.; Seebach, D.; Winter, R. E.; Borretzen, B.; Brune, H.-A. *Chem. Ber.* **1965**, *98*, 2339.

30. Branton, G. R.; Frey, H. M.; Skinner, R. F. *Trans. Faraday Soc.* **1966**, 1546.

31. Maier, G.; Bothur, A. *Eur. J. Org. Chem.* **1998**, 2063.

32. Saltiel, J.; Lim, L.-S. N. *J. Am. Chem. Soc.* **1969**, *91*, 5404.

33. Leigh, W. J.; Clark, K. B. *J. Am. Chem. Soc.* **1987**, *109*, 6086.

34. Zheng, K.; Leigh, W. J. *J. Am. Chem. Soc.* **1991**, *113*, 2163.

35. Postigo, J. A.; Leigh, W. J. *J. Am. Chem. Soc.* **1995**, *117*, 1688.

36. Clark, K. B.; Zheng, K.; Leigh, W. J. *J. Org. Chem.* **1991**, *56*, 1574.

37. Zheng, K.; Leigh, W. J. *J. Am. Chem. Soc.* **1991**, *113*, 4019.

38. Dauben, W. G.; Haubrich, J. E. *J. Org. Chem.* **1988**, *53*, 600.

39. Leigh, W. J. Diene/Cyclobutene Photochemistry; In *CRC Handbook of Organic Photochemistry and Biology*; Horspool, W., ed. CRC Press: Boca Raton, 1996.

40. Tai, J. C.; Allinger, N. L. *J. Am. Chem. Soc.* **1976**, *98*, 7928.

41. Roth, W. R.; Lennartz, H. W.; Doering, W. v. E.; Dolbier, W. R. Jr.; Schmidhauser, J. C. *J. Am. Chem. Soc.* **1988**, *110*, 1883.

42. Mui, P. W.; Grunwald, E. *J. Am. Chem. Soc.* **1982**, *105*, 6562.

43. Boue, S.; Srinivasan, R. *Mol. Photochem.* **1972**, *4*, 93.

44. Laarhoven, W. H.; Jacobs, H. J. C. Photochemistry of Acyclic 1,3,5-Trienes and Related Compounds; In *CRC Handbook of Organic Photochemistry and Biology.*; Horspool, W., ed. CRC Press: Boca Raton, 1996; pp 143-154.

45. Squillacote, M. E.; Semple, T. C.; Mui, P. W. *J. Am. Chem. Soc.* **1985**, *107*, 6842.

46. Boue, S.; Srinivasan, R. *J. Am. Chem. Soc.* **1970**, *92*, 3226.

47. Inoue, Y.; Hagiwara, S.; Daino, Y.; Hakushi, T. *J. Chem. Soc. Chem. Comm.* **1985**, 1307.

48. Nebe, W. J.; Fonken, G. J. *J. Am. Chem. Soc.* **1969**, *91*, 1249.

49. Daino, Y.; Hagiwara, S.; Hakushi, T.; Inoue, Y.; Tai, A. *J. Chem. Soc. Perkin Trans. II* **1989**, 275.

50. Venneri, P. C.; Postigo, J. A.; Leigh, W. J. *J. Am. Chem. Soc.* **1995**, *117*, 7826.

51. Lawless, M. K.; Wickham, S. D.; Mathies, R. A. *J. Am. Chem. Soc.* **1994**, *116*, 1593.

52. van der Lugt, W. Th. A. M.; Oosterhoff, L. J. *J. Am. Chem. Soc.* **1969**, *91*, 6042.

53. Grimbert, D.; Segal, G.; Devaquet, A. *J. Am. Chem. Soc.* **1975**, *97*, 6629.

54. Robb, M. A.; Bernardi, F.; Olivucci, M. *Pure Appl. Chem.* **1995**, *67*, 783.

55. Bernardi, F.; Olivucci, M.; Robb, M. A. *Chem. Soc. Rev.* **1996**, 321.

56. Bernardi, F.; Olivucci, M.; Robb, M. A. *J. Photochem. Photobiol. A. Chem.* **1997**, *105*, 365.

57. Bernardi, F.; De, S.; Olivucci, M.; Robb, M. A. *J. Am. Chem. Soc.* **1990**, *112*, 1737.

58. Bernardi, F.; Olivucci, M.; Robb, M. A. *Acc. Chem. Res.* **1990**, *23*, 405.

59. Michl, J. *Mol. Photochem.* **1972**, *4*, 243.

60. Zimmerman, H. E. *J. Am. Chem. Soc.* **1966**, *88*, 1566.

61. Fuss, W.; Lochbrunner, S.; Muller, A. M.; Schikarski, T.; Schmid, W. E.; Trushin, S. A. *Chem. Phys.* **1998**, *232*, 161.

62. Trushin, S. A.; Fuss, W.; Schikarski, T.; Schmid, W. E.; Kompa, K. L. *J. Chem. Phys.* **1997** , *106*, 9386.

63. Fuss, W.; Schikarski, T.; Schmid, W. E.; Trushin, S. A.; Kompa, K. L. *Chem. Phys. Lett.* **1996**, *262*, 675.

64. Bernardi, F.; Olivucci, M.; Michl, J.; Robb, M. A. *Spectrum* **1996**, *9*, 1.

65. Bernardi, F.; Olivucci, M.; Robb, M. A. *Isr. J. Chem.* **1993**, *33*, 265.

66. Olivucci, M.; Ragazos, I. N.; Bernardi, F.; Robb, M. A. *J. Am. Chem. Soc.* **1993**, *115*, 3710.

67. Celani, P.; Bernardi, F.; Olivucci, M.; Robb, M. A. *J. Chem. Phys.* **1995**, *102*, 5733.

68. Squillacote, M. E.; Semple, T. C. *J. Am. Chem. Soc.* **1990**, *112*, 5546.

69. Leigh, W. J.; Postigo, J. A. *J. Chem. Soc. Chem. Comm.* **1993**, 1836.

70. Pasto, D. J.; Kong, W. *J. Org. Chem.* **1989**, *54*, 4028.

71. Bernardi, F.; Olivucci, M.; Ragazos, I. N.; Robb, M. A. *J. Am. Chem. Soc.* **1992**, *114*, 2752.

72. Olivucci, M.; Bernardi, F.; Celani, P.; Ragazos, I. N.; Robb, M. A. *J. Am. Chem. Soc.* **1994**, *116*, 1077.

73. Celani, P.; Bernardi, F.; Robb, M. A.; Olivucci, M. *J. Phys. Chem.* **1996**, *100*, 19364.

74. Celani, P.; Ottani, S.; Olivucci, M.; Bernardi, F.; Robb, M. A. *J. Am. Chem. Soc.* **1994**, *116*, 10141.

75. Garavelli, M.; Celani, P.; Bernardi, F.; Robb, M. A.; Olivucci, M. *J. Am. Chem. Soc.* **1997** , *199*, 11487.

76. Garavelli, M.; Celani, P.; Fato, M.; Bearpark, M. J.; Smith, B. R.; Olivucci, M.; Robb, M. A. *J. Phys. Chem. A.* **1997**, *101*, 2023.

77. Garavelli, M.; Celani, P.; Yakamoto, N.; Bernardi, F.; Robb, M. A.; Olivucci, M. *J. Am. Chem. Soc.* **1996**, *118*, 11656.

78. Vreven, T.; Bernardi, F.; Garavelli, M.; Olivucci, M.; Robb, M. A.; Schlegel, H. B. *J. Am. Chem. Soc.* **1997**, *119*, 12687.

79. Garavelli, M.; Bernardi, F.; Clifford, S.; Robb, M. A.; Olivucci, M. *J. Photochem. Photobiol. A. Chem.* **1998**, *114*, 109.

80. Garavelli, M.; Vreven, T.; Celani, P.; Bernardi, F.; Robb, M. A.; Olivucci, M. *J. Am. Chem. Soc.* **1998**, *120*, 1285.

81. Bernardi, F.; Garavelli, M.; Olivucci, M.; Robb, M. A. *Mol. Phys.* **1997**, *92*, 359.

82. Inoue, Y.; Mukai, T.; Hakushi, T. *Chem. Lett.* **1983**, 1665.

83. Nguyen, N.; Harris, B. E.; Clark, K. B.; Leigh, W. J. *Can. J. Chem.* **1990**, *68*, 1961.

84. Kropp, P. J. Photoreactions of Alkenes in Protic Media; In *CRC Handbook of Organic Photochemistry and Photobiology*; Horspool, W., ed. CRC Press, Inc.: Boca Raton, 1995; pp 105-114.

85. Kropp, P. J.; Reardon, E. J., Jr.; Gaibel, Z. L. F.; Williard, K. F.; Hattaway, J. H., Jr. *J. Am. Chem. Soc.* **1973**, *95*, 7058.

86. Fravel, H. G.; Kropp, P. J. *J. Org. Chem.* **1975**, *40*.

87. Fields, T. R.; Kropp, P. J. *J. Am. Chem. Soc.* **1974**, *96*, 7559.

88. Collin, G. J.; Deslauriers, H. *Can. J. Chem.* **1985**, *63*, 1424.

89. Leigh, W. J.; Clark, K. B. *Can. J. Chem.* **1988**, *66*, 1571.

90. Postigo, J. A.; Leigh, W. J. *Can. J. Chem.* **1995**, *73*, 1.

91. Brauman, J. I.; Archie, W. C., Jr. *J. Am. Chem. Soc.* **1972**, *94*, 4262.

92. Reeve, W.; Reichel, D. M. *J. Org. Chem.* **1972**, *37*, 68.

93. Lew, C. S. Q.; Brisson, J. R.; Johnston, L. J. *J. Org. Chem.* **1997**, *62*, 4047.

94. Inoue, Y.; Daino, Y.; Tai, A.; Hakushi, T.; Okada, T. *J. Am. Chem. Soc.* **1989**, *111*, 5584.

95. Hirayama, F.; Lipsky, S. *J. Chem. Phys.* **1975**, *62*, 576.

96. Klessinger, M.; Michl, J. *Excited States and Photochemistry of Organic Molecules*; VCH Publishers,Inc.: New York, 1995; pp 320-322.

97. Elsaesser, T.; Kaiser, W. *Annu. Rev. Phys. Chem.* **1991**, *42*, 83.

98. Hippler, H.; Troe, J. Recent Direct Studies of Collisional Energy Transfer in Vibrationally Highly Excited Molecules in the Ground Electronic State; In *Bimolecular Collisions*; Ashfold, M. N. R., Baggott, J. E., eds. Royal Society of Chemistry: London, 1986; pp 209-262.

99. Troe, J. *J. Phys. Chem.* **1983**, *87*, 1800.

100. Hippler, H.; Luther, K.; Troe, J.; Wendelken, H. J. *J. Chem. Phys.* **1983**, *79*, 239.

101. Calvert, J. G.; Pitts, J. N. Jr. *Photochemistry*; John Wiley & Sons,Inc.: New York, 1966.

102. Troe, J. *Pure & Appl. Chem.* **1997**, *69*, 841.

103. Haller, I.; Srinivasan, R. *J. Org. Chem.* **1965**, *16*, 2977.

104. Chung, G.-Y.; Carr, R. W. *J. Phys. Chem.* **1987**, *91*, 2831.

105. Inoue, Y.; Takamuku, S.; Sakurai, H. *J. Chem. Soc. Perkins II* **1977**, 1635.

106. Inoue, Y.; Takamuku, S.; Sakurai, H. *Bull. Chem. Soc. Jpn.* **1975**, *48*, 3101.

107. Roquitte, B. C. *J. Phys. Chem.* **1965**, *69*, 2475.

108. Roquitte, B. C. *J. Am. Chem. Soc.* **1963**, *85*, 3700.

109. Andrews, G. D.; Davalt, M.; Baldwin, J. E. *J. Am. Chem. Soc.* **1973**, *95*, 5044.

110. Andrews, G. D.; Baldwin, J. E. *J. Am. Chem. Soc.* **1977**, *99*, 4851.

111. Andrews, G. D.; Baldwin, J. E. *J. Am. Chem. Soc.* **1977**, *99*, 4853.

112. Elsaesser, T.; Kaiser, W. *Annu. Rev. Phys. Chem.* **1991**, *42*, 83.

113. Schriebmann, A. A. P. *Tet. Lett.* **1970**, *49*, 4271.

114. Kuhn, H. J.; Braslavsky, S. E.; Schmidt, R. *Pure Appl. Chem.* **1989**, *61*, 187.

115. Robinson, P. J.; Holbrook, K. A. *Unimolecular Reactions*; Wiley-Interscience: London, 1972.

116. Frisch, M. J., Trucks, G. W., Schlegel, H. B., Gill, P. M. W., Johnson, B. G., Robb, M. A., Cheeseman, J. R., Keith, T., Petersson, G. A., Montgomery, J. A., Raghavachari, K., Al-Laham, M. A., Zakrzewski, V. G., Ortiz, J. V., Foresman, J. B., Cioslowski, J., Stefanov, B. B., Nanayakkara, A., Challacombe, M., Peng, C. Y., Ayala, P. Y., Chen, W., Wong, M. W., Andres, J. L., Replogle, E. S., Gomperts, R., Martin, R. L., Fox, D. J., Binkley, J. S., Defrees, D. J., Baker, J., Stewart, J. P., Head-Gordon, M., Gonzalez, C., and Pople, J. A. Gaussian 94, Revision E.2. 1995. Pittsburgh, PA, Gaussian, Inc.

117. Scott, A. P.; Radom, L. *J. Phys. Chem.* **1996**, *100*, 16502.

118. Rondan, N. G.; Houk, K. N. *J. Am. Chem. Soc.* **1985**, *107*, 2099.

119. Tien, C. L.; Lienhard, J. H. *Statistical Thermodynamics*; Hemisphere Pucblishing Corporation: Washington, 1979; pp 211-240.

120. Benzler, J.; Linkersdorfer, S.; Luther, K. *J. Chem. Phys.* **1997**, *106*, 4992.

121. Benzier, J.; Linkersdorfer, S.; Luther, K. *Ber. Bunsenges. Phys. Chem.* **1996**, *100*, 1252.

122. Collin, G. J.; Deslauriers, H. *Can. J. Chem.* **1983**, *61*, 1970.

123. Tardy, D. C.; Ireton, R.; Gordon, A. S. *J. Am. Chem. Soc.* **1979**, *101*, 1508.

124. Herndon, W. C.; Lowry, L. L. *J. Am. Chem. Soc.* **1964**, *86*, 1922.

125. Marvell, E. N. *Thermal Electrocyclic Reactions.*; Academic Press: New York, 1980; pp 124-189.

126. Leigh, W. J. and Cook, B. H. O. 2000. Personal Communication

127. Diau, E. W. G.; Herek, J. L.; Kim, Z. H.; Zewail, A. H. *Science* **1998**, *279*, 847.

128. Negishi, E.; Liu, F.; Choueiry, D.; Mohamud, M. M.; Silveira, A. Jr.; Reeves, M. *J. Org. Chem.* **1996**, *61*, 8325.

129. Gerson, F.; Qin, X.-Z.; Bally, T.; Aebischer, J.-N. *Helv. Chim. Acta* **1988**, *71*, 1069.

130. Bellville, D. J.; Chelsky, R.; Bauld, N. L. *J. Comp. Chem.* **1982**, *3*, 548.

131. Barone, V.; Rega, N.; Bally, T.; Sastry, G. N. *J. Phys. Chem. A.* **1999**, *103*, 217.

132. Negishi, E.; Holmes, S. J.; Tour, J. M.; Miller, J. A.; Cederbaum, F. E.; Swanson, D. R.; Takahashi, T. *J. Am. Chem. Soc.* **1989**, *111*, 3336.

133. Nugent, W. A.; Thorn, D. L.; Harlow, R. L. *J. Am. Chem. Soc.* **1987**, *109*, 2788.

134. Dass, C.; Sack, T. M.; Gross, M. L. *J. Am. Chem. Soc.* **1984**, *106*, 5780.

135. Dass, C.; Gross, M. L. *J. Am. Chem. Soc.* **1983**, *105*, 5724.

136. Gross, M. L.; Russel, D. H. *J. Am. Chem. Soc.* **1978**, *101*, 2082.

137. Kawamura, Y.; Thurnauer, M. C.; Schuster, G. B. *Tetrahedron* **1986**, *42*, 6195.

138. Miyashi, T.; Wakamatsu, K.; Akiya, T.; Kikuchi, K.; Mukai, T. *J. Am. Chem. Soc.* **1987**, *109*, 5270.

139. Aebischer, J.-N.; Bally, T.; Roth, K.; Haselbach, E.; Gerson, F.; Qin, X.-Z. *J. Am. Chem. Soc.* **1989**, *111*, 7909.

140. Sastry, G. N.; Bally, T.; Hrouda, V.; Carsky, P. *J. Am. Chem. Soc.* **1998**, *120*, 9323.

141. Dunkin, I. R.; Andrews, L. *Tetrahedron* **1985**, *41*, 145.

142. Haselbach, E.; Bally, T.; Lanyiova, Z. *Helv. Chim. Acta* **1979**, *62*, 577.

143. Wiest, O. *J. Am. Chem. Soc.* **1997**, *119*, 5713.

144. Evleth, E. M.; Sevin, A. *J. Am. Chem. Soc.* **1981**, *103*, 7414.

145. Gruber, E. E.; Adams.R. *J. Am. Chem. Soc.* **1935**, 2555.

146. Dauben, W. G.; Cargill, R. L.; Coates, R. M.; Saltiel, J. *J. Am. Chem. Soc.* **1966**, *88*, 2742.

147. Moore, W. R.; Moser, W. R. *J. Am. Chem. Soc.* **1970**, *92*, 5469.

148. Forbes, W. F.; Shilton, P.; Balasubramanian, A. *J. Org. Chem.* **1964**, *29*, 3527.

149. Leighton, W. G.; Forbes, G. S. *J. Am. Chem. Soc.* **1930**, *52*, 3139.

150. Volman, D. H.; Seed, J. R. *J. Am. Chem. Soc.* **1964**, *86*, 5095.

151. Pitts, J. N. Jr.; Margerum, J. D.; Terry, R. P.; Brim, W. *J. Am. Chem. Soc.* **1955**, *77*, 5499.

152. Forbes, G. S.; Heidt, L. J. *J. Am. Chem. Soc.* **1934**, *56*, 2363.